CONTRACTION SCOUR IN COMPOUND CHANNELS WITH COHESIVE SOIL BEDS

A Thesis

by

BENJAMIN PRAISY ISRAEL DEVADASON

Submitted to the Office of Graduate Studies of
Texas A&M University
in partial fulfillment of the requirements for the degree of

MASTER OF SCIENCE

December 2007

Major Subject: Civil Engineering

CONTRACTION SCOUR IN COMPOUND CHANNELS WITH COHESIVE SOIL BEDS

A Thesis

by

BENJAMIN PRAISY ISRAEL DEVADASON

Submitted to the Office of Graduate Studies of
Texas A&M University
in partial fulfillment of the requirements for the degree of

MASTER OF SCIENCE

Approved by:

Chair of Committee,	Kuang-An Chang
Committee Members,	Jean-Louis Briaud
	Ming-Han Li
	Francisco Olivera
Head of Department,	David Rosowsky

December 2007

Major Subject: Civil Engineering

ABSTRACT

Contraction Scour in Compound Channels with Cohesive Soil Beds. (December 2007)

Benjamin Praisy Israel Devadason, B.S., Government College of Engineering,

Tirunelveli, India

Chair of Advisory Committee: Dr. Kuang-An Chang

Bridge scour, which is the removal of bed materials from near the bridge foundations, is observed to be the most predominant cause of bridge failures in the United States. Scour in cohesive soils is greatly different from scour in cohesionless soils owing to the differences in critical shear stresses, scour extents and the time taken to reach the maximum scour depth in the scour process. The present solutions available for the cohesionless soils cannot be applied to cohesive soils because of the above crucial reasons. Also, a compound channel model with main channel and flood plain arrangement represents more closely the field stream conditions rather than a simple rectangular prismatic model.

In this study, a systematic investigation of the scour process due to flow contractions in a compound channel with cohesive soil bed is made by conducting a series of flume tests representing typical field conditions. The effect of the most crucial factors causing contraction scour namely flow velocity, depth of flow and the shape of the abutment is examined. Correction factors are developed for changes in flow

geometries incorporating simulation results from the one dimensional flow simulation model HEC RAS.

Most importantly, a methodology to predict the depth of the deepest scour hole and its location in the vicinity of the contraction structure is developed for compound channels through an extension of the presently available methodology to predict maximum scour depths in simple rectangular channels. A prediction method to identify the extent of the uniform scour depth is also developed. Finally, an investigation of precision of the proposed methodology has been carried out on the field data from a number of real life contraction scour cases.

The results obtained from this study indicate that depth of flow and geometry of the contraction section significantly influence final scour depth in cohesive soils with deeper flows and harsh contractions resulting in increased scour depths. However, corrections for different contraction inlet skew angles and long contractions need to be further explored in future studies.

ACKNOWLEDGEMENTS

First and foremost, I would like to thank Dr. Kuang-An Chang for his continued guidance, instruction and encouragement throughout this research and till the completion of this thesis. Without his support and help, this work would not have been possible. The critical insights and the reviews he provided from time to time at every discussion were greatly helpful in gaining valuable understanding of both the subject matter, as well as, understanding the bigger picture in research.

I would like express my profound gratitude to Dr. Jean-Louis Briaud for the thought provoking discussions he initiated everytime during the project meetings. His kind, but intense approach, towards solving problems and the art of connecting ideas to arrive at solutions were truly inspiring at different stages of this work. I wish to thank him for the great learning experience he offered to me and the inspiration he provided to me, which resulted in a major milestone in my life. At this juncture, I would also like to express my thanks for the financial support received from the National Cooperative Highway Research Program through Dr. Jean-Louis Briaud to complete this research.

My thanks go to Dr. Francisco Olivera for teaching me the basics of Hydraulic Engineering in such an effective way that helped me clearly understand the fundamental principles in fluid flow, which immensely helped me while working in this research. I would also like to express my thanks to Dr. Ming-Han Li for his inputs through this thesis.

Last but not the least, I would like to express my gratitude to my lab partner Seung-Jae Oh for his continuous support even when we teamed up together while performing the experiments, and providing experimental data for three test cases in the experiments (Cases 7, 8 and 9 shown in Table 6.1. and erosion function experiment results as shown in Fig. 4.1). I would also like to express my thanks to Xingnian Chen for his support and interesting ideas while analyzing the results from the experiments.

TABLE OF CONTENTS

Page

ABSTRACT iii

ACKNOWLEDGEMENTS v

TABLE OF CONTENTS vii

LIST OF FIGURES x

LIST OF TABLES xii

CHAPTER

I INTRODUCTION AND RESEARCH OBJECTIVES 1

1.1 Introduction 1
1.2 Research Objectives 4
1.3 Approaches And Methodologies 5

II BASIC CONCEPTS AND PARAMETERS IN BRIDGE SCOUR 8

2.1 Introduction 8
2.2 Classification Of Bridge Scour 9
2.3 Contraction Scour In Compound Channels 11
2.4 Factors Affecting Contraction Scour Process 12

III EXISTING CONTRACTION SCOUR PREDICTION METHODS 13

3.1 Introduction 13
3.2 Contraction Scour In Cohesionless Soils 13
3.3 Contraction Scour In Cohesive Soils 19

IV MODEL DEVELOPMENT – CONTRACTION SCOUR 23

4.1 Introduction 23
4.2 Theoretical Background 24

CHAPTER Page

4.3 Shear Stress And Flow Velocity 28
4.4 Design Of Flume Tests For Contraction Scour In Compound Channel 31
4.5 General Test Arrangement 35

V FLUME TESTS – THE COMPOUND CHANNEL MODEL 43

5.1 The Compound Channel Model 43
5.2 False Bottoms 45
5.3 Scour Bed Preparation 45
5.4 Measurement Equipment 47

VI TEST DATA AND OBSERVATIONS 50

6.1 Introduction 50
6.2 General Test Procedure 50
6.3 Scour Depth 51
6.4 Flow Velocity And Water Depth 76
6.5 HEC RAS 81

VII METHODOLOGY DEVELOPMENT AND SCOUR PREDICTION 85

7.1 Background 85
7.2. Maximum Scour Depth 86
7.3 Location Of Maximum Scour Depth 94
7.4 Uniform Scour Depth 96
7.5 Verification Case Study 98

VIII CONCLUSIONS AND RECOMMENDATIONS 101

8.1 Conclusions 101
8.2 Recommendations 104

REFERENCES 105

APPENDIX A 110

APPENDIX B 113

APPENDIX C 116

VITA 118

LIST OF FIGURES

FIGURE Page

3.1 Scour Profile In A Contracted Channel (Li, 2002) 20

4.1 Erosion Rate Vs Shear Stress For Porcelain Clay 30

4.2 Schematic Representation Of The Geometry Of The Contracted Channel Section 32

4.3 Scour Depth Measurement Grid Points 36

4.4 Spectral Plot Of Flow Velocity For Test Case 3 38

4.5 Velocity Measurement Grid Points 39

5.1 Schematic Representation Of The Flume System (Not To Scale) 43

6.1 Contour Plots Of Compound Channel Flume Tests On Cohesive Soil 52

6.2 Contraction Scour Boundary – Half-Depth Of Maximum Scour 71

6.3 Influence Of Contraction Ratio On Contraction Scour Profile 74

6.4 Influence Of Approach Velocity On Contraction Scour Profile 75

6.5 Influence Of Water Depth On Contraction Scour Profile 75

6.6 Influence Of Abutment Shape On Contraction Scour Profile 76

6.7 Velocity Contours At The Start Of Test Cases 3 And 5 77

6.8 Longitudinal Velocity Profiles At The For Test Case 3 78

6.9 Vorticity Plot For Test Case 3 79

6.10 Water Surface Profile At Different Time Steps For Test Case 15 81

FIGURE Page

6.11 Comparison Of HEC RAS Predicted Velocities And Flume Test Velocities....82

6.12 Relationship Between Hec Ras Estimate Of Velocities And Flume Test Velocities....83

7.1 Velocity Stream Line Plots For Test Cases 3 And 5....87

7.2 Geometry Of The Contracted Section....88

7.3 Correlation Of Scour Depth Against Reynolds Number....89

7.4 Relationship Between Maximum Scour Depth And Froude Number....90

7.5 Relationship Between X_{max} And Contraction Geometry....96

7.6 Relationship Between Z_{unif} And Froude Number....98

7.7 Verification Case Studies – Prediction Vs Measurement....100

LIST OF TABLES

TABLE Page

4.1 Dimensionless Form Of Test Matrix For Compound Channel Cases.....34

4.2. Dimensionless Form Of Test Matrix For Rectangular Channel Cases 34

4.3 Dimensional Form Of Test Matrix For Compound Channel Cases.....34

4.4 Dimensional Form Of Test Matrix For Rectangular Channel Cases 35

4.5 Comparison Of The Experimental Measurements And Data Acquired– Rectangular Channel Vs. Compound Channel..... .. .40

6.1 Results From The Contraction Scour Tests In Compound Channel With Clay Bed 73

7.1 Contraction Scour Estimates On Real Life Rivers With Compound Channel Geometry.....99

CHAPTER I

INTRODUCTION AND RESEARCH OBJECTIVES

1.1 INTRODUCTION

Scour is the removal of bed material from the stream bed and stream banks due to the flow of water in the streams with high velocities. Flow acceleration happening around bridge structures can enhance such scour action resulting in enormous material removal. Scour is found to be the major cause of bridge failures all over the world. According to a survey conducted by Shirole and Holt (1991), 60% of the bridge failures are due to one or the other form of scour. According to Wang (2004), United States alone has lost about 1000 bridges to adverse scour action over the last 30 years. Bridges in general are high-investment infrastructures and any process that undermines the integrity of the bridges poses a huge threat to the hefty financial investments and causes a potential danger to the safety of human activities. A clear understanding of the scouring process is important in order to counter the effects of scour while structuring and designing bridge foundations.

Although, scour in general is material-removal, such a material-removal action is

---

This Thesis follows the style and format of *Journal of Geotechnical and Environmental Engineering*, ASCE.

more pronounced during high flows during storm and flood events when the water velocities and depths of flow are higher. During such high flood events, enormous energy transfer and energy losses happen between water and the soil grains around the bridge structures resulting in the soil particles getting excited and removed from the bed and banks. This can be mainly attributed to the turbulence patterns that happen due to sudden changes in flow geometries.

Contraction scour is classified as the scour that happens due to contracted flow patterns resulting from geometrical constrictions around bridges. Whenever contraction in area of flow occurs in between bridge abutments or piers, the velocity of flow increases rapidly due to the flow being forced through a reduced sectional area resulting in an increased shear stress near the soil bed. Whenever the shear stress at the soil-water interface exceeds the critical shear stress of the soil particles, excitation of the bed materials happen resulting in material removal. Such erosion of soil particles result in a general lowering of the bed level resulting in scour holes in the contracted flow section. Such a contraction scour action is found to be different in intensities between cohesionless soils and cohesive soils.

According to Briaud et al., (2001) scour and erosion rates in cohesive soils can be 1000 times slower than scour in cohesionless soils like sand. Therefore an estimate of scour in cohesive soils based on the characteristics of cohesionless soils can be an unnecessarily conservative estimate. The need for the differentiation between scour estimates in cohesive and non-cohesive soils is of particularly significant importance to

the bridge design community as it can mean huge differences in infrastructure expenditure in the form of very deep and massive foundations evenwhile making the scour estimates overly conservative. Currently, though a significant amount of research has been done to estimate the maximum depth of scour in cohesionless soils because of contraction scour, very little research can be accredited to the same on cohesive soils. Though thorough experimental investigations have been conducted in gravel beds (Carollo et al., 2005) or in sand beds (Richardson & Davis, 2001; Lagasse et al., 1991) to understand scour around bridge abutments in cohesionless soils resulting from complex turbulence patterns in flow fields, scour in cohesive soils is a phenomena less understood and is still under study with little research material available. Even among cohesive soils, maximum scour prediction methodology is available only for a simple rectangular channel (Li, 2002) without any flood plain-main channel arrangement like the most typical fluvial geomorphologies. A better understanding of the flow field patterns is also vital in better comprehending the contraction scour phenomena in cohesive soils, especially in the context of a compound channel with flood plain-main channel arrangement.

This research aims to develop a prediction methodology to estimate the maximum scour depth value in a compound channel with a flood plain-main channel arrangement with cohesive soils as the bed material. This research, in addition aims at understanding the physical processes during contraction scour by studying the effects of crucial flow parameters namely the flow depth and flow velocity and the geometry of the

abutment. This research is also an attempt to model a compound channel and also it's changing flow fields at a scale much closer to the typical real-life stream and approximately six times larger than previously studied models at reduced scales (Barbhuiya & Dey, 2003).

1.2 RESEARCH OBJECTIVES

This research is an attempt to understand the following key points with regard to contraction scour in compound channels with cohesive soil beds. Key questions that have been attempted to be answered through the current study of contraction scour on compound channels are as follows.

1. To evaluate the general trend of contraction scour in compound channels, its extent and geometry.

2. To develop a methodology to predict contraction scour depth and its location with reference to the bridge structure.

3. To evaluate the effect of changing flow fields on the location of contraction scour for compound channels and to identify the difference between abutment and contraction scours in compound channels.

4. To develop a method to construct a complete contraction scour profile for compound channels in cohesive soils.

1.3 APPROACHES AND METHODOLOGIES

In order to achieve the research objectives, flume tests in porcelain clay are conducted to study the behavior of scour for different case scenarios. The results of the flume tests are evaluated to arrive at generalized scour patterns.

1.3.1 Flume Tests

Flume tests are conducted to physically measure scour action under different conditions. The experiments on the flume model result in instant scour depth at different time steps and this data is extrapolated through a hyperbolic model to arrive at the maximum scour depth at equilibrium state. With special focus on the dominant factors causing scour action namely the approaching flow velocity, water depth and the contraction ratio, nine critical cases are evaluated to construct a basic formula to predict contraction scour.

1.3.2 Hyperbolic Model

According to Li (2002), the major difference between the scour phenomena in cohesionless and cohesive soils is the time taken to reach the maximum scour depth in the scour hole. In cohesionless soils such as sands, equilibrium scour state can occur fairly quick while on the other hand, cohesive soils can take as much as ten to thousand times more time to reach the equilibrium state in scour (Li, 2002). Since the scour rate in

cohesive soils is very low, it is practically difficult to conduct flume experiments till the maximum scour depth is reached at equilibrium scour state. Thus, according to Li (2004) and Briaud et al (1999,2001a), the first primary challenge that is faced while flume tests are conducted on porcelain clay is that the time to reach maximum scour depth Z_{max} could be as much as several months. The second challenge for cohesive soils is that the scour rate at later stages of the tests could be so low that it is almost impossible to judge and ascertain if the maximum scour depth has been reached. The answer to both of these challenges have been worked out by Briaud et al. (1999,2001a) through Scour Rate in Cohesive Soils (SRICOS) method wherein the maximum scour depth can be reliably extrapolated through fitting the flume test data of scour depth versus time as measured with a hyperbola.

The above said hyperbolic model can be written as

$$Z(t) = \frac{t}{\frac{t}{Z_{\max}} + \frac{1}{Z_{\text{ini}}}} \tag{1.1}$$

This can be rewritten as

$$\frac{1}{Z(t)} = \frac{1}{Z_{\max}} t + \frac{1}{Z_{\text{ini}}} \tag{1.2}$$

Where Z(t) is the scour depth at time t, Z_{max} is the maximum scour depth at equilibrium state and Z_{ini} is the initial scour rate. Both Z_{max} and Z_{ini} can be arrived by fitting the parabola given in Equation 1.2. Though the approach to extrapolate scour depth to arrive

at maximum scour depths based on the hyperbolic Equation 1.2. was developed for pier scour initially, it is also found to predict well contraction scour depth.

1.3.3 Shear Stresses in Soil Bed

Considering the erosion due to sediment transport to be negligible for clay, the only mechanism causing the removal of soil materials from the bed can be attributed to the erosive action of water. This erosive action of water flow can be represented by the shear stress the water exerts over the soil material. The initial represents the stress exerted by water on the soil bed before the scour process starts. The resistance offered by the soil particles against this erosive action of water can be quantified by the critical shear stress of the bed materials. The critical shear stress of the porcelain clay sample can be arrived at by the Erosion Function Apparatus developed by Briaud et al. (1999). This critical shear stress is assumed to be an unchanging characteristic throughout the scour development. The scour action is sustained until the shear stress in the clay bed, due to flow of water, drops down to the critical shear stress of soil bed material at the bottom of scour hole. Here, it is to be noted that any scour is initiated only if the erosive action of water, or in other words, the initial shear stress is greater than the critical shear stress of the soil bed. And therefore, it is the difference between the initial shear stress and the critical shear stress of the soil bed that governs the maximum scour depth and the time at which it is reached and all the associated equations developed based on these experiments.

CHAPTER II

BASIC CONCEPTS AND PARAMETERS IN BRIDGE SCOUR

2.1 INTRODUCTION

Scour phenomena results from the interaction between the water that flows in the stream and the soil particles that make the bed of the stream. When the erosive action of the water exceeds the erosion resistance offered by the soil particles, scour starts and continues till the shear stresses generated by the water is equal to the shear resistance of soil particles. In other words, scour action continues till shear stress drops down to the critical shear stress of the soil. In this chapter, different types of scour action that can happen in stream beds have been introduced with details about scour pattern that can result due to different flow patterns around hydraulic structures. The soil characteristics that are found to be a factor in causing scour have also been introduced in this chapter. In the following chapters, all of these factors are explored in further detail with the focus being on contraction scour in compound channels.

2.2 CLASSIFICATION OF BRIDGE SCOUR

Any scour that happens around and undermines bridge foundations can be termed as bridge scour. Bridge scour can be broadly classified into aggradation and degradation, local scour and contraction scour.

2.2.1 Aggradation and Degradation

According to Richardson and Davis (2001), aggradation and degradation refer to the gradual changes in the streambed elevation due to the natural or man-made causes over a very long time. Also, according to them, aggradation refers to the increase in streambed elevation due to depositing action of the waters and degradation refers to the erosive action of the waters. Aggradation or degradation can happen due to the changes in flow characteristics of the stream due to construction of dams and reservoirs, changes in the land use patterns in the floodplains and watersheds, channelization, gravel mining from the channel bed, cutting off of meander stream beds and the movement of bend and stream movement in relation to crossing at a far upstream location (Richardson and Davis, 2001). Here, it is to be noted that aggradation and degradation do not include the local cutting or filling that happens due to the change in flow geometry in the vicinity of bridge infrastructure. In summary, aggradation and degradation refer to the increase or decrease in the general stream bed elevation on a long-term basis due to changes that happen at a far upstream location which affect sediment transfer.

2.2.2. Local Scour

The presence of hydraulic structural obstacles such as abutments, embankments, spurs or piers can alter the flow patterns around these structures. This results in an increased erosive action around these structures. Since the area of influence of such an obstacle-induced erosion is limited, they are called local scour. Horseshoe vortex and wake vortex around these hydraulic obstacles are found to be the primary cause for local scour (Li, 2002).

2.2.3. Contraction Scour

Contraction scour is the type of scour that is caused at flow constrictions due to man-made or natural causes. The reduction in flow area increases the flow velocity which thereby increases the shear stresses near the flow constriction. The scour due to such an increased erosive action happens in the vicinity of the contraction and can be a result of factors such as (1) natural flow area decrease in the form of channel constrictions, (2) abutments and piers, intruding into and blocking the flow area, (3) ice formations, (4) sediment depositions along the length of the banks forming natural berms, (5) islands or bars of soil formations formed at the upstream or downstream side of bridge openings, and (6) vegetation that can contract the flow area either in the main channel or in the floodplain (Richardson et al., 2001). Among all these causes, the most common cause is the contraction effect caused by the protrusion of bridge abutments

either into the main channel or into the flood plain below the bridge structure (Wang, 2004).

2.3 CONTRACTION SCOUR IN COMPOUND CHANNELS

In a typical stream, flow is not only conveyed through the main channel but also through the flood plain during events of flood and high flows. Flood plains offer hydraulic buffer space for flow transfer in stream systems when the discharge through the stream exceeds the capacity of the main channel. Such a compound arrangement of main channel and flood plain complicates the flow characteristics near the bridges and other hydraulic structures. Contraction scour caused due to the channel constriction can be very different between a stream with main channel alone and a stream with a combined main channel-flood plain arrangement. The flow transfer characteristics between the flood plain and the main channel can vary the quantity of contraction scour that happens around the flow constriction. Though a clear experimental study of contraction scour in cohesive soils has been undertaken for channels with a rectangular cross-section (Li, 2002), contraction scour in a compound channel with cohesive soil beds and with the complicated geometry of a flood plain-main channel arrangement is yet to be thoroughly evaluated. This research aims at exploring the compound channel more in detail with respect to contraction scour.

2.4 FACTORS AFFECTING CONTRACTION SCOUR PROCESS

Shear stress increase in flow contractions can be influenced by a number of factors. Flow velocity increases at flow constrictions due to reduced area of conveyance. Such an accelerated flow happens even before the scour starts. Any factor that affects flow velocity or flow depth will increase the generation of contraction scour.

The initial flow velocity directly affects the initial shear stress while the flow depth is directly related to the shear stress decay rate with scour depth (Li, 2002). The flow velocity in the contracted section is found to be non uniform due to a number of factors. The major reason for such a non-uniform variation is the generation of turbulence in the wake of a hydraulic structure (Wang, 2004).

CHAPTER III

EXISTING CONTRACTION SCOUR PREDICTION METHODS

3.1 INTRODUCTION

Bridge scour has been extensively researched and systematic methods to evaluate scour have been put forward with respect to sandy soils. But research on scour in cohesive soils is still in its primitive state. With respect to contraction scour, only the live-bed and clear-water contraction scour in cohesionless soils have been the major concern in previous studies. The fundamental differences between the scour action in cohesionless soils and cohesive soils thus open up a horizon of areas where research is yet to be detailed and comprehensive. In this chapter, previous research on cohesionless contraction scour and cohesive contraction scour has been summarized with specific comments on the differences between the methodologies of the previous researches.

3.2 CONTRACTION SCOUR IN COHESIONLESS SOILS

Encroachment of bridge abutments or piers into the flow area in the main channel or in the flood plains is found to be the most common cause of bridge contraction scour (Li, 2002). All of the previous research on long contraction scour has focused on uniform rectangular channels with sand as bed material. The predominant assumption

that the flow in the far upstream approach section is uniform has governed the theoretical solutions. Since uniformity in flow characteristics has been the primary assumption and the flow section has been a simple rectangle, fundamental open channel theories and continuity relationships have been employed to easily arrive at the flow characteristics in unknown contracted sections. Though live-bed and clear-water scour have been dealt differently, a similar approach using uniform flow assumption has been used to evaluate the flows and sediment transport in the constricted and unconstricted portions of the channel. The major difference between the live-bed scour and clear-water scour equations is the sediment transport term.

According to Laursen (1963), clear water scour reaches an equilibrium state when the boundary shear stress reaches the critical shear stress of the soil bed. This observation forms the basis for several clear-bed scour equations to follow wherein the scour can be estimated based on a continuity relationship between the flow conditions in the uncontracted approach section and the constricted section. Clear water contraction scour equations of Laursen (1963) and Iverson (1998) for silica sands and clays respectively have been as follows.

Laursen's equation: $$\frac{H_2}{H_1} = 0.13\left(\frac{Q}{D^{1/3} H_1^{7/6} B_2}\right)^{6/7} \tag{3.1}$$

Iverson's equation: $$\frac{H_2}{H_1} = \left(\frac{2.32\, q_2{}^3 n^2 Q}{H_1{}^{10/3} (\log S_u - 2.367)} \right)^{3/10} \quad (3.2)$$

Where H_2 is the average water depth in the contracted section, m; H_1 or d_1 is the average water depth in the main upstream channel, m; Q is the discharge through the bridge or on the over bank at the bridge associated with the width, m^3/s; B_2 is the width of the main channel in the contracted section, m; S_u is the unconfined compressive strength of clay, lbs/ft^2; D is the effective mean diameter of the bed material ($1.25D_{50}$), m; n is the Manning's roughness coefficient and q_2 is the flow per unit width, m^2/s.

Also, according to Laursen (1963), the start of sediment transfer acts as a threshold between clear water scour and live bed scour and live bed scour prediction equations are found to lie well below this threshold interface under the levels of clear water scour. The head losses at the contraction inlet due to changes in velocity head are found to have less impact on the amount of scour observed in a long contracted section, according to Laursen (1963). This served as a basis for the development of several scour prediction equations by future researchers considering the scour action as a factor of contraction alone neglecting the loss in the velocity head at the contraction inlet. According to Laursen's (1963) findings, the error introduced through neglecting such kinetic head losses caused by the hindrance for uniform velocity at the bridge entrance section is found to be no greater than the possible error through the assumptions made

about the particle shear and critical shear of the soil bed. In general, it is observed that Laursen's study on long contracted channels with sand beds is found to be a stepping stone for further studies.

Biglari and Sturm (1998) experimented the relevance of the contraction scour studies conducted on rectangular channels and how they can be implemented for cases where a compound channel set up is present with a main channel and flood plain. In general, most of the real life streams are found to have distinct main channels and flood plains and therefore any methodology based on a simple rectangular channel may not be directly applicable to a compound channel. Through flume tests and computational approaches on compound channels, they have observed that there is a strong transverse movement of longitudinal momentum transfer between the flow in the main channel, where the water is flowing at a higher velocity to the flood plain where the water flows at a relatively lower velocity. According to Biglari and Sturm (1998), as the water flow increases, the velocity of flow in both the main channel as well as the flood plain increases, but the difference between the velocities decreases. Also, they inferred that the velocity in the center of the main channel was mostly unaffected by any projection of abutment into the flood plain or the edge of the main channel. On the other hand, the velocity in the flood plain increased greatly due to such encroachment. Also, according to them, the water depth and the velocity around the abutment can be approximately estimated by assuming that the water in the flood plain portion went only in to the flood

plain of the contracted channel and thus it could be assumed to be a rectangular section with the flow in the main channel considered separately for scour estimates.

The first most important shortcoming in the presently available methods for contraction scour prediction is that all the experimental evaluations are based on sandy soils which have significantly different erosive characteristics compared to cohesive soils. Although Iverson (1998) has developed an equation to predict contraction scour depth in clear water scour through an empirical relationship between critical shear stress and direct shear strength of cohesive soils, any experimental result or case studies to validate the empirical relationship is unavailable.

The present studies including that of Laursen (1963) have conducted experiments on long contraction channels to study contraction scour which may not realistically represent the most common short encroachments in the form of bridge piers and abutments (Melville and Coleman, 1999). Therefore application of correction factors to expand the usage of the contraction scour equations based on long contractions to short contractions becomes necessary. This need is particularly important with respect to predicting the location of the deepest scour hole.

Another shortcoming in all the presently available texts except for Li (2002) on contraction scour research is that the lack of distinction between the maximum scour depth and the uniform scour depth. The present scour estimate methodologies have put forward equations to predict the scour values that could be considered uniformly around the contraction zone. But, based on flume experiments conducted by Li (2002) on a

rectangular channel with cohesive soil bed, it has been shown that the scour profile distinctly contains a maximum scour hole and a zone of roughly uniform scour depth. Also, a methodology to estimate the location of the maximum scour hole is yet to be explored within the context of a compound channel. The distance of the maximum scour hole (X_{max}) from the start of the contraction section could be of significant importance to the bridge design community in making crucial structural decisions while considering the effects of scour.

Since most of the above mentioned equations have been derived based on a channel with a simple rectangular cross section, the turbulence phenomena associated with the formation of eddies at the wake of the encroachment structures and the corresponding increase in the shear stresses have not been documented well. The possible formation of recirculation waves at the downstream side of the constriction and their mixing with the main stream flow could give rise to complex flow mixing with subsequent effect on the shear stress exerted on the soil bed. This points towards the need for an improved model of a compound channel with main channel and flood plain which resembles a natural stream to realistically evaluate the turbulence patterns around the flow constrictions and their effects on contraction scour.

3.3 CONTRACTION SCOUR IN COHESIVE SOILS

The higher cohesive binding between the clay particles can cause the scour rate in clayey soils to be ten to thousand times slower than that in cohesionless sandy soils (Briaud et al., 1999). Though studies on contraction scour in cohesive soils are very limited, the contraction flume tests conducted by Li (2002) on cohesive soil bed offers critical insights on the contraction scour phenomena. A number of flume tests have been conducted on a rectangular channel with porcelain clay bed to evaluate the scour responses in cohesive bed.

Based on his research, three specific characteristics of contraction scour have been identified namely the maximum scour depth, Z_{max} or the depth of the most critical scour hole, the location of the maximum scour hole as measured from the start of the contracted section, X_{max} and the uniform scour depth, Z_{unif} which gives an estimate of the uniform scour depth that is observed beyond the maximum scour hole. According to Li (2002), the scour profile in a contracted channel with cohesive soil bed can be schematically represented as in Figure 3.1.

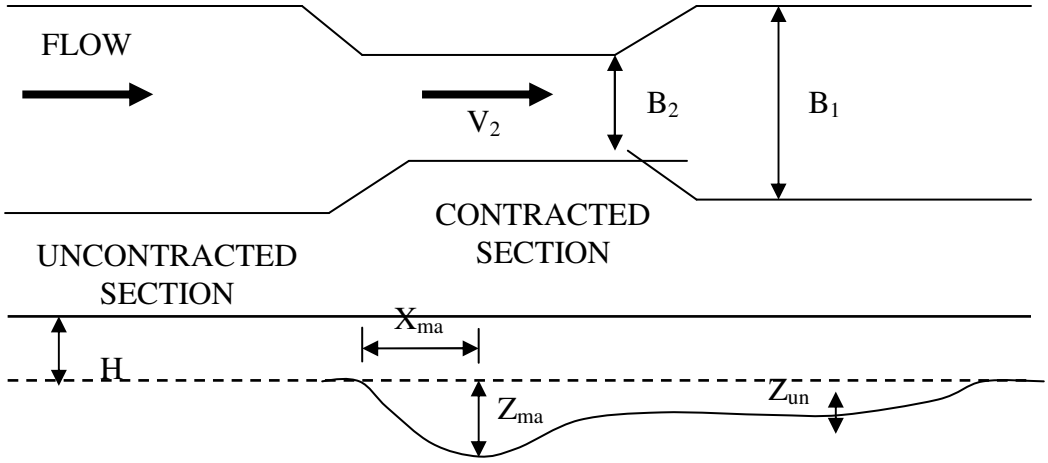

FIG 3.1 Scour Profile In A Contracted Channel (Li, 2002)

The equations suggested by Li (2002) for evaluating contraction scour in cohesive soils can be gives as follows.

$$\frac{Z_{max}}{H_1} = 1.9 \left\{ \frac{1.38\left[v_1 \frac{B_1}{B_2} \right] - v_c}{\sqrt{gH_1}} \right\} \tag{3.3}$$

where Z_{max} is the maximum scour depth, mm; H_1 is the depth of flow at a far upstream section where the effect of contraction is not pronounced, mm; v_1 is the velocity of flow in the uncontracted upstream section, cm/s; B_1 and B_2 are the widths of the uncontracted

and contracted portions of the stream respectively, cm and v_c denotes the critical velocity of the bed material, cm/s. The first term in this equation $\frac{1.38\left[v_1 \frac{B_1}{B_2}\right]}{\sqrt{gH_1}}$ refers to the Froude number in the contracted section. In the above term, the velocity of flow in the contracted channel (v_2) has not been used and instead, it is arrived by dividing the average upstream velocity (v_1) by the contraction ratio (B_2/B_1). The second term in Li's equation 3.1, $\frac{v_c}{\sqrt{gH_1}}$ denotes the critical Froude number. This quantity signifies the amount of erosive resistance that is offered by the soil bed. According to Li, the difference between the first and the second term explains the erosive potential. The factors 1.9 and 1.38 are applied as dimensionless factors.

According to Li, the scour phenomenon gives rise to an uniform scour zone apart from the maximum scour hole. This uniform scour zone extends beyond the immediate maximum scour hole and is found to be uniform because of the flow stabilization that occurs in the wake of the constriction. The expression to predict uniform scour depth according to Li (2002) is given as follows,

$$\frac{Z_{unif}}{H_1} = 1.41\left\{\frac{1.31\left[v_1 \frac{B_1}{B_2}\right] - v_c}{\sqrt{gH_1}}\right\} \tag{3.4}$$

where all the parameters in the above Equation 3.2 are the same as in Equation 3.1, except for Z_{unif} which is the uniform scour depth, mm.

Li (2002) has also put forward an equation to predict the location of the maximum scour based on the geometry of the contracted section. According to him,

$$\frac{X_{max}}{B_2} = 2.25\frac{B_2}{B_1} + 0.15 \tag{3.5}$$

In the above equation, X_{max} denotes the distance of the maximum scour hole from the start of the channel in mm while B_1 and B_2 stand for the width of the non-contracted and contracted portions of the channel respectively.

CHAPTER IV

MODEL DEVELOPMENT – CONTRACTION SCOUR

4.1 INTRODUCTION

Contraction scour has been an important phenomenon and has been studied by a number of researchers in the past (Straub 1934; Laursen 1960; 1963; Komura 1966; Gill 1981; Lim 1998; Chang 1998; Li 2002). Though contraction scour in cohesion soils have been studied thoroughly in the past, a comprehensive scour estimation methodology is not available for predicting cohesive contraction scour in compound channels. Even among the research on cohesionless soil contraction scour, it is only long contraction scour where the length of the contraction is more than twice the approaching channel width that has been focused on. But in reality, bridges typically impose short contractions in the form of abutments and piers and also, uniform flows as assumed by most of the previous methodologies may not be closely relevant assumptions with in the case of a compound channel. Besides, the applicability of the scour estimation methodologies based on cohesionless soils to cohesive soils is questionable. Another pressing need for the present research on compound channels is the necessity to distinguish uniform scour from the maximum scour hole and to identify its location.

In this chapter, the experiments on contraction scour are introduced. The theoretical background and the design of each flume test on contraction scour are

elaborately discussed. Comparisons are been made between the previous studies on contraction scour in cohesive soils with special emphasis being on cohesive solid bed and compound channel scour. In the later part of the chapter, the data from flume test observations is discussed along with the results.

4.2 THEORETICAL BACKGROUND

In this chapter the background behind the design of flume tests is discussed and analyzed in the light of cohesive soil scour. The most common cause for contraction scour is the reduction of flow area near abutments which causes flow constriction with subsequent increase in flow velocities followed by scour. Contraction scour typically occupies a larger area than other forms of local scour and therefore can result in a general lowering of the bed elevation over a long time (Li, 2002). Here open channel theories can provide the general background for the study on contraction scour. The equations and solutions used to generalize scour area according to Li (2002) are as follows.

Continuity equation describes that the input flow must be equal to the output flow when there is no channel loss involved.

$$V_1 B_1 H_1 = V_2 B_2 H_2 \tag{4.1}$$

Where V_1, B_1, H_1 are the stream velocity, m/s; channel width, m; flow depth, m respectively of the stream in the upstream side of the contraction and V_2, B_2, H_2 are the stream velocity, m/s; channel width, m; flow depth, m respectively of the stream at the contraction.

In the event of a head loss at the contraction inlet, the energy conservation law that is used to calculate the head losses can be given as the Bernoulli's law on a frictionless, steady and incompressible flow.

$$Z_1 + \frac{v_1^2}{2g} + H_1 = Z_2 + \frac{v_2^2}{2g} + H_2 \tag{4.2}$$

Where g is acceleration due to gravity, m/s^2; Z_1, v_1 and H_1 are the stream bed elevation, m; flow velocity, m/s; flow depth, m respectively in the upstream side of the contraction and Z_2, v_2 and H_2 are the stream bed elevation, m; flow velocity, m/s; flow depth, m respectively at the contraction.

4.2.1 Application of Hyperbola Model on Contraction Scour

The idea of using a hyperbolic model to predict scour was proposed, tried and verified in the prediction of pier scour by Li (2002), but it can also be extended for application in contraction scour. Hyperbolic models can help extrapolate the test results

of contraction scour unto very long time periods to which conduction of experiments may not be practically feasible (Li, 2002). Two assumptions that are used by other researchers (Lauren, 1960; Komura, 1966) to simplify the flow conditions are as follows.

(1) Flow is uniformly distributed in the rectangular channel.

(2) The velocity head is negligible when compared with the flow depth and therefore the water elevation in the contracted channel remains the same throughout scour development.

Based on the above two assumptions by the earlier researchers, Li (2002) has carried out the derivations as per Lauren (1960) and Komura (1966) as follows.

(1) Continuity equation of flow is

$$V_1 B_1 H_1 = V_2 B_2 H_2 = Q \tag{4.3}$$

Where Q is channel discharge, m^3/s.

(2) The bed of the stream is subjected to a shear stress of

$$\tau = \frac{\rho g n^2 V_2^{\,2}}{H^{1/3}} \tag{4.4}$$

Where τ is shear stress, N/m^2 ; ρ is the mass density of water, kg/m^3;

H is flow depth, m. By rearranging the above equation, the critical velocity ($V_{c)}$ can be expressed in terms of critical shear stress τ_c as

$$V_c = \sqrt{\frac{\tau_c H^{1/3}}{\rho g n^2}} \tag{4.5}$$

(3) By replacing V_2 by V_c in Equation 4.4, the final water depth in the contracted portion of the channel after equilibrium state has reached can be written as

$$H_2 = \left(\frac{\rho g n^2 \left(\frac{V_1 B_1 H_1}{B_2} \right)^2}{\tau_c} \right)^{3/7} \tag{4.6}$$

(3) A soil erosion function model in linear form can be given as

$$\frac{dH}{dt} = s(\tau - \tau_c) \tag{4.7}$$

Where H is the soil bed elevation, m; and S is a constant coefficient.

(4) Bringing equation 4.6 into Equation 4.7, the equation for scouring process can be obtained as

$$\frac{dH}{dt} = \left(\frac{a}{H^{7/3}} - b\right) \tag{4.8}$$

Where $a = S\rho g n^2 \left(\frac{V_1 B_1 H_1}{B_2}\right)^2$

$b = S\tau_c$

4.3 SHEAR STRESS AND FLOW VELOCITY

Shear stress exerted by water at the top of the soil bed plays a crucial role in exciting the bed materials, resulting in scour. Also, the shear resistance offered by the soil grains is of crucial importance. The critical shear stress (τ_c) of the soil bed can be experimentally estimated directly through the Erosion Function Apparatus (EFA) developed by Briaud et al. (1999) by measuring the erosion rates of the clay sample at different flow velocities. According to Briaud et al. (1999), in cohesive soils, the velocity of flow which gives rise to scour at the rate of 1 mm/hour can be regarded as the critical velocity (V_c) of the soil. The shear stress at the top of the bed material corresponding to the critical velocity gives the critical shear stress of the soil (τ_c) . A

number of EFA tests were conducted on Porcelain Clay samples from the cohesive test beds used in the experiments to evaluate the critical velocity of the bed material used and thereby, the critical shear stress of the bed material. The results have been shown in Figure 4.1. A median value of 1.5 N/m^2 was used for the critical shear stress value of test bed material in all the calculations in the following chapters.

Flow velocity is another major factor in the development of contraction scour. Though the velocity distribution across the stream at a far upstream approach section is fairly uniform, flow velocity variations occur to a great extent at the contraction section. This is mainly due to the convergence of flow into the constricted area. The portion of flow near the centerline of the stream has a higher velocity than the portion close to the abutment. This is due to the higher deflection of flow near the abutment contractions while the flow is fairly undisturbed near the channel centerline. Because of the uneven distribution of flow velocities across the contracted section, the actual velocity to be used in the calculations is based on the average velocity in the contracted section. A similar approach has been followed by the ABSCOUR program while estimating contraction scour. According to the ABSCOUR methodology developed by the Maryland State Highway Administration Scour Program in their Manual for Hydrologic and Hydraulic Design, Office of Bridge Development, Maryland SHA, when the setback of the abutment in to the floodplain from the main channel slope is less than 5 times the depth of water in the main channel, it is classified as a short set back case. And according to ABSCOUR methodology, there is uniform mixing among the main channel

waters and the flood plain waters thereby validating the assumption that the velocity used in the computation of flow parameters in the contraction channel can be the averaged velocity at the contraction section. In this research, a similar approach has been followed with the velocity with the suggestion that the velocity in the contraction section can be obtained by dividing the total discharge by the sectional area at the contraction section.

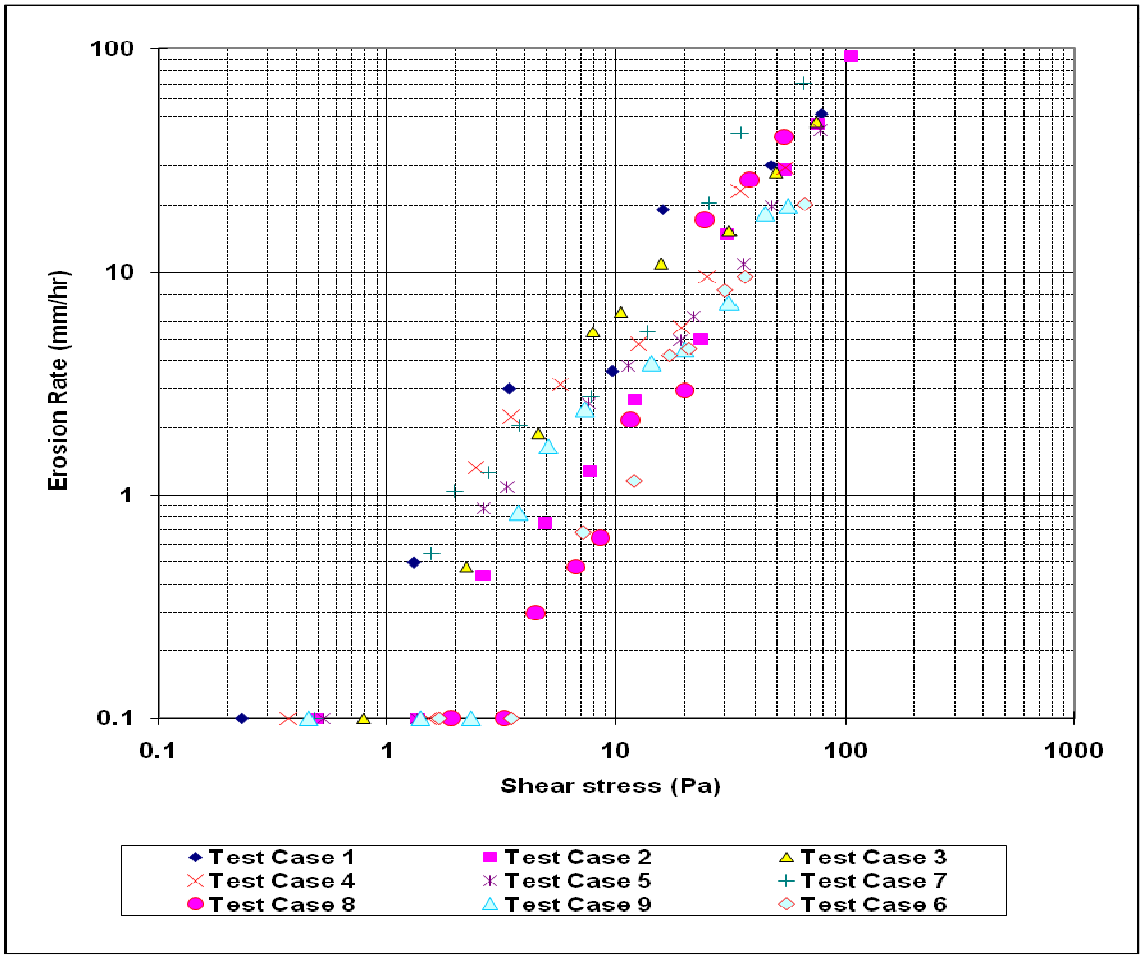

FIG 4.1 Erosion Rate Vs Shear Stress For Porcelain Clay

4.4 DESIGN OF FLUME TESTS FOR CONTRACTION SCOUR IN COMPOUND CHANNEL

The main factors that influence contraction scour in compound channels can be listed as the approach velocity V_1, the approach water depth H_m in the main channel, the contraction ratio (A_2/A_1), the abutment transition angle Θ and the contraction length L. But in this research, the focus has been only on the first three parameters which are the most influential parameters. The scour depth can therefore be expressed as these factors as below

$$Z = \mathrm{f}\,(H_c,\ V_1,\ V_2, \tau_c,\ g,\ \rho,\ \mu,\ \Theta\ ,\ S) \tag{4.9}$$

The explanation for the notations used in Equation 4.9 are given below the schematic diagram of the experimental set up shown in Fig. 4.2.The flume tests are designed to evaluate the effect of the following four factors.

(1) The effect of the approach velocity V_1 on scour development.

(2) The effect of the approach water depth H_c on scour development.

(3) The effect of shape of the abutment on scour development.

(4) The effect of contraction ratio on scour development.

To model the effects of the above parameters, two sets of experiments were conducted. One set is to study the effects of approach velocity, water depth and the

shape of the abutment on a compound channel while the other set was conducted to study the effect of blockage ratio on a rectangular channel.

Since the objective of these set of experiments were to bring about a set of solutions that can be applicable both for the compound channel and the rectangular channel geometries, all the above factors have been discussed with the primary focus being on the compound channel setup.

The following schematic diagram 4.2 represents the different variables used to define the geometries of the contraction section.

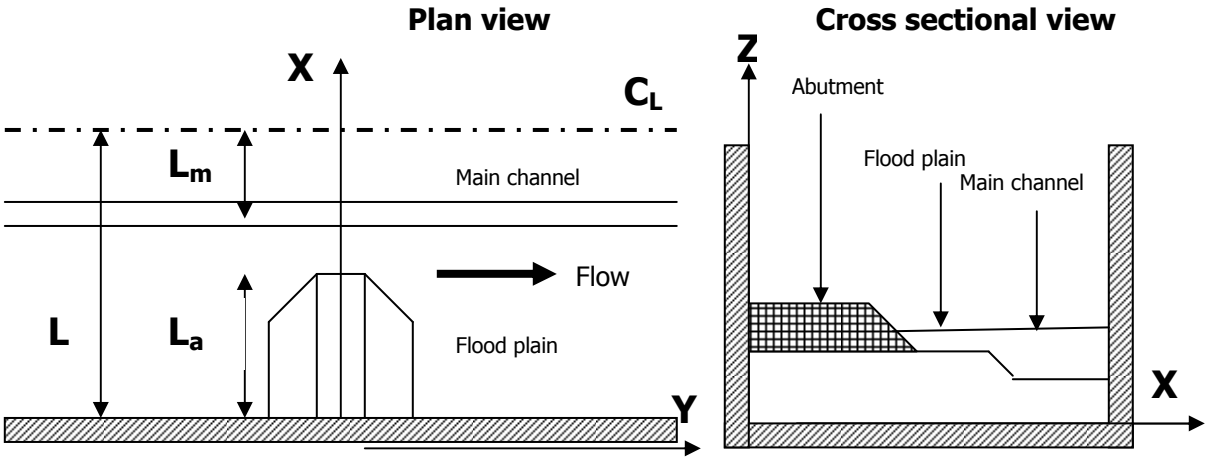

FIG 4.2 Schematic Representation Of The Geometry Of The Contracted Channel Section

L – Width of the flume.

L_m – Width of the main channel.

L_a – Width of the abutment.

L_f – Width of the flood plain

$L_f = L - L_m$

H_c – Depth of flow in the main channel.

H_{fp} – Depth of flow in the flood plain.

Q – Discharge.

β – Inclination angle of the abutment side walls.

Θ – Angle of the abutment.

Fr – Froude number.

S – Longitudinal slope of the channel bed.

ν - Kinematic viscosity of water.

V_1 – Velocity of flow in the uncontracted channel

V_2 – Velocity of flow at the contraction.

It is to be noted that since scour experiments were performed on a symmetric channel model, the centerline of the channel is replaced by a boundary wall. Table 4.1 and Table 4.2 show the variables and the different ratios in the dimensionless form for compound channel cases and rectangular channel cases respectively. Table 4.3 and Table 4.4 show the values of variables in the flume model for the compound and rectangular cases respectively.

Table 4.1 Dimensionless Form Of Test Matrix For Compound Channel Cases

Test Case	H_{fp}/L_a	F_r	L_a/L	TAN(β_a)	Θ (^{o})	L/L_m	H_c/L_m	L_a/L_m
1	0.16	0.23	0.5	0.5	90	3	0.41	1.50
2	0.1	0.23	0.5	0.5	90	3	0.32	1.50
3	0.22	0.23	0.5	0.5	90	3	0.50	1.50
4	0.16	0.18	0.5	0.5	90	3	0.41	1.50
5	0.16	0.28	0.5	0.5	90	3	0.41	1.50
6	0.16	0.23	0.5	vertical	90	3	0.41	1.50

Table 4.2. Dimensionless Form Of Test Matrix For Rectangular Channel Cases

Test Case	Fr	La/L
7	0.18	0.28
8	0.18	0.44
9	0.18	0.61

Table 4.3 Dimensional Form Of Test Matrix For Compound Channel Cases

Test Case	L		L_m		L_f		L_a		H_{fp}		V_{avg}		TAN(β_a)	Θ (^{o})	VARIABLE
	(ft)	(m)	(ft)	(m)	(ft)	(m)	(ft)	(m)	(ft)	(m)	(ft/s)	(m)			
1	12	3.66	4	1.2	8	2.4	6	1.8	0.96	0.29	1.41	0.43	0.5	90	Reference case
2	12	3.66	4	1.2	8	2.4	6	1.8	0.60	0.18	1.17	0.35	0.5	90	Water Depth (Low)
3	12	3.66	4	1.2	8	2.4	6	1.8	1.32	0.40	1.61	0.49	0.5	90	Water Depth (High)
4	12	3.66	4	1.2	8	2.4	6	1.8	0.96	0.29	1.10	0.33	0.5	90	Velocity (Low)
5	12	3.66	4	1.2	8	2.4	6	1.8	0.96	0.29	1.71	0.52	0.5	90	Velocity (High)
6	12	3.66	4	1.2	8	2.4	6	1.8	0.96	0.29	1.71	0.52	vertical	90	Abutment shape

Table 4.4 Dimensional Form Of Test Matrix For Rectangular Channel Cases

Test Case	L		L_m (ft)		L_f (ft)		L_a (ft)		H_c (ft)		V_{avg}		TAN(β_a)	Θ (°)	VARIABLE
	(ft)	(m)	(ft)	(m)	(ft)	(m)	(ft)	(m)	(ft)	(m)	(ft/s)	(m/s)			
7	12	3.66	-	-	-	-	3.33	1.01	1.20	0.37	1.09	0.33	vertical	90	Contraction ratio
8	12	3.66	-	-	-	-	5.33	1.62	1.20	0.37	1.09	0.33	vertical	90	Contraction ratio
9	12	3.66	-	-	-	-	7.33	2.23	1.20	0.37	1.09	0.33	vertical	90	Contraction ratio

4.5 GENERAL TEST ARRANGEMENT

The flume tests were designed to be conducted till an appreciable portion of the scour prediction hyperbola model has been constructed from the available experimental data for each test case. Stream bed elevations are measured across a grid of points after 24 hours in every test case in order to measure the changes in the bed topography and to identify scour. A plan view of the measurement grid is shown in Figure 4.3. The grid is more closely spaced towards the center of the abutment in order to capture the trends of scour development more precisely.

Mechanical profilers attached to the movable carriage described in Chapter 5 are used to measure to the bed elevation at the grid points after every 24 hours. After the first 144 hours of the test run, bed elevations were measured at a frequency of 48 hours so as to obtain more extensive points for fitting the hyperbolic model.

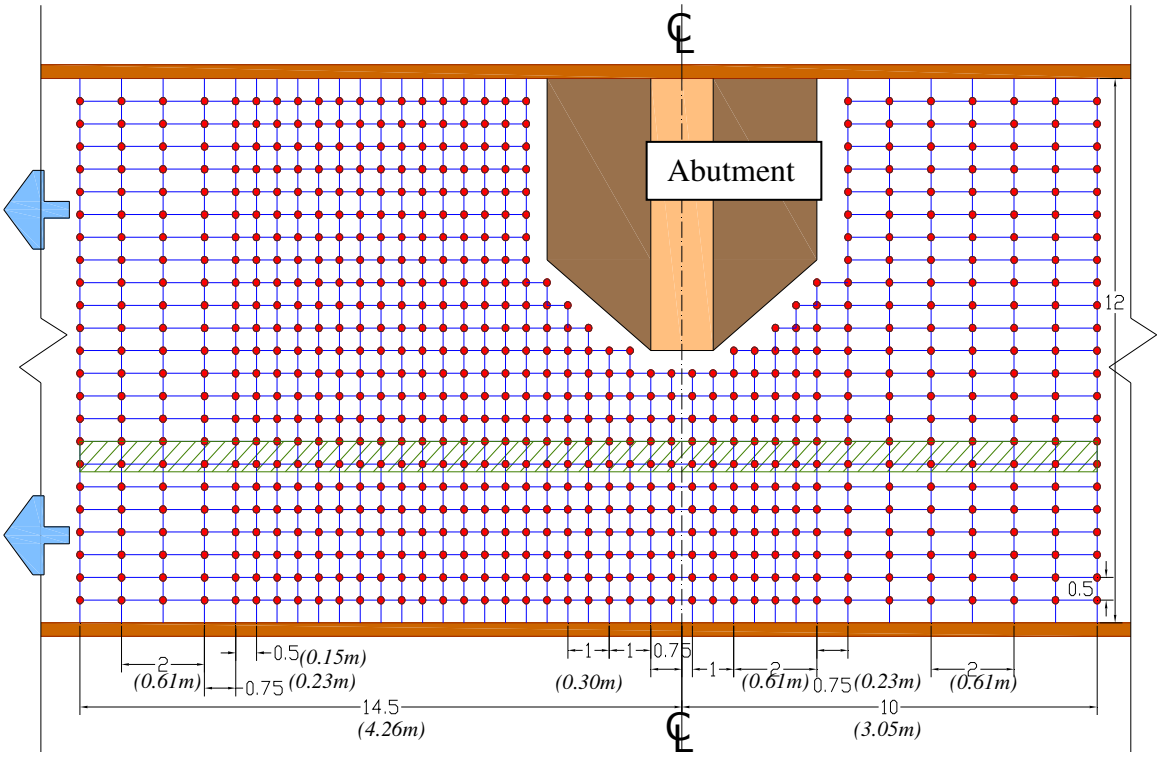

All dimensions of the flume shown are in units of ft (SI units are within brackets)

FIG 4.3 Scour Depth Measurement Grid Points

Flow velocity measurement around the abutment contraction and in the far upstream approach section is essential in understanding the velocity trends around the abutment contraction. Flow velocity was measured along a grid of points after the start of each test run. The grid points where velocity measurements were made is given in the Figure 4.5. Similar to the bed topography measurement grid, velocity measurement grid is also more intensive towards the abutment contraction as shown in Figure 4.5. Velocity measurement was made every 120 hours in the entire grid and every 24 hours in the far

upstream section in order to identify any changes in the velocity patterns due to the development of scour and change in bed geometry. Advanced Doppler Velocimeters as described in Chapter 5 were used measure the velocities at each of the grid points. A spectral analysis of the velocities around the contraction zone were conducted for Cases 3 and 5 to evaluate the velocity time history of flow and thereby to identify the time-duration of the eddies and recirculation waves formed at the wake of the contraction. The spectral analysis is performed on the basis of plotting the frequency of the eddy in the wake of the contraction opening against the power of the wave. The frequency corresponding to the intersection of a line with a negative slope of 5/3 against the power fluctuations gives average time period of the wave. Therefore, in the flume tests, the duration of the measurement ranges from 100 seconds near the abutment upto 10 minutes near the far downstream section. This change in the time of measurement is due to the fact that eddies and recirculation waves are generated near the abutment contraction with low time periods while as they move downstream their time period increases. This explains the need for measurements made over a longer time period in the sections away from the abutment so as not to miss the velocity pattern of any of the recirculation vortices in the vicinity of the contraction zone. An example of the conducted spectral analysis for Test Case 3 of the experiment is shown in Figure 4.4.

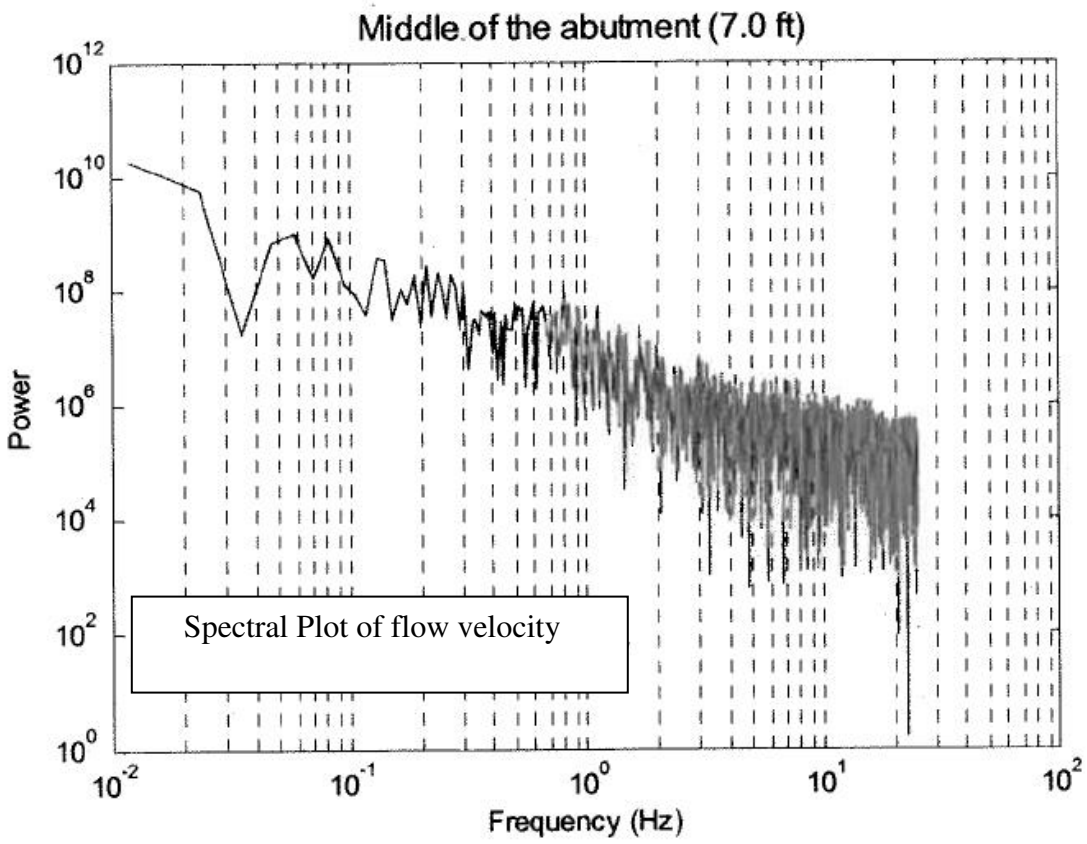

FIG 4.4 Spectral Plot Of Flow Velocity For Test Case 3

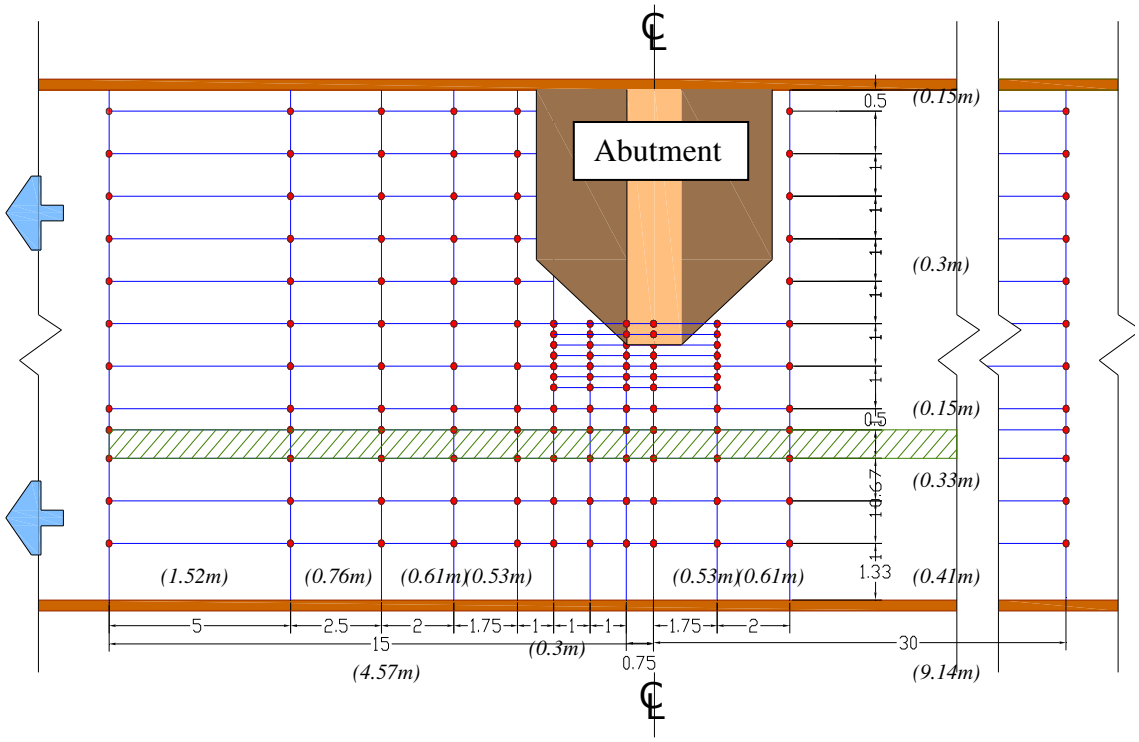

All dimensions are in units of ft (SI units are given within brackets)

FIG 4.5 Velocity Measurement Grid Points

Water surface elevations are measured using a point gage at the start of every test along the main channel to record the changes in the water surface profile near the contraction zone. Water level is also measured after every 24 hours to monitor the changes in the water elevation due to changes in the scour bed geometry.

The following Table 4.5 compares the observations and measurements that were made in the previous research conducted by Li (2002) on contraction scour in cohesive soils in a rectangular channel and the measurements carried out in this present research on compound channel contraction scour in cohesive soil beds.

Table 4.5 Comparison Of The Experimental Measurements And Data Acquired– Rectangular Channel Vs. Compound Channel

Rectangular channel (Li, 2002)	Compound channel
Velocity measurement (using an ADV): 1. Longitudinal velocity profile along the centerline of the channel once at the initial state and then at the final state. Initial vertical velocity profile in the middle of the channel at a location of 1.2 m upstream of the contraction.	Velocity measurement (using an ADV): 1. Velocity measurement at a 2-D grid of points (grid is shown below) at initial state and after every 120 hours till final state (viz. 0hour, 120hour, 240hour, 360hour). • Closer grid points near the channel contraction to capture the changes in flow fields precisely. 2. Initial vertical velocity profile in a section across the channel at the contracted portion for two cases.

Table 4.5 (Continued)

Water surface elevation (measured using a point gage): 1. Initial water surface elevation measured along the centerline of the channel. 2. Final water surface elevation measured along the centerline of the channel.	Water surface elevation (measured using a point gage): 1. Initial water surface elevation measured along the centerline of the main channel. 2. 120-hour water surface elevation measured along the centerline of the main channel. 3. 240-hour water surface elevation measured along the centerline of the main channel. 360-hour water surface elevation measured along the centerline of the main channel (for Case 2 only)
<u>Contraction scour profile:</u> Contraction scour profile along the centerline of the bottom of the channel, as a function of time (measured using a point gage).	<u>Contraction scour profile:</u> Contraction scour profile across a 2-D grid of points at the bottom of the flood plain and the main channel, as a function of time (measured using a profiler).

Table 4.5 (Continued)

Abutment scour measurements: Two abutment scour measurements as a function of time (measured using a point gage).	-
1. Photos of the final scour hole shape (taken by a digital camera).	1. Photos of the final scour hole shape (taken by a digital camera). Video clips of water flow across the contracted zone taken from the upstream, downstream and an aerial perspective using a digital camcorder.

CHAPTER V

FLUME TESTS – THE COMPOUND CHANNEL MODEL

5.1 THE COMPOUND CHANNEL MODEL

A compound channel model was constructed to perform a series of flume tests at the Haynes Coastal Engineering Laboratory, Texas A&M University, College Station. The tests were aimed at experimentally studying the proposed hyperbolic model. Porcelain clay was used to set up the bed of the compound channel and was sourced from Armadillo Clay and Supplies in Austin, Texas. A schematic representation of the compound channel model along with the instrumentation is shown in the following Figure 5.1. Details of the test set-up are described in the following paragraphs.

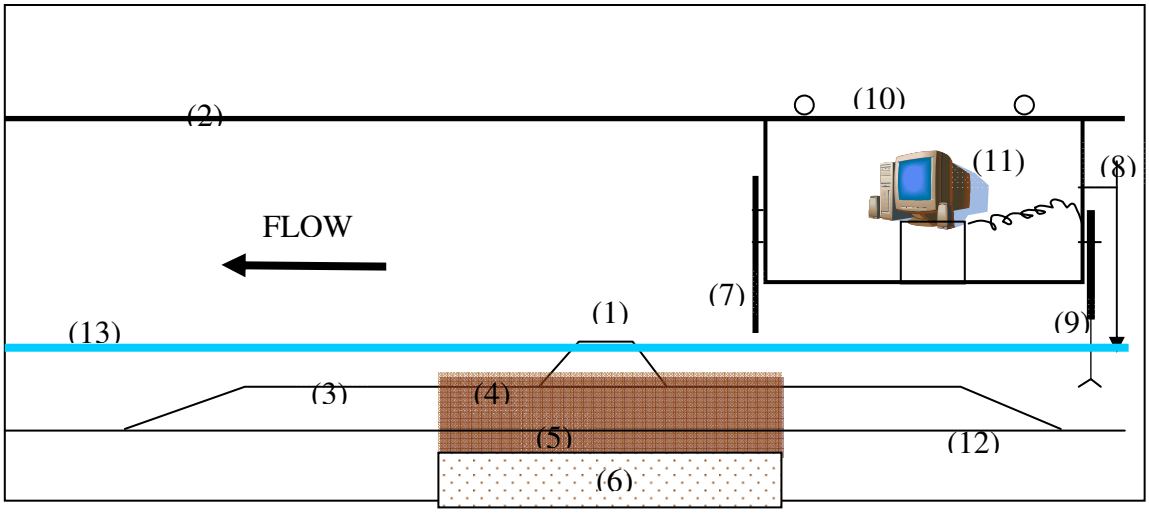

FIG 5.1 Schematic Representation Of The Flume System (Not To Scale)

(1) – Contraction Abutment

(2) – Steel Rails

(3) – False Bottom

(4) – Flood Plain

(5) – Main Channel

(6) - Sediment Pit

(7) – Scour Bed Mechanical Profiler

(8) – Point Gage

(9) – Advanced Doppler Velocimeter

(10) – Carriage

(11) – Computer Controls

(12) – Concrete Flume Bed

(13) – Water level

A long two-dimensional test flume with the dimensions 150 feet (45.72 m) long, 12 feet (3.66 m) wide and 11 feet (3.35 m) deep was used to conduct the scour experiment. The flume is part of a closed system and two pumps supply water into the flume part of this recirculation system at desired velocities and discharge levels based on accurate electronic adjustments of pump speeds. Therefore the total volume of water in the system remains constant except for few minor losses in the form of leakage or evaporation. The flume also includes an adjustable gate on one end so as to impound water if necessary to adjust flows and water levels. A sediment pit measuring 25 feet (7.62 m) long and 5 feet (1.52 m) deep starting at about one half of the flume length is available inside the flume which is used as the test bed.

5.2 FALSE BOTTOMS

False bottoms are necessary on either side of the test bed to ensure a smooth transition of the channel waters into the compound channel portion, which extends only for about 25 feet (7.62 m) length within the 150 feet (45.72 m) long flume. False bottoms were provided with the same geometrical cross-section as that of the compound channel geometry. In this experiment, false bottoms were provided with concrete beams of cross-sectional dimension 8" x 2' (0.203m x 0.61m). Placement and alignment of these heavy beams were done with the help of the gantry crane available at the laboratory. The gaps between these beams were sealed with liquid sealants to avoid any infiltration of water into the beams. The false bottoms were also provided with an entry ramp and an exit ramp with the slope 1:3 (vertical to horizontal) to ensure a smooth transition and to avoid the introduction of eddies. The slope of the main channel in the false bottom portion was provided with a framework of wooden members with plywood facing. These wooden members were fastened to the floor of the flume to avoid any uplift thrust exerted by the flowing waters.

5.3 SCOUR BED PREPARATION

The flume contains a sediment pit which is 25 feet (7.62 m) long, 12 feet (3.66 m) wide and 5 feet (1.52 m) deep. The sediment pit was filled with sand for about 3 feet (0.91 m) depth and the remaining depth was filled with Porcelain clay with a median

particle diameter of D_{50} = 0.003mm, plastic index of 14% and a critical shear stress (τ_c) of 1.5 $N/_m^2$. The abovementioned physical properties of clay were ascertained through the ASTM standard test procedures and the Erosion Function Apparatus test procedure (Briaud et al., 1999). The Porcelain Clay used for these experiments were sourced from Armadillo Clay and Supplies, Austin, Texas. The Erosion Function Apparatus (EFA) (Briaud et al., 1999) estimates the critical shear stress (τ_c) of the clay sample based on the erosion rates of the sample at different flow velocities. EFA tests were conducted on samples from the Porcelain Clay supplies and their critical shear stresses have been plotted in the Figure 4.1. The Porcelain Clay was delivered from the source in sealed plastic bags of size 250 mm x 180 mm x 180 mm. These bags were opened and the clay blocks were placed carefully upon the concrete floor of the flume. Compaction was performed to get rid of the air voids between adjacent blocks of clay. Compaction is necessary as any gaps between clay blocks could result in excessive scour holes. Care was taken to see to it that the clay was not deformed or its homogeneity lost in an effort to compact the bed.

The test bed was constructed with a flood plain arrangement along the length of the flume with a side slope of 1:1 and an elevation of 8 inches (0.2 m) relative to the main channel, for the tests on compound channels. The flood plain arrangement was made with plywood material with braces and connections to keep the shape intact. Abutments of two different shapes were tested in these experiments. One of them was a vertical wall abutment with a 45° wing wall, 18 inch (0.46 m) wide crest, 44 inch (1.12

m) height, and 90 inch (2.29 m) width and the other one was a spill-through abutment with the same dimensions. The side slope for the wing-wall shape is to be 2:1 (horizontal: vertical). The abutment was firmly seated in the flood plain with the right orientation.

Figure 5.1 shows the proposed experimental setup and the definition of the flow parameters are given below. The different test conditions that are to be investigated are shown in Table 4.3 and Table 4.4. After the completion of every test, the eroded and top slimy part of the clay was removed and was replaced with fresh unused clay. The removal of the top soft film of clay is essential to ensure that the old soil and the new soil can stick tight. Otherwise, the new clay might possibly be washed away in lumps when water exerts shearing and uplifting forces at higher velocities of flow.

5.4 MEASUREMENT EQUIPMENT

5.4.1 Equipment for Velocity Measurement

Acoustic Doppler Velocimeter (ADV) is an electronic instrument that uses acoustic sensors to measure the flow velocity in the flume by way of measuring the delay in the reflected waves between the impurities that are carried by the flow. ADVs can accurately measure velocities of flow without disturbing the flow or generating eddies through their probes. The used ADVs were sensitive for a velocity range of +-2.5

m/s and to a resolution of 0.1 mm/sec. Two ADVs were used in the compound channel flume tests, one each for the flood plain and the main channel set at 0.6 times the depth of water in order to measure the average velocity at that point. ADV's can measure velocities in all the three principal directions x, y and z. The two ADVs were set at measuring velocities four times every second. ADVs were primarily used in this experiment to measure the flow velocity across a grid of points as shown in Figure 4.4. The ADVs were fitted to a metal sliding piece and were mounted on a movable carriage that was used for making measurements across the test bed. The movable carriage was fabricated for mounting measurement devices and was towed by an electrically operated crane during the experiments.

5.4.2 Equipment for Flow Depth Measurement

Point gage is an accurate, inexpensive and efficient instrument to measure depth of flow. It is designed on the principle that electrical conductivity changes between different media such as air, water and soil. It has a needle attached to a vertical rule. The needle is connected to an electrical circuit which in turn in connected to a resistance gage. When the needle is lowered into the water and when the tip of the needle just touches the top surface of water, there is a sudden change of current flow in the closed circuit, which in turn is displayed in the resistance gage.

An electronic display unit is also provided to accurately measure water depths with a precision of 1/100 mm. A point gage was mounted on the movable carriage to measure flow depths along the length of the flume during the flume tests.

5.4.3 Equipment for Elevation Measurement

Elevation of the clay bed is to be measured after every 24 hours or 36 hours in order to record the changes in the bed topography with time. Measurement of elevation changes in a grid of points in the contraction zone as shown in Figure 4.3 are necessary to evaluate the scour trends and extents.

In this experiment, a hand-operated mechanical profiler arrangement is used to measure the elevations of the bed after every run of the test. A series of 0.5 inch (1.27 cm) diameter tubes are affixed with measurement tapes. These tubes can be lowered to rest on the bed after every test and the change in elevations can be noted down at the level of the carriage against a fixed mark. This is a simple yet effective method to measure the bed elevations. It takes roughly about three to four hours to measure the surface elevations of all the grid points whose elevations are measured.

After every test case, the skewed tubes are replaced with new ones in order to avoid any errors due to the nonlinearity of the profiler tubes. These profilers are mounted on the downstream side of the movable carriage. A measurement tape was affixed on the wall of the flume to identify the exact locations along the length of the flume where the scour bed elevation measurements were made.

CHAPTER VI

TEST DATA AND OBSERVATIONS

6.1 INTRODUCTION

In this chapter, the experimental results from the flume tests are introduced. For each test case, scour depth across a grid of points are measured at regular time intervals to obtain the trend of scour development and the maximum scour depth is thereby obtained from the hyperbolic model. Measurements of flow velocity at different sections were also carried out to obtain the trends in velocity change across the abutment contraction. Water depth measurement was also made for every test case. A brief discussion of the observed significant trends has been made for each of those measurements.

6.2 GENERAL TEST PROCEDURE

Pumps were operated and discharges were adjusted to match proposed discharge of the test conditions as shown in Tables 4.3 and 4.4 which in turn have been decided from a comprehensive dimensionless analysis of the typical bridge geometry conducted by Briaud et al., (2005) at Texas A&M University, College Station and are shown in Table 4.1 and Table 4.2 of Chapter 4. At the beginning of every test case, water

elevations and the test bed topography (bed elevation) were measured. The pump operation is followed by measurements of water depth and bed elevations at the grid points every 24 hours using an electronic point gage and a mechanical bed profiler respectively.

Flow velocities along all the three principal directions were measured while the experiment is in process using two Advanced Doppler Velocimeters, one for the main channel and one for the flood plain every 120 hours as explained in chapter 4.

6.3 SCOUR DEPTH

Contour plots of channel bed elevation measurements have been shown in Figures 6.1 and 6.2. These plots show the changes in the scour patterns over time.

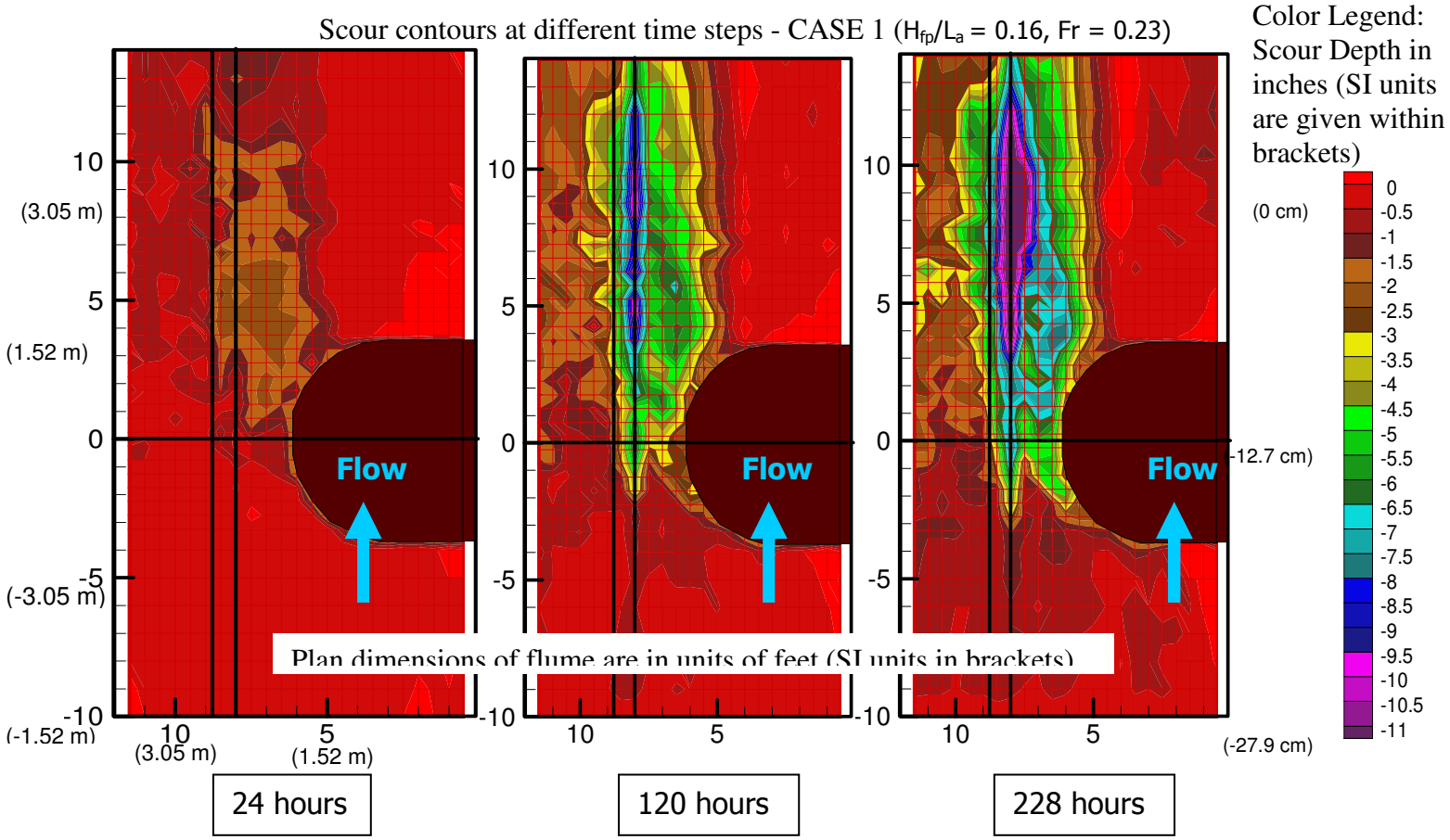

FIG 6.1 Contour Plots Of Compound Channel Flume Tests On Cohesive Soil

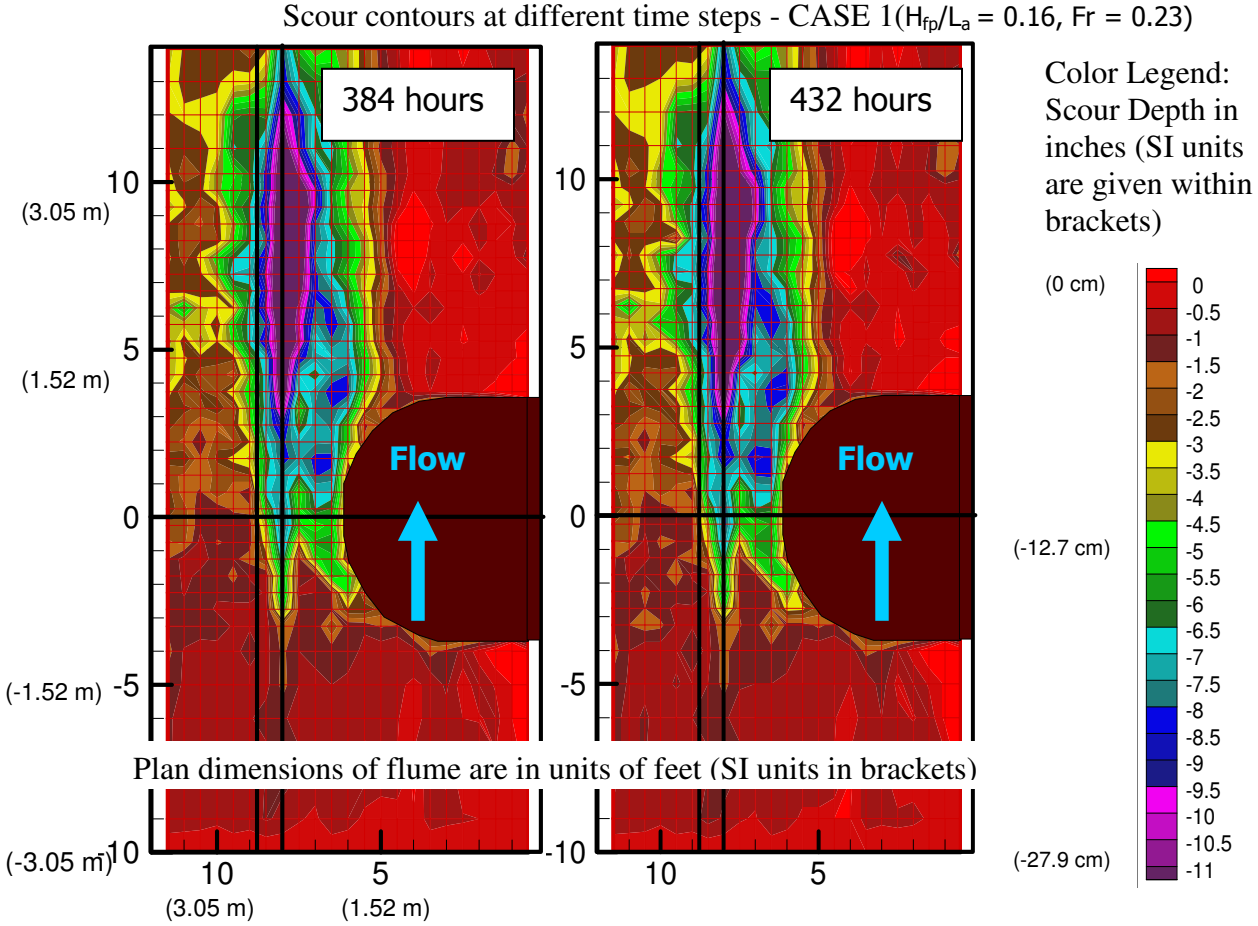

FIG 6.1 (Continued)

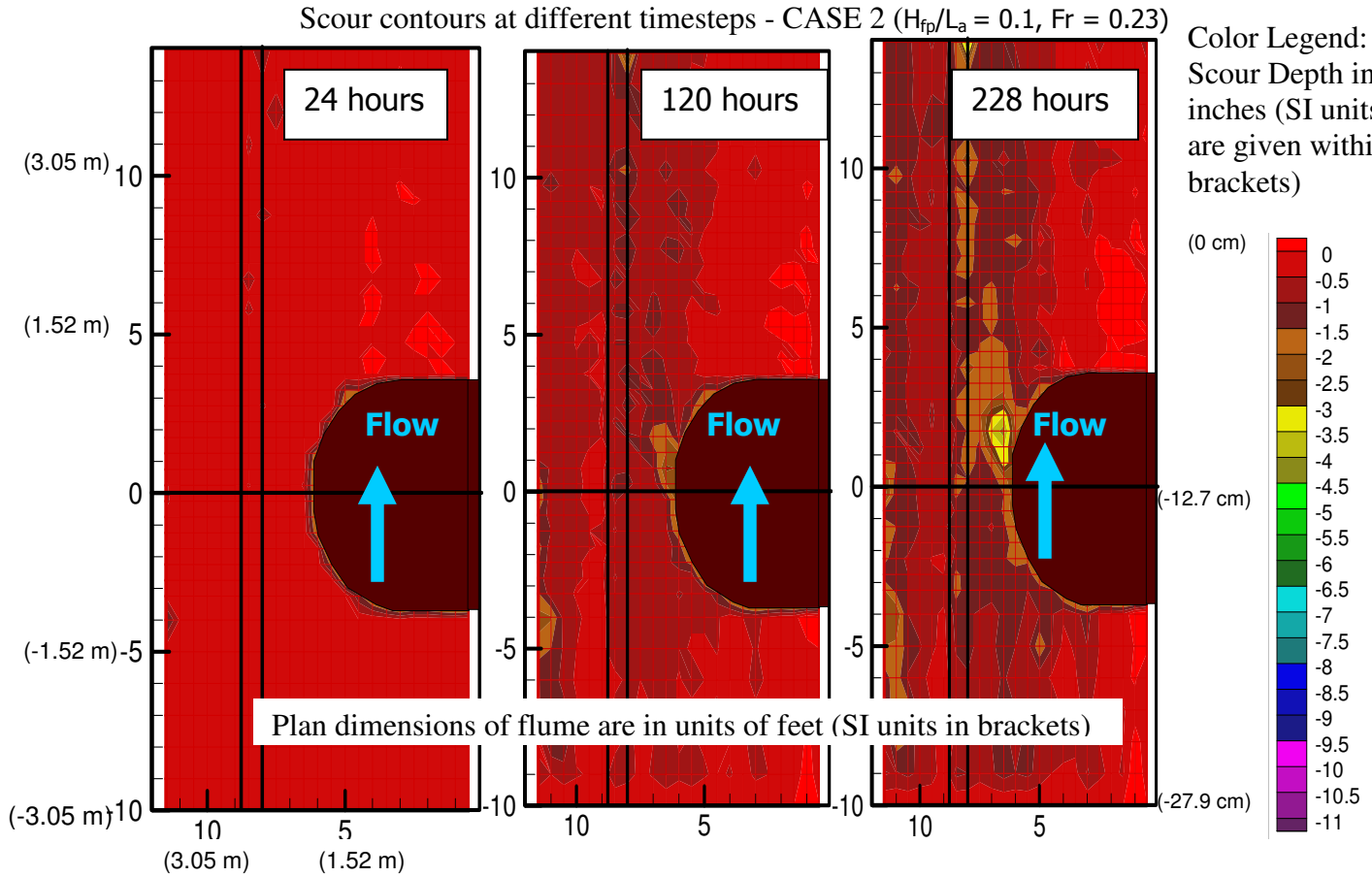

FIG 6.1 (Continued)

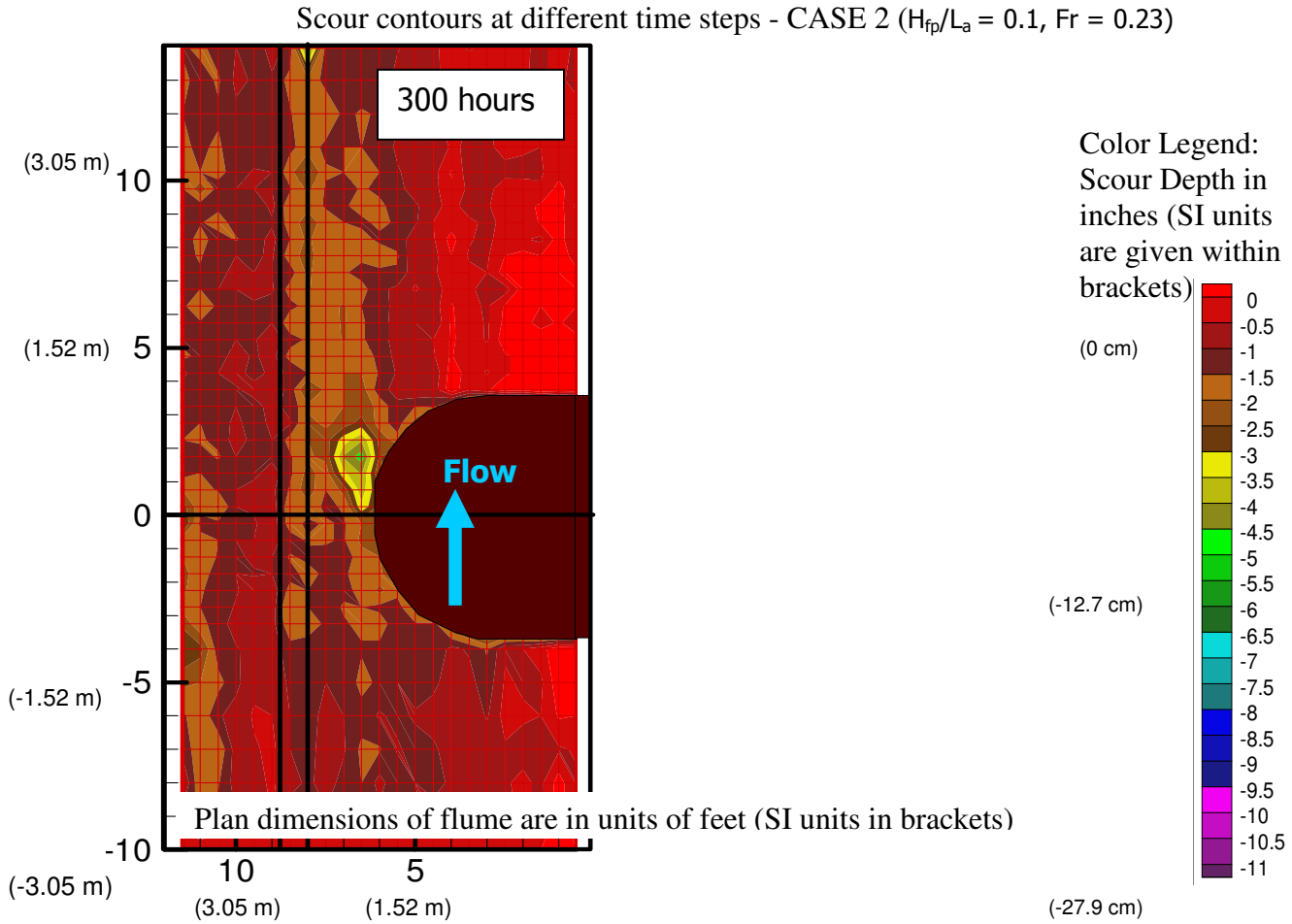

FIG 6.1 (Continued)

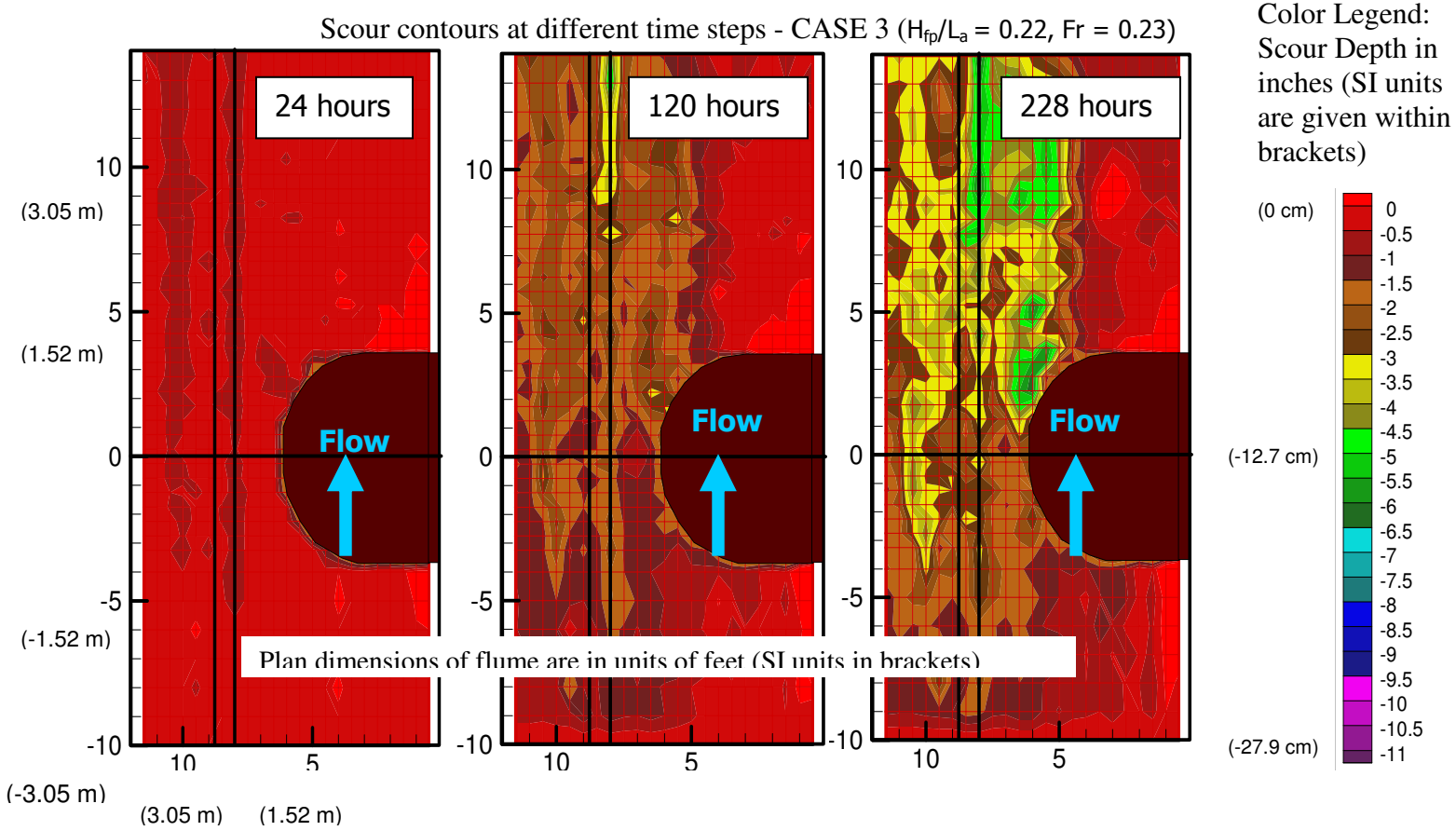

FIG 6.1 (Continued)

Scour contours at different time steps – CASE 3 (H_{fp}/L_a = 0.22, Fr = 0.23)

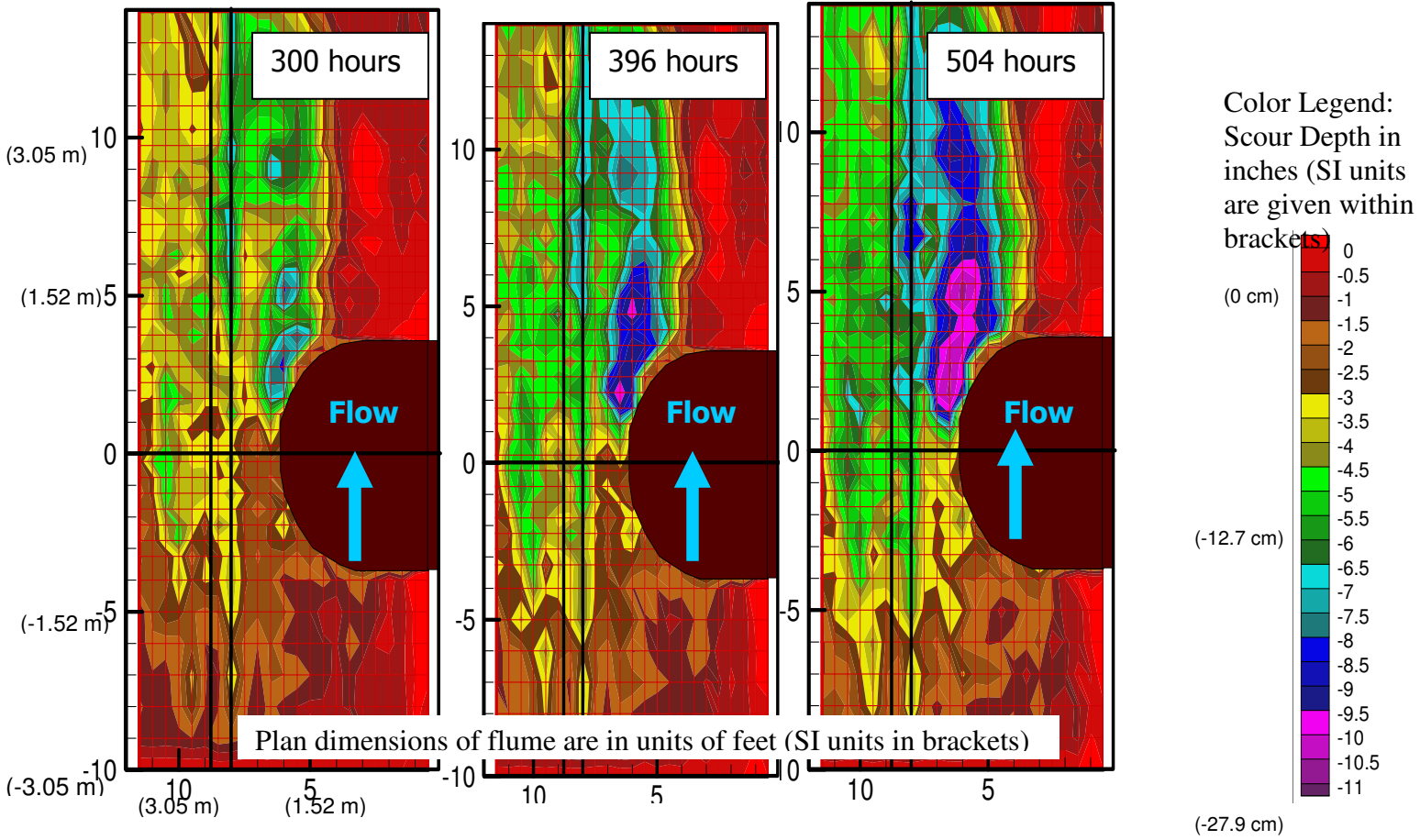

FIG 6.1 (Continued)

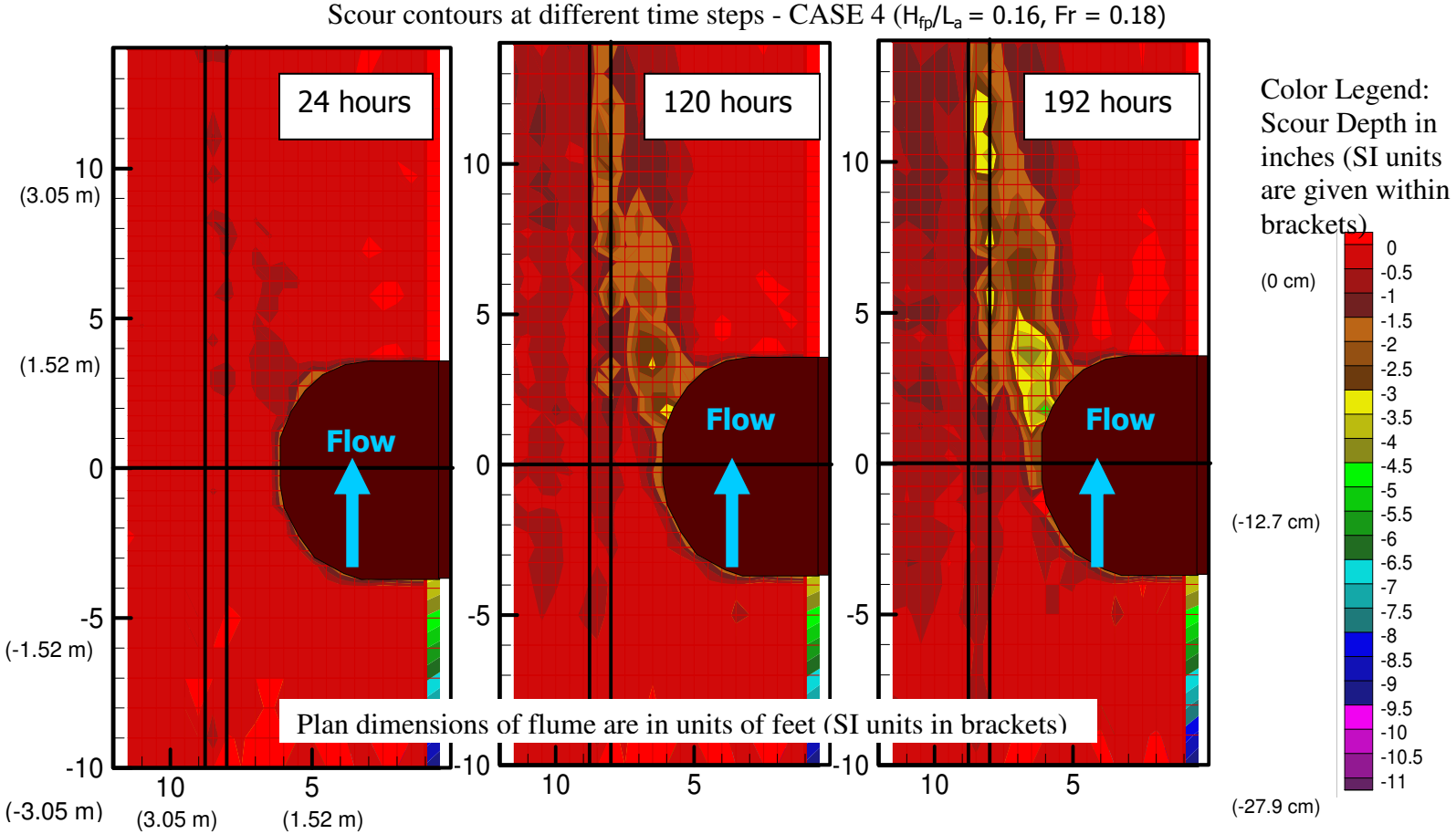

FIG 6.1 (Continued)

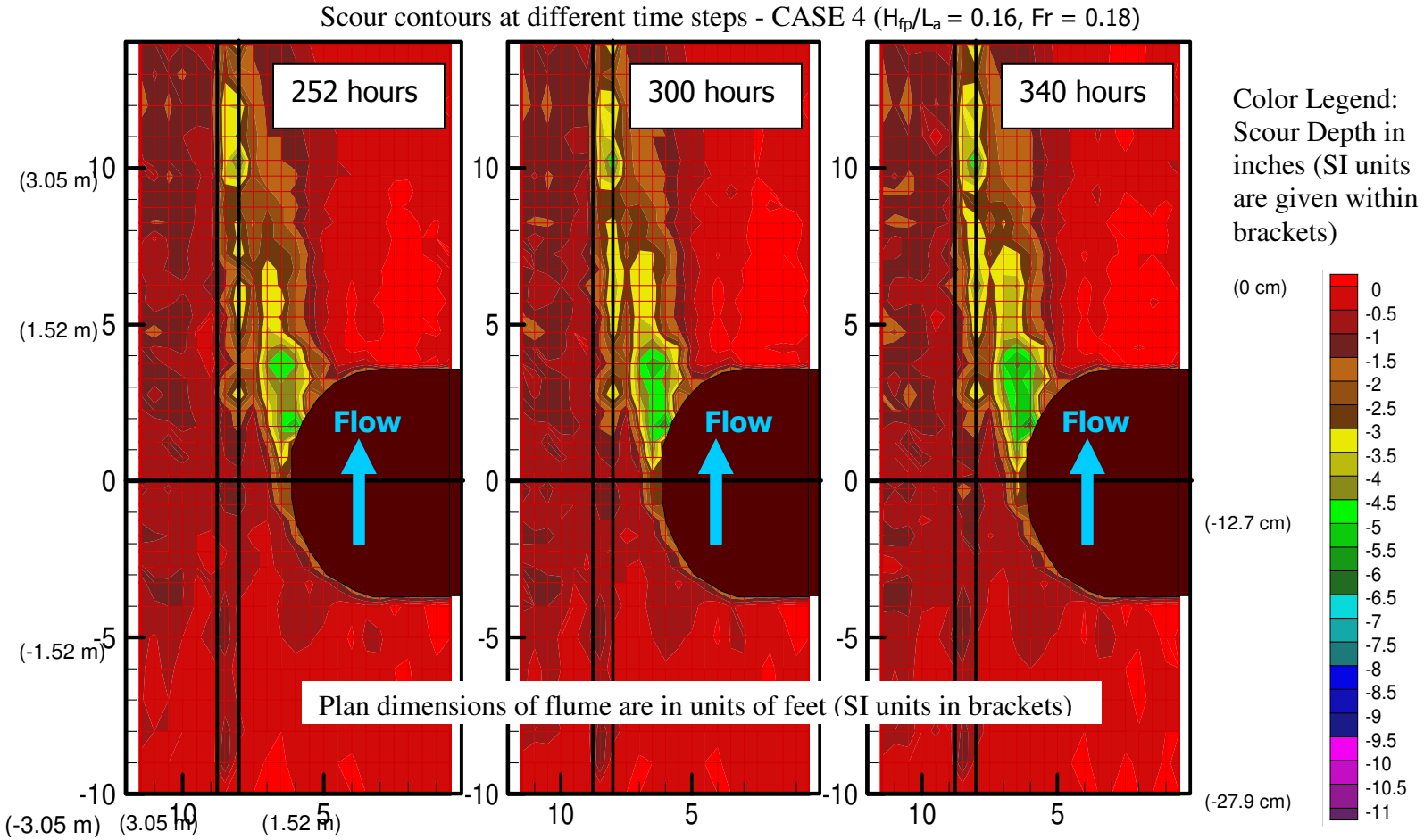

FIG 6.1 (Continued)

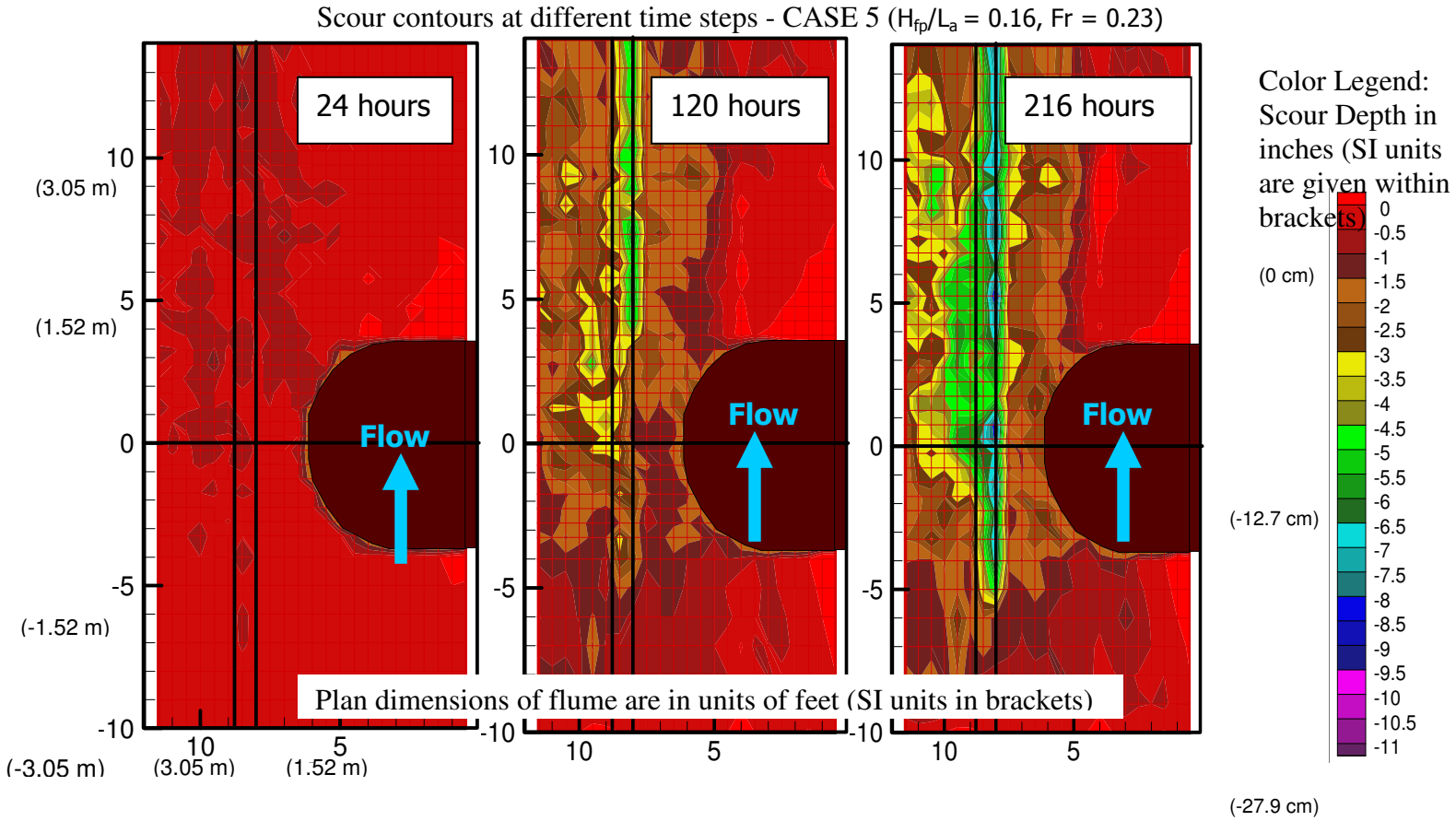

FIG 6.1 (Continued)

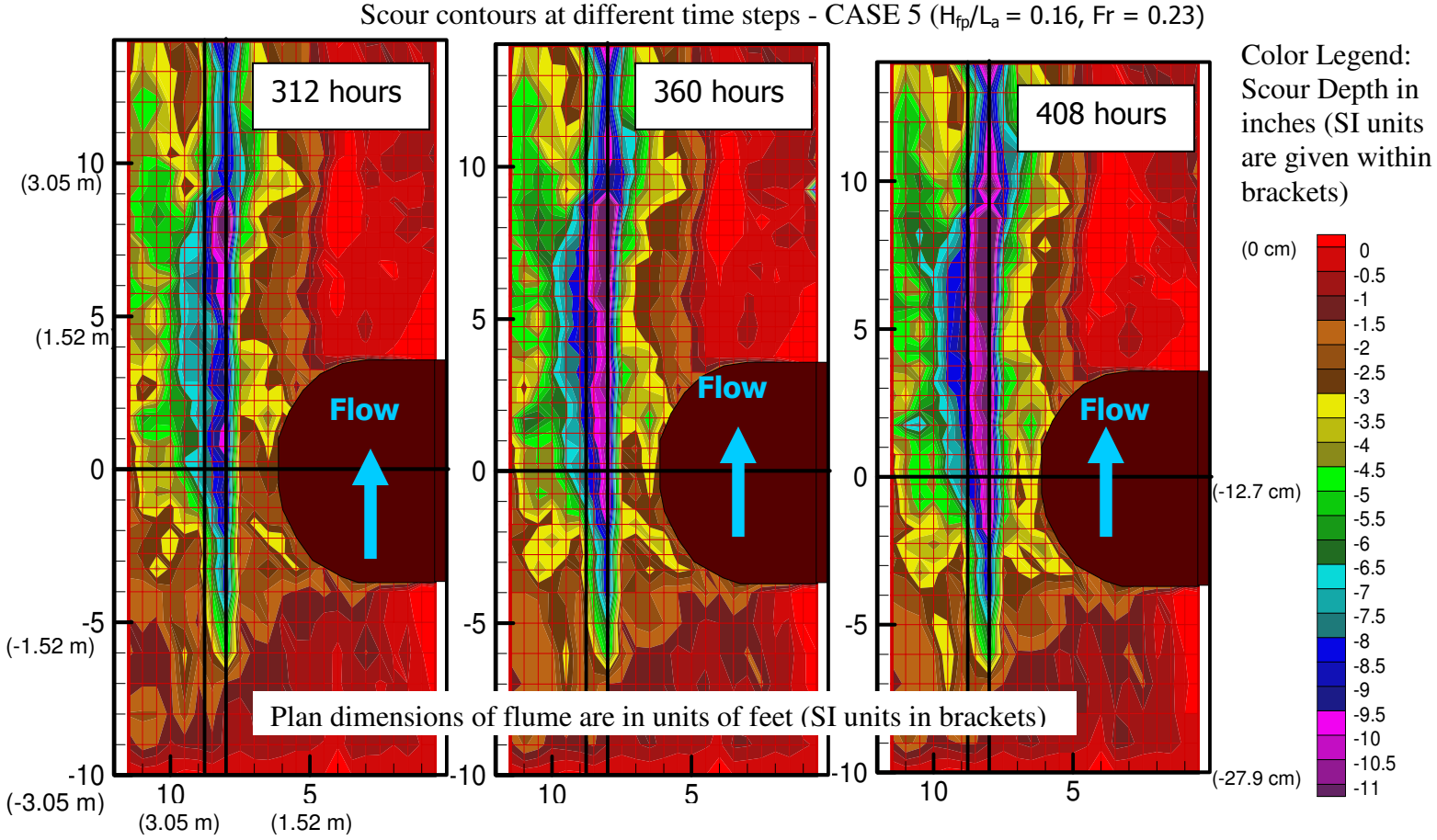

FIG 6.1 (Continued)

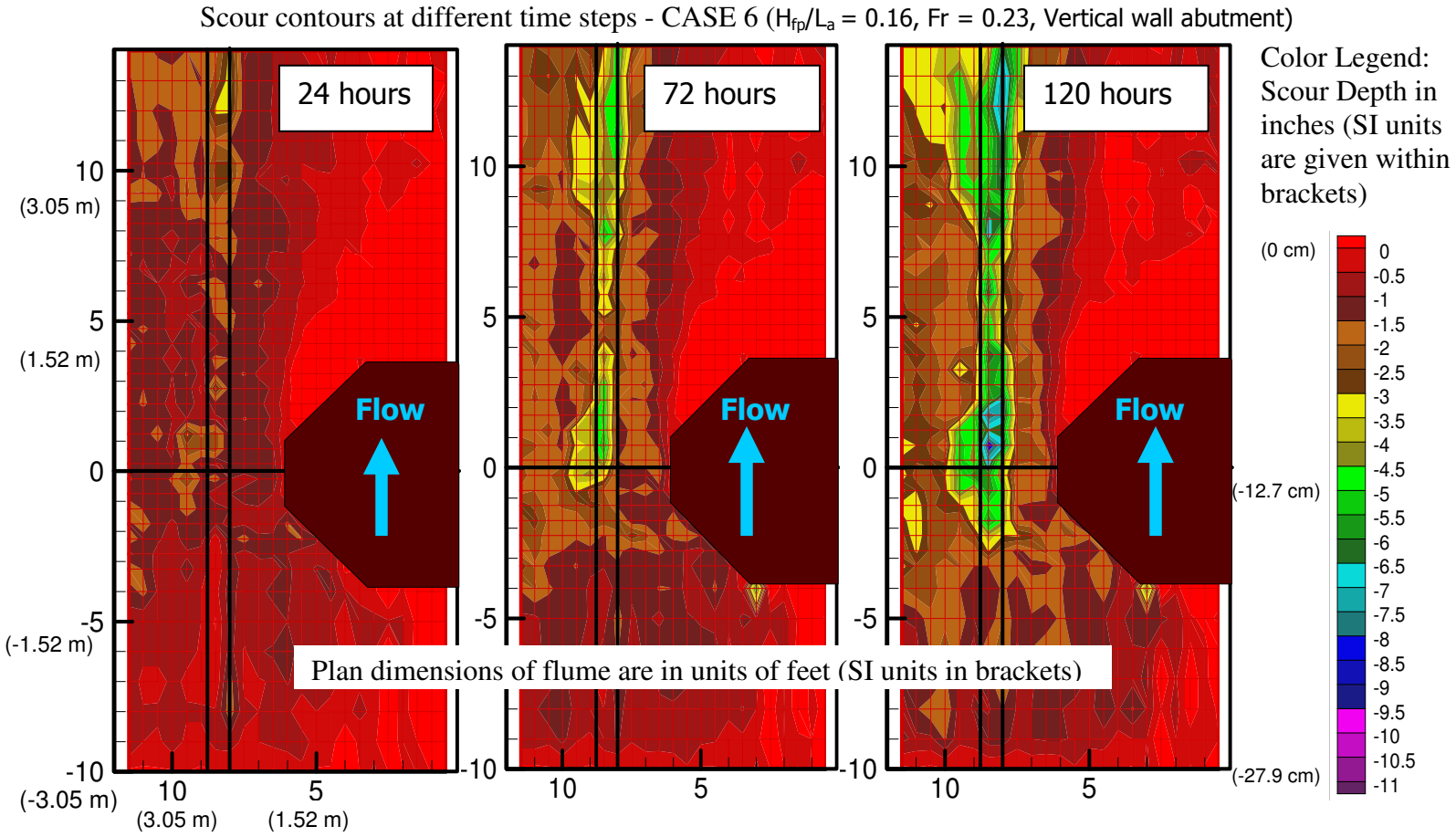

FIG 6.1 (Continued)

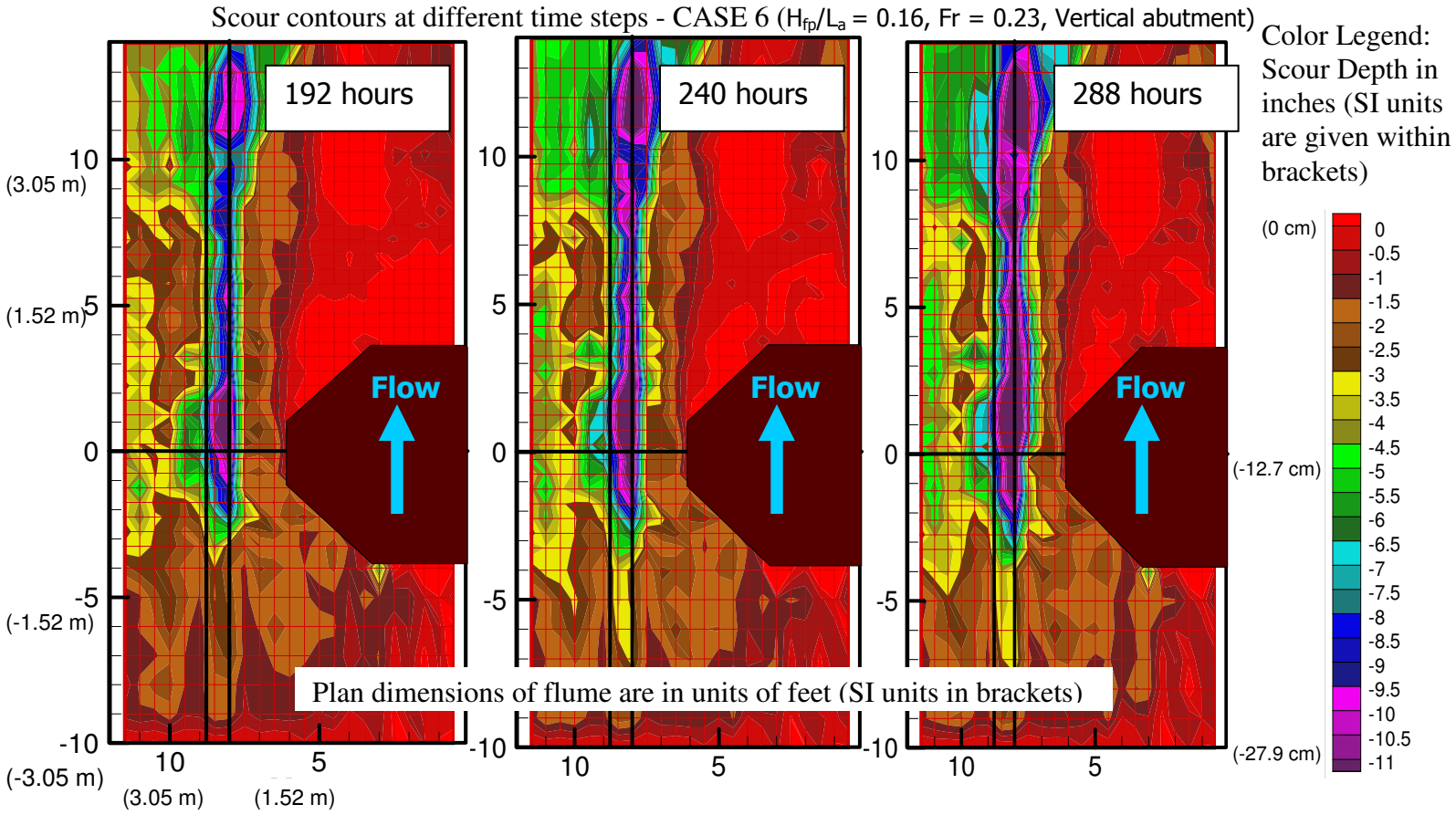

FIG 6.1 (Continued)

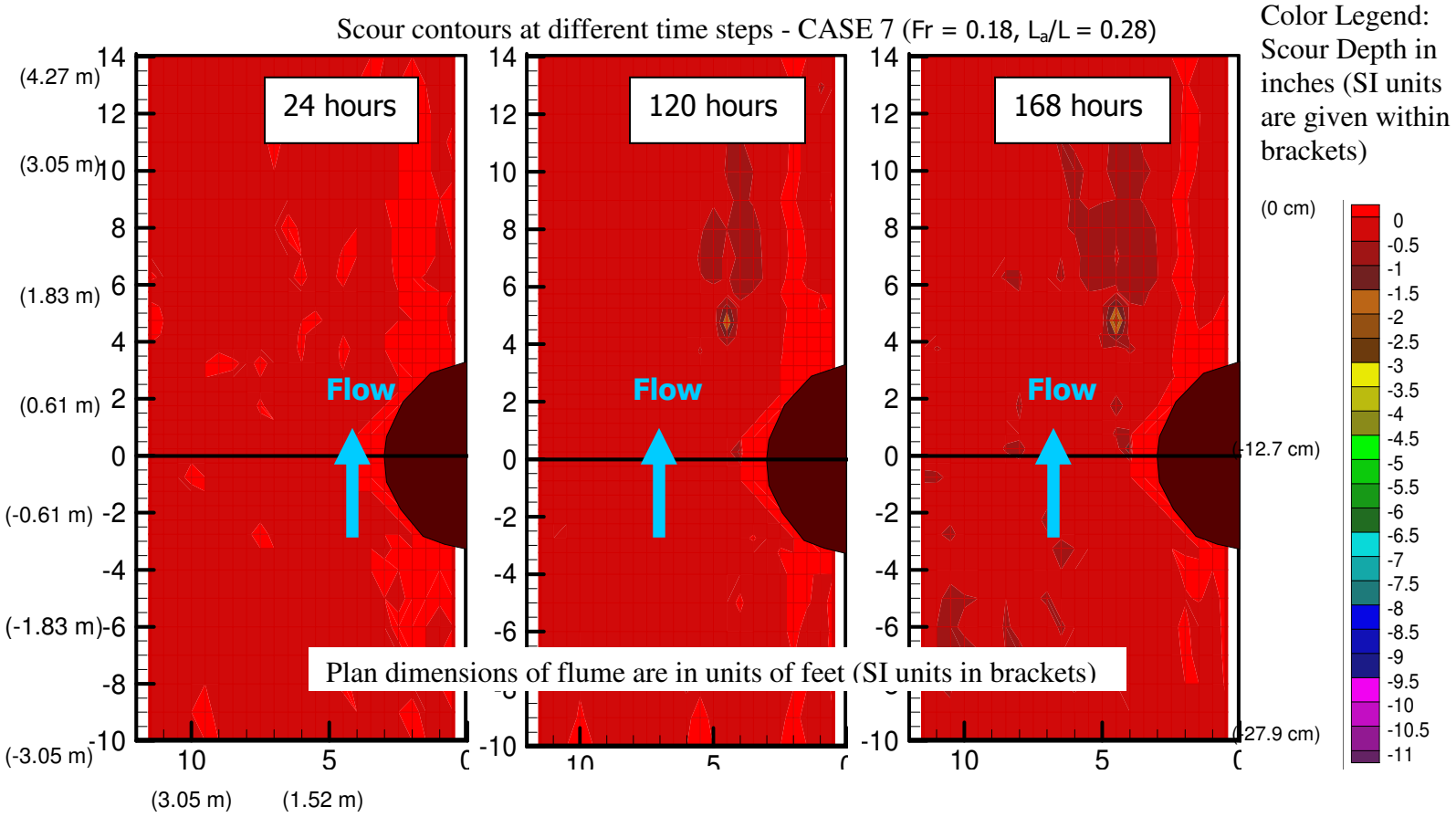

FIG 6.1 (Continued)

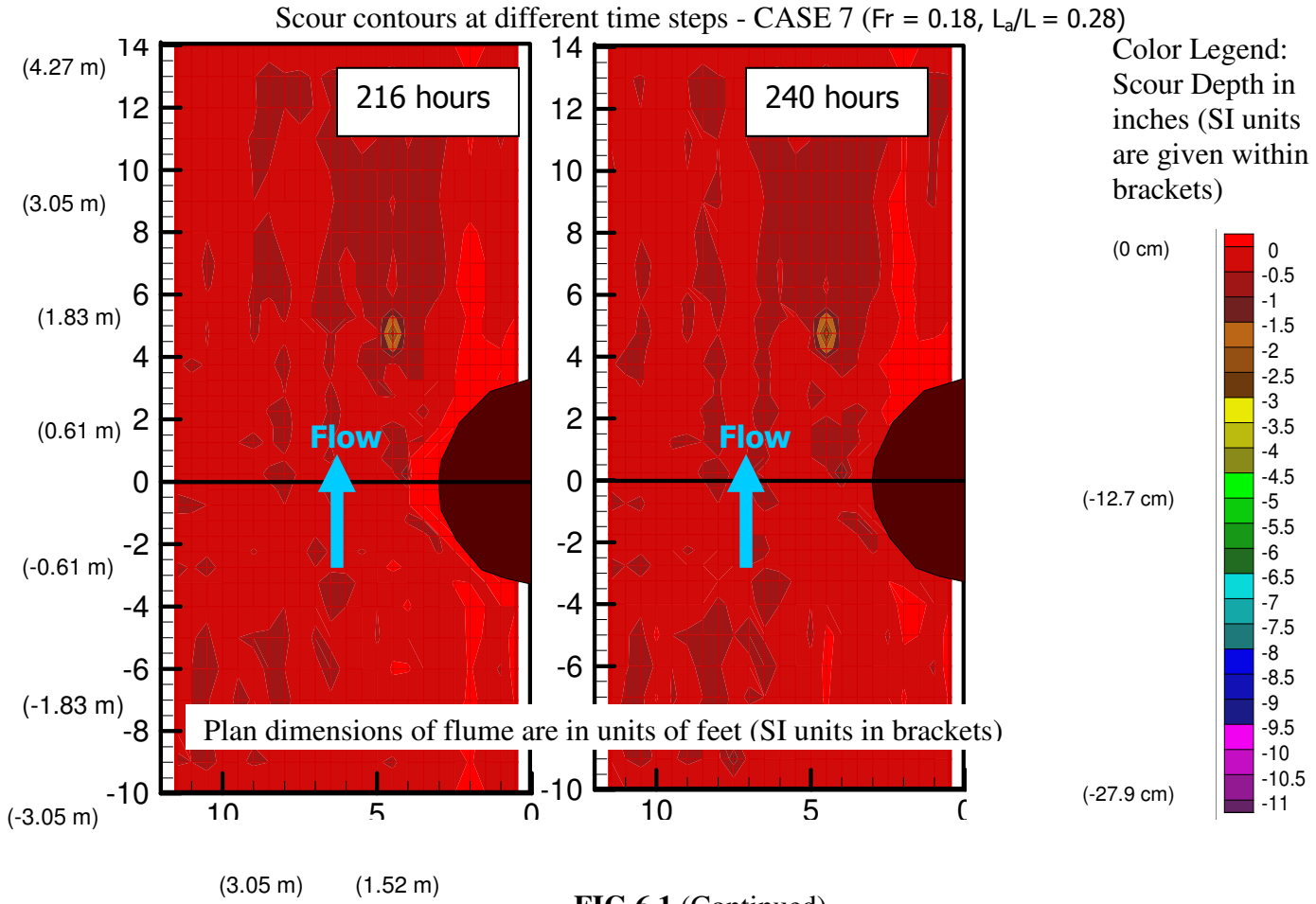

FIG 6.1 (Continued)

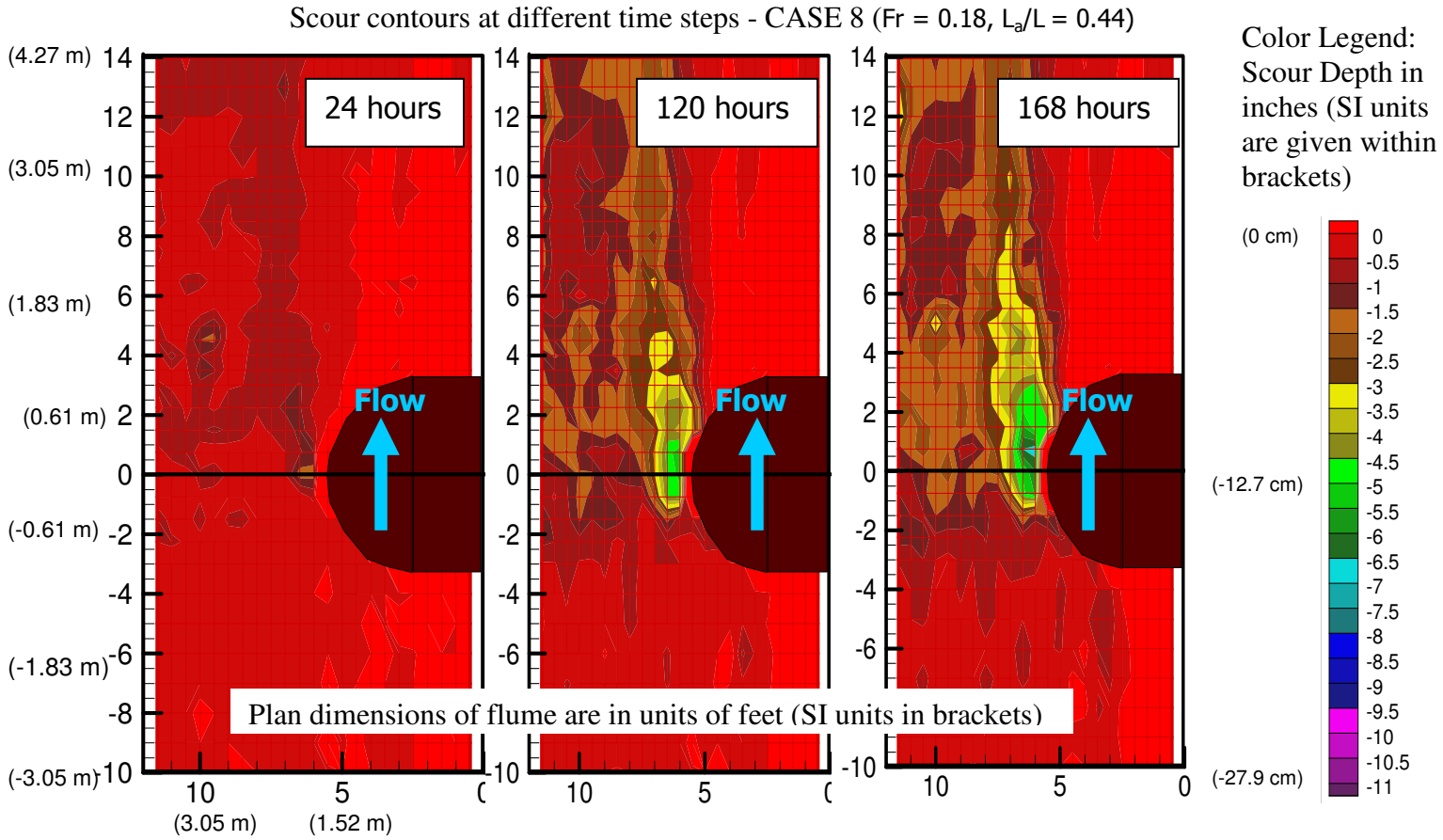

FIG 6.1 (Continued)

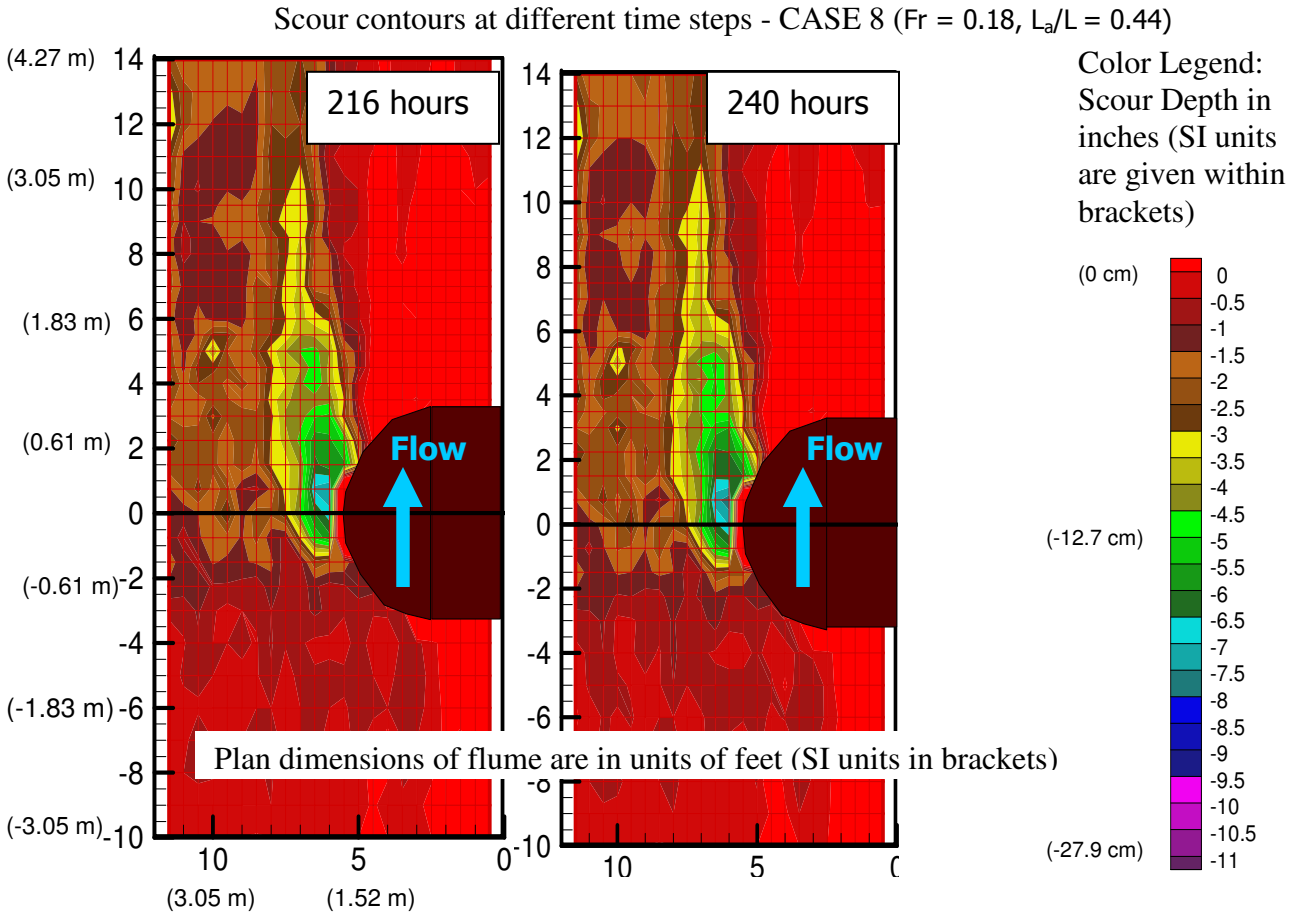

FIG 6.1 (Continued)

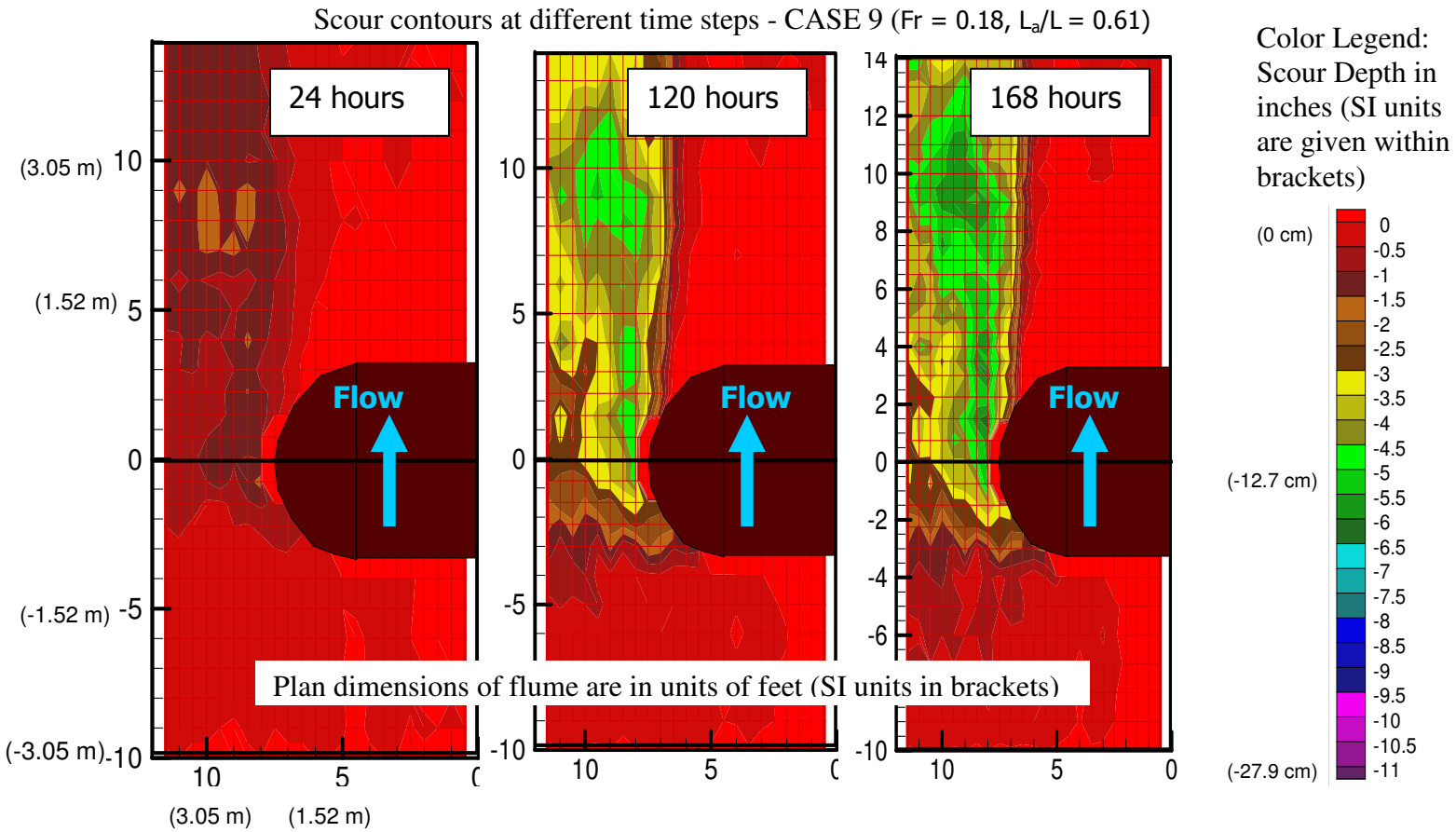

FIG 6.1 (Continued)

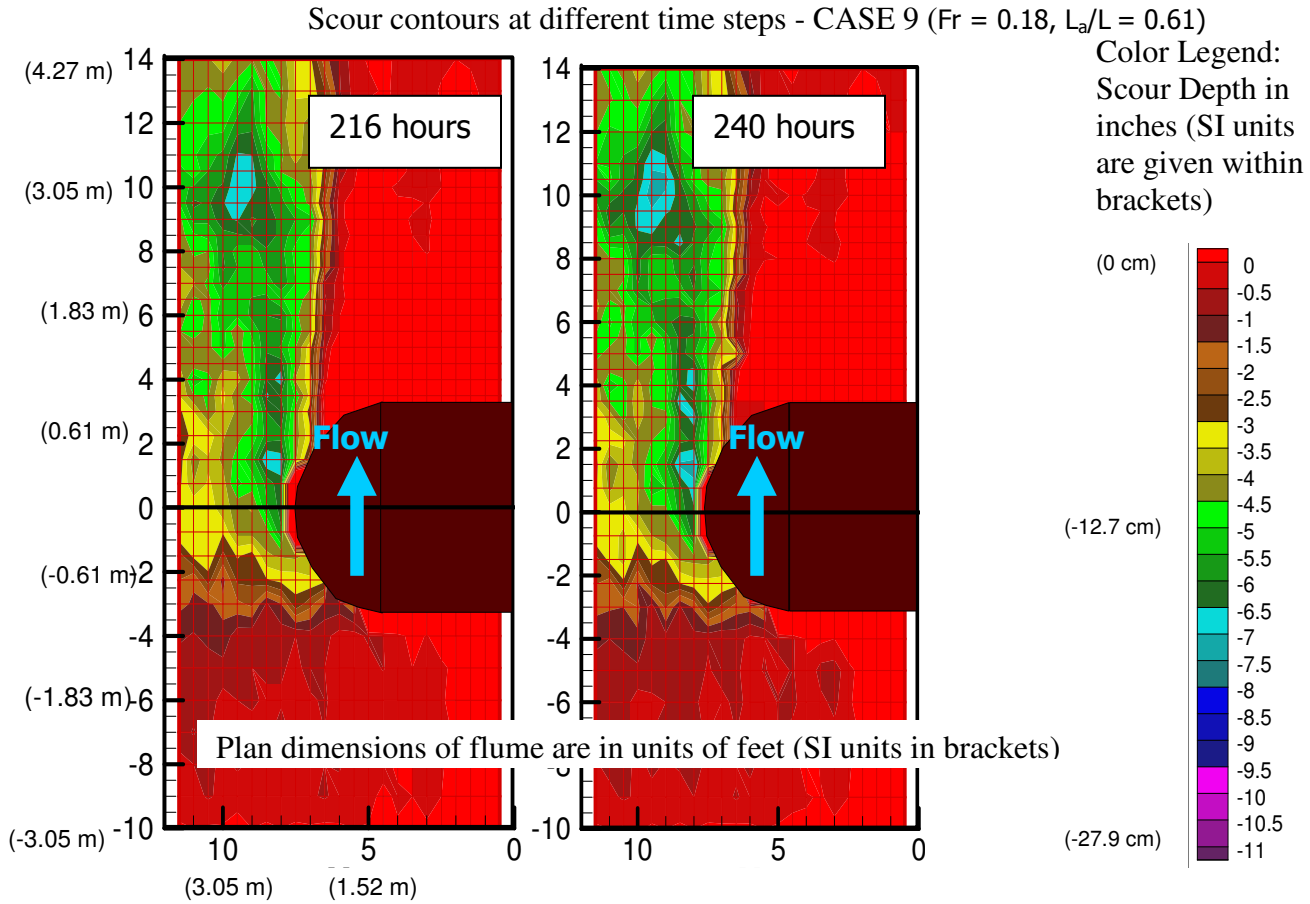

FIG 6.1 (Continued)

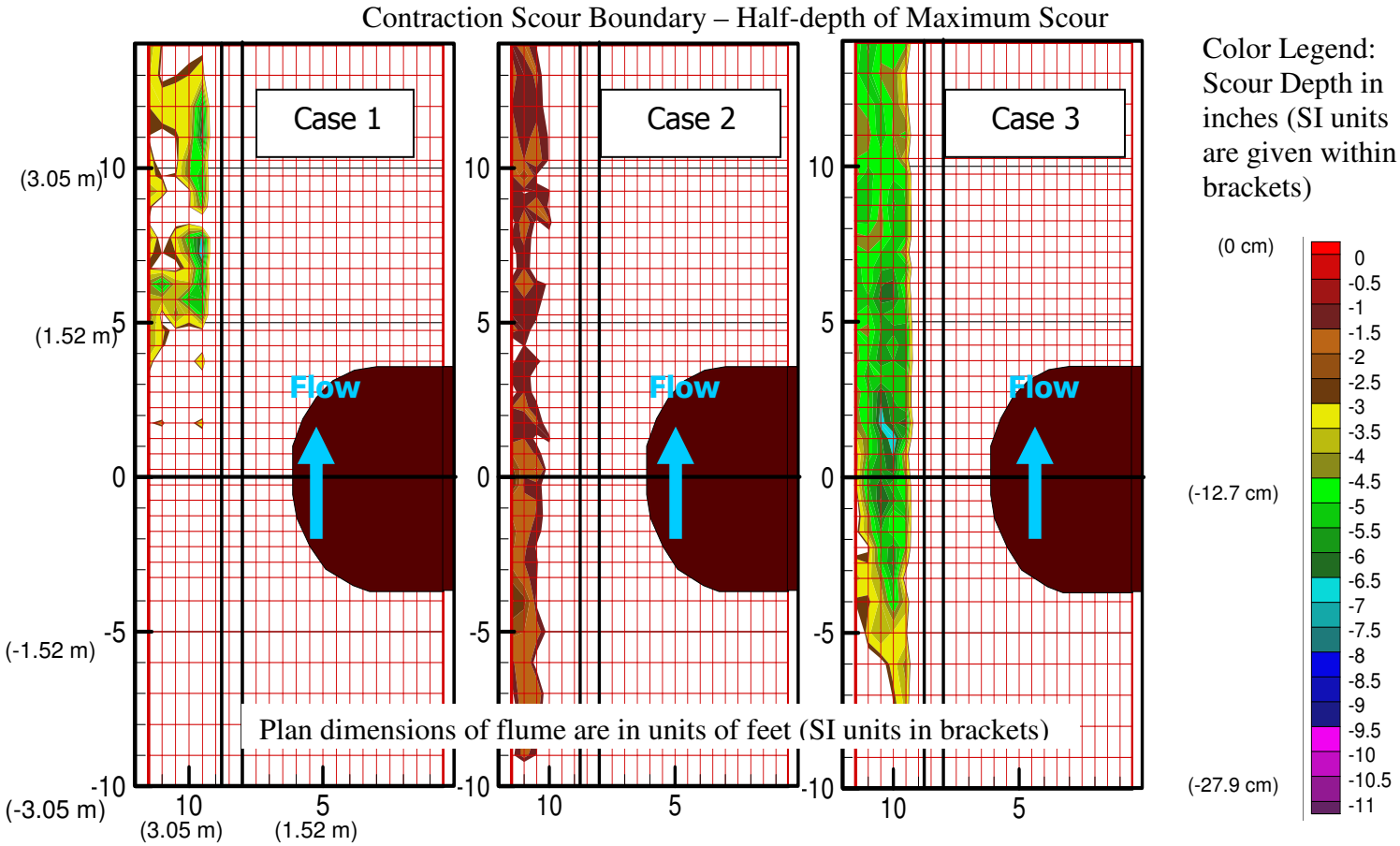

FIG 6.2 Contraction Scour Boundary – Half-Depth Of Maximum Scour

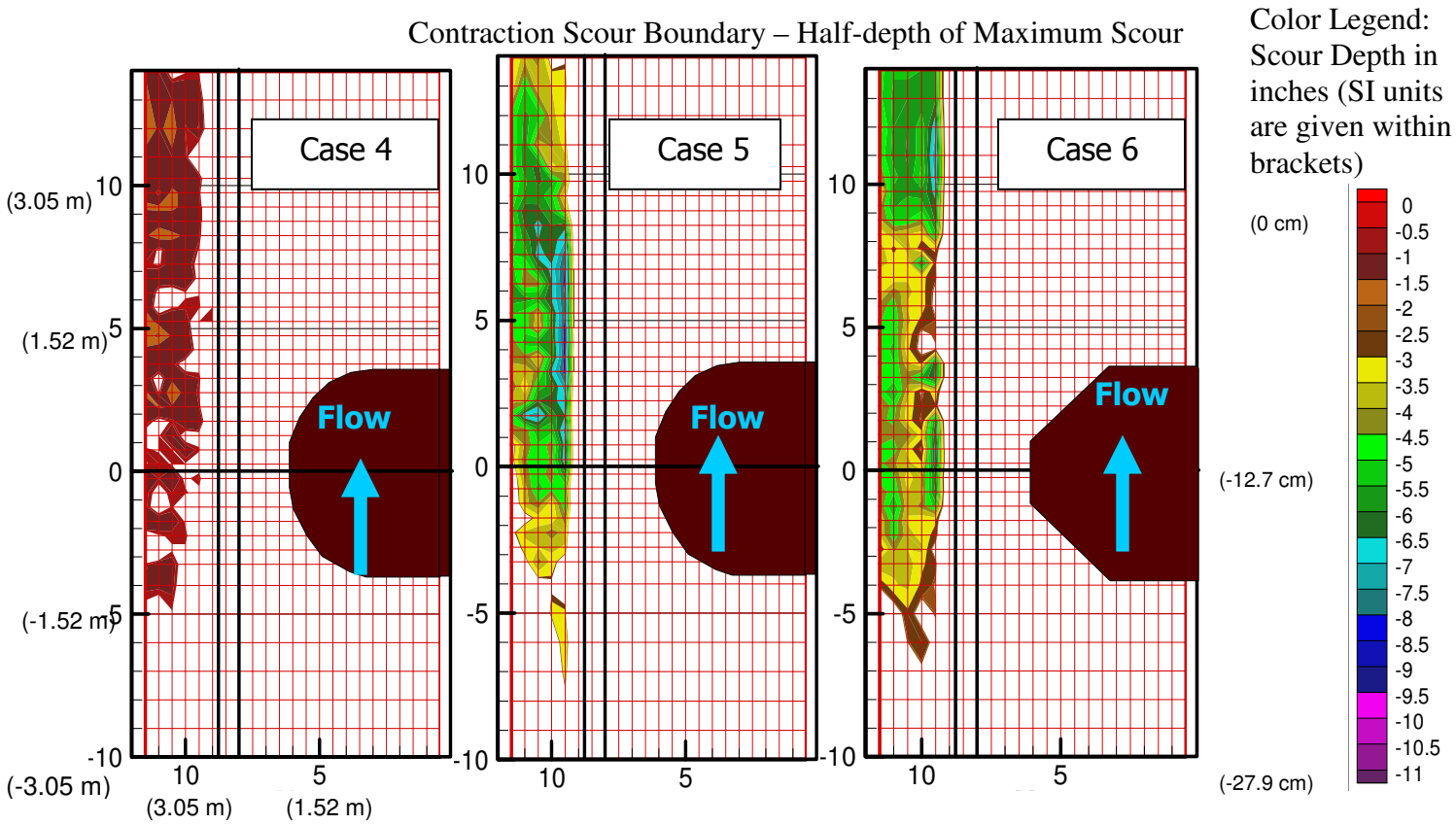

FIG 6.2 (Continued)

For Test Cases 1 to 5, the contraction abutment in the compound channel is provided with a spill-through shaped abutment while the Test Case 6 on the compound channel geometry and the rectangular channel cases from Test Case 7 through Test Case 9 are provided with a wing and vertical wall shaped abutments respectively. Test Case 1 is considered as the reference case whose dimensionless parameters were arrived through a statistical analysis conducted by Briaud et al. of Texas A&M University after conducting a survey of bridge geometries in the United States. Test Cases 1, 2 and 3 simulate the effect of water depth on contraction scour. Test Cases 1, 4 and 5 simulate the effect of flow velocity of contraction scour. Test Cases 1 and 6 study the effect of the shape of the abutment on contraction scour. Test Cases 7, 8 and 9 test analyze the effect of contraction ratio on contraction scour.

Contraction scour in a compound channel is more pronounced near the center line of the channel. With the increase in depth of flow, the scour trend broadens throughout the contraction zone. This is also accompanied by the faster development of a deeper scour hole.

Table 6.1 Results From The Contraction Scour Tests In Compound Channel With Clay Bed

Test Case No.	H_c		Q		V_1		V_2		V_{HEC}		Z_{max}		Z_{unif}		X_{max}	
	(ft)	(m)	(cfs)	(m^3/s)	(ft/sec)	(m/s)	(ft/sec)	(m/s)	(ft/sec)	(m/s)	(inch)	(cm)	(inch)	(cm)	(ft)	(m)
Case 1	1.62	0.49	20.23	0.57	1.44	0.44	2.21	0.67	2.22	0.68	8.13	20.65	3.86	9.80	5.75	1.75
Case 2	1.27	0.39	11.29	0.32	1.17	0.36	1.77	0.54	1.75	0.53	3.53	8.97	2.25	5.72	4.00	1.22
Case 3	1.98	0.60	28.69	0.81	1.58	0.48	2.39	0.73	2.22	0.68	10.17	25.83	5.55	14.10	4.25	1.30
Case 4	1.63	0.50	15.61	0.44	1.12	0.34	1.72	0.52	1.76	0.54	2.87	7.29	3.51	8.92	4.75	1.45
Case 5	1.63	0.50	23.37	0.66	1.67	0.51	2.56	0.78	2.64	0.80	10.62	26.97	5.31	13.49	4.00	1.22
Case 6	1.63	0.50	26.79	0.76	1.91	0.58	3.26	0.99	3.46	1.05	8.42	21.39	4.84	12.29	3.75	1.14
Case 7	1.20	0.37	15.15	0.43	1.06	0.32	1.47	0.45	1.47	0.45	2.2	5.59	0.72	1.83	2.75	0.84
Case 8	1.22	0.37	15.27	0.43	1.04	0.32	1.87	0.57	1.86	0.57	5.66	14.38	2.45	6.22	4.00	1.22
Case 9	1.23	0.37	14.69	0.42	0.99	0.30	2.54	0.77	3.00	0.91	8.29	21.06	4.36	11.07	3.00	0.91

Comparison between the contour plots of scour between the Test Cases 1 and 6 (Effect of the shape of the abutment) show the interesting fact that there is no scour near the toe of the abutment in case of a vertical wall abutment. This could be the result of the portion of flow from the flood plain getting harshly deflected into the main channel owing to the shape of the vertical wing wall contraction abutment.

An increase in contraction ratio increases the depth and extent of the contraction scour hole. This has also been observed by the previous researchers (Laursen, 1960; Li, 2002). Though a very harsh contraction combines the effect of contraction scour and abutment scour near the upstream tow of the contraction abutment, there is a well-

marked delineation between contraction and abutment scour patterns in mild contractions as abutment scour occurs localized around the abutment while contraction scour is more towards the center of the channel and extends longer than abutment scour.

Figure 6.3 shows the influence of contraction ratio on contraction scour profile. Figure 6.4 shows the influence of approach velocity on contraction scour profile. Figure 6.5 and Figure 6.6 show the influence of water depth and abutment shape, respectively on contraction scour development. Detailed Tables showing the development of the maximum depth scour hole with time have been given in Appendix C.

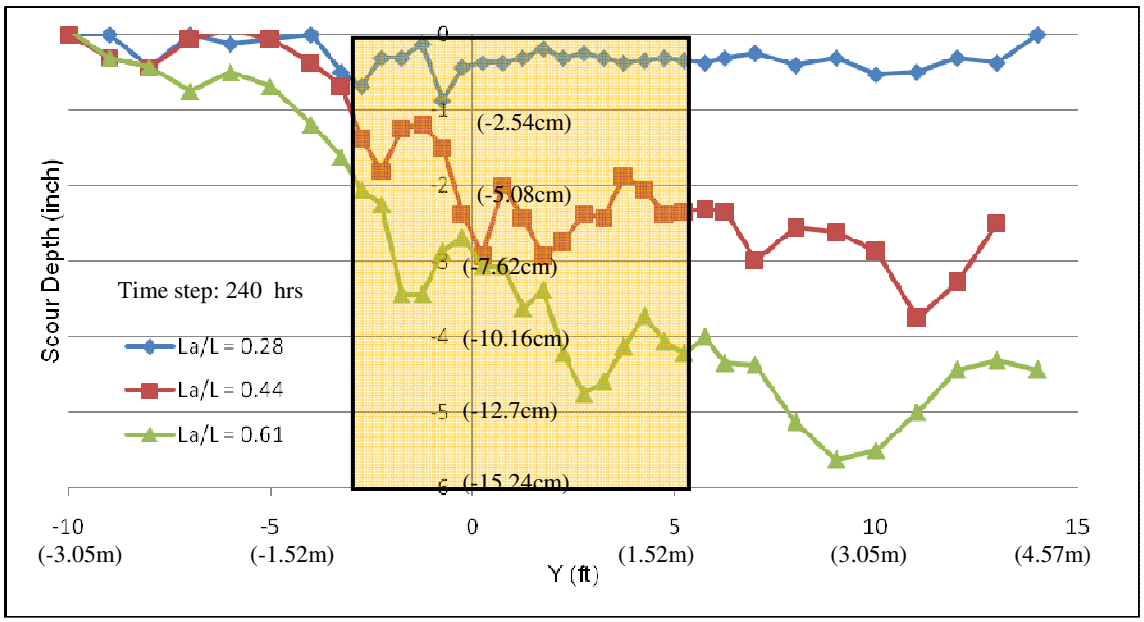

FIG. 6.3 Influence Of Contraction Ratio On Contraction Scour Profile

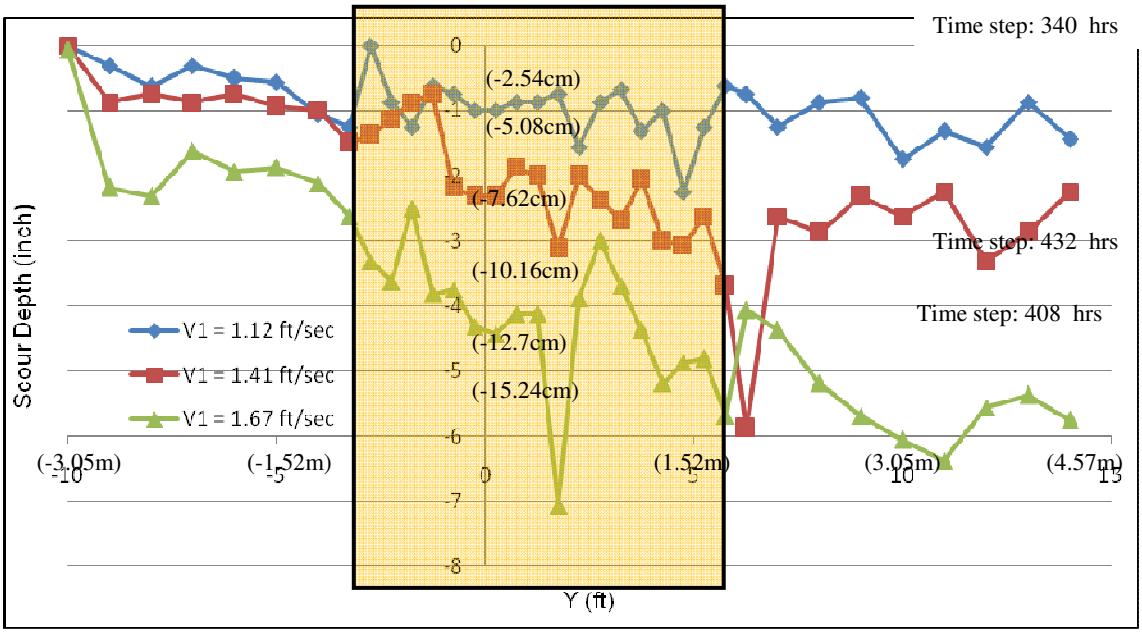

FIG. 6.4 Influence Of Approach Velocity On Contraction Scour Profile

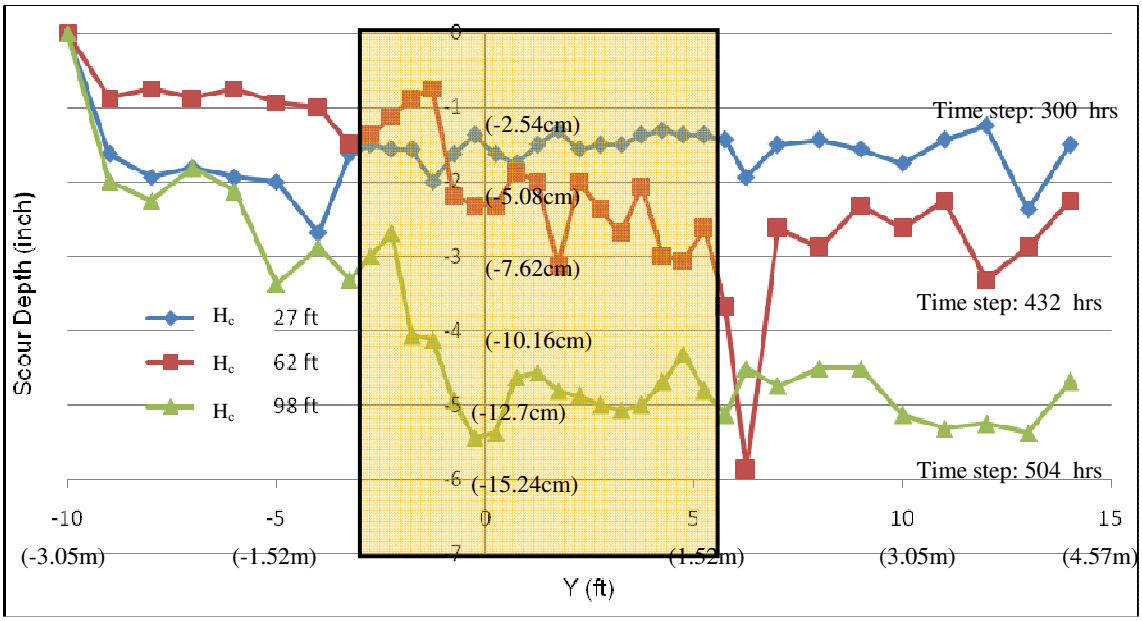

FIG. 6.5 Influence Of Water Depth On Contraction Scour Profile

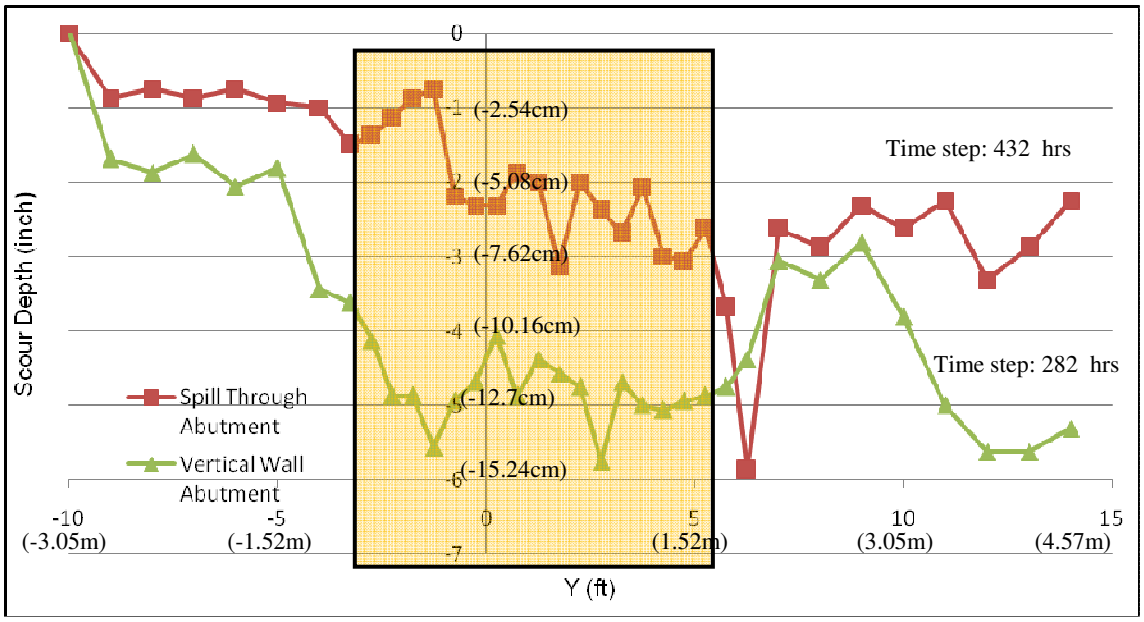

FIG. 6.6 Influence Of Abutment Shape On Contraction Scour Profile

6.4 FLOW VELOCITY AND WATER DEPTH

Flow velocities at the various grid points were obtained from the Advanced Doppler Velocimeter measurements. A contour plot of the velocities in Test Case 2 and Test Case 3 at the start of the flume tests have been shown in the Figure 6.7. The changes in velocities at different longitudinal sections at the contraction zone have been shown in the Figure 6.8.

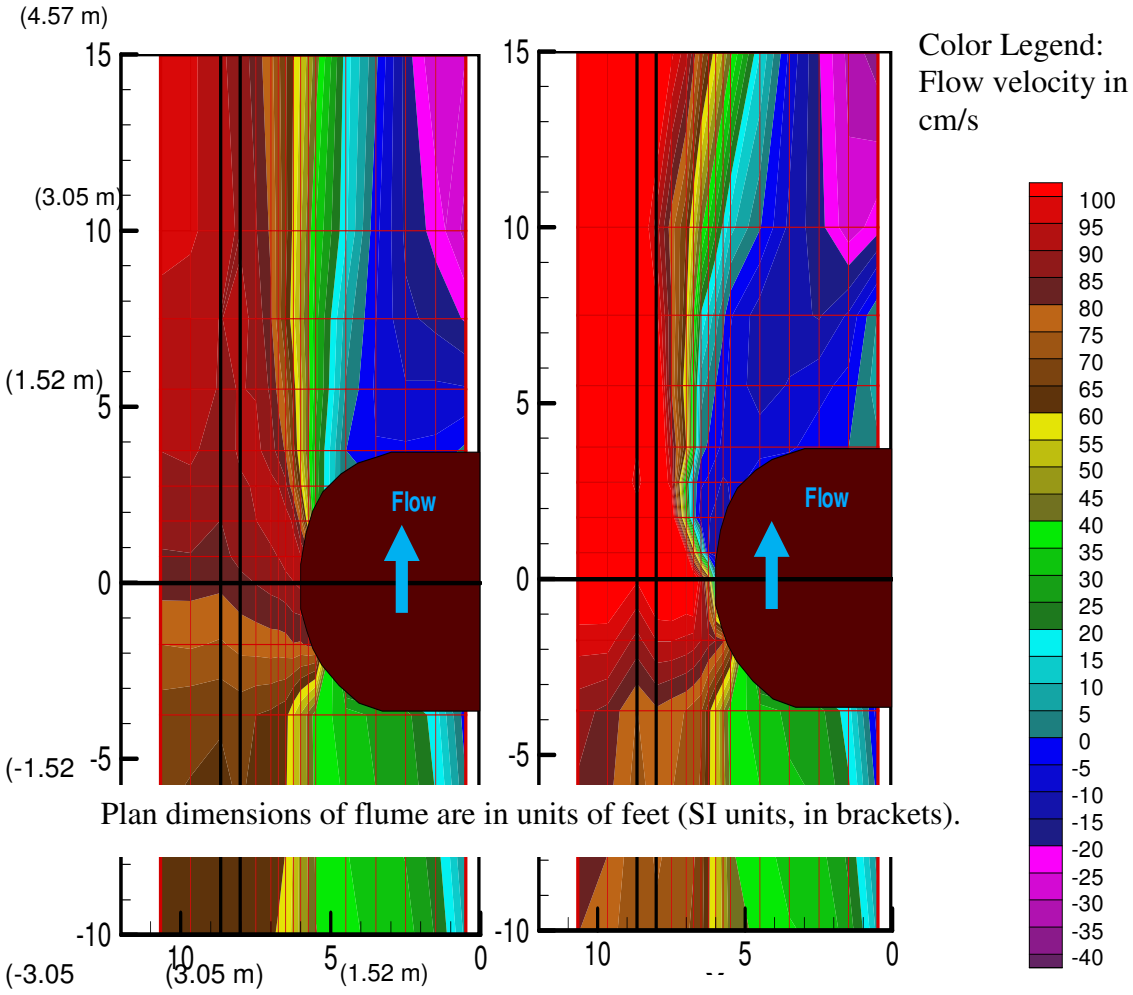

FIG 6.7 Velocity Contours At The Start Of Test Cases 3 And 5

A reverse circulation in the downstream side of the contraction abutment gives rise to negative velocities just downstream of the abutment. In all the test cases, velocity increases rapidly near the abutment contraction and particularly near the toe of the abutment and gradually slows down as the waters move downstream. There is no uniform increase across the center of the abutment section. This again reinforces the fact

that the mixing of flood plain waters in to the main channel waters gives rise to the sudden increase of flow velocity causing enormous erosive forces near the soil bed.

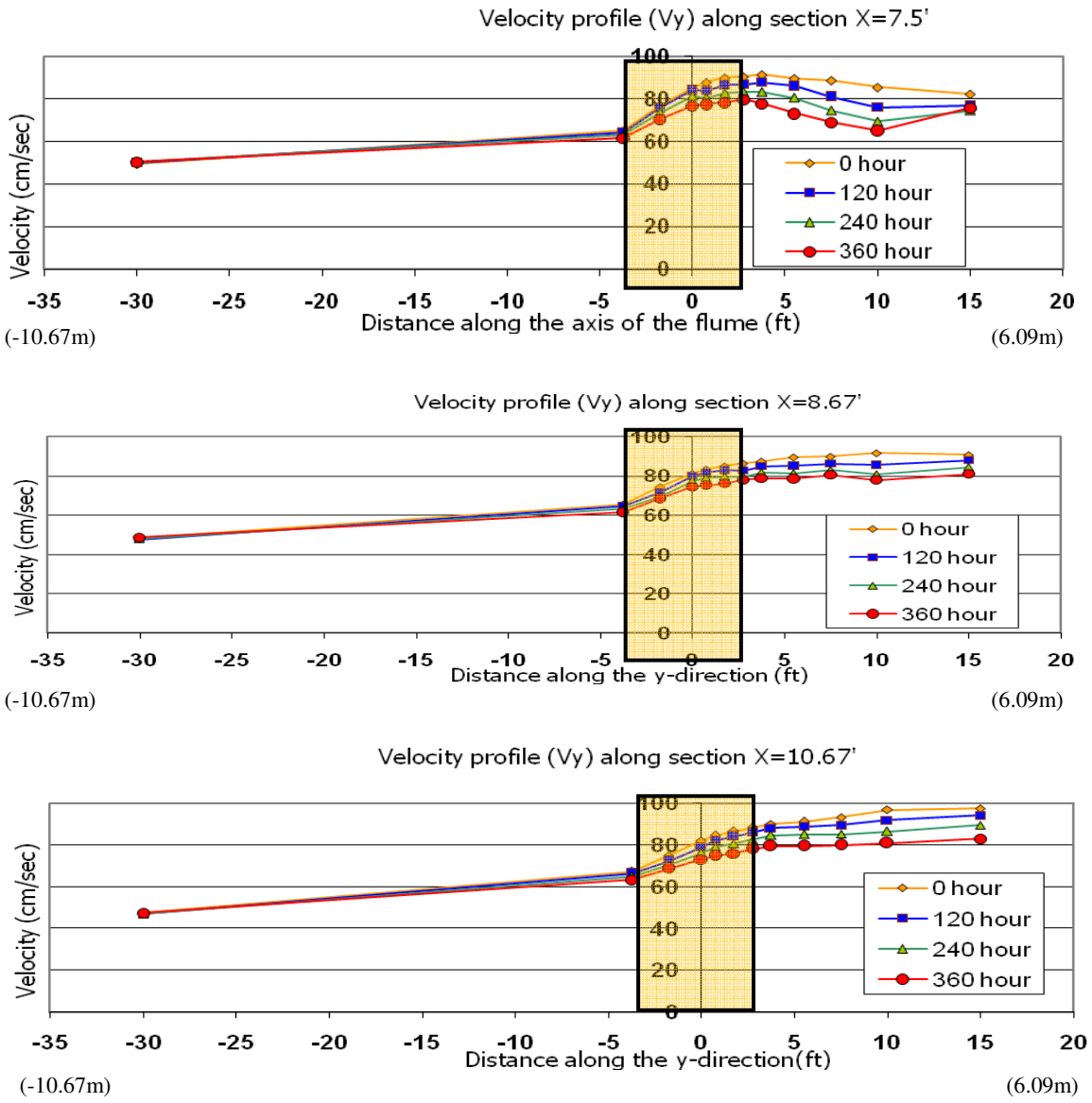

FIG 6.8 Longitudinal Velocity Profiles At The For Test Case 3

A plot of the vorticity of flow near the abutment from the velocity data shows the amount of flow "rotation" that takes place around the contraction section. Figure 6.9 shows the vorticity pattern observed in Test Case 3 of the flume tests. It is to be noted that there is a clear recirculation pattern that takes place just downstream of the abutment (shown in the figure with blue contours) signifying the introduction of a rotational motion which could give rise to local abutment scour.

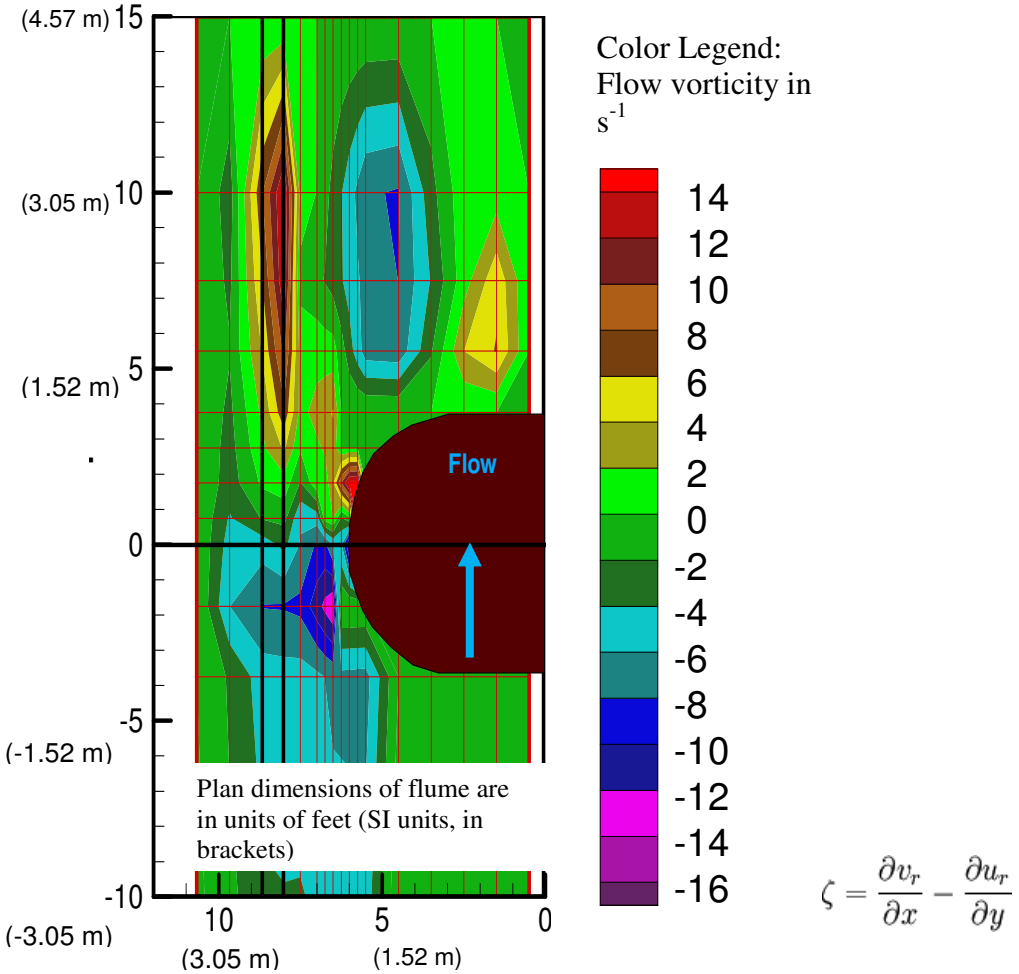

FIG 6.9 Vorticity Plot For Test Case 3

In the above equation, ζ gives a measure of vorticity, which is obtained from the difference between the change in velocity components along the longitudinal and transverse directions.

The water surface elevation drops near the contracted zone for the compound channel tests, which has been observed by previous researchers in rectangular channels (Laursen 1960, Komura 1966) as well. Also, the water depth is found to rise at the contracted section with time and tends to get equal with the upstream water level. This is in agreement with the findings of Li (2002) for a simple rectangular channel with cohesive soil bed. Since the flow in the channel is subcritical, downstream control exists suggesting the changes in the water surface elevations could be the result of the development of scour in the downstream side of the contraction zone. Figure 6.10 shows the change in water surface profiles at different time steps for Test Case 15.

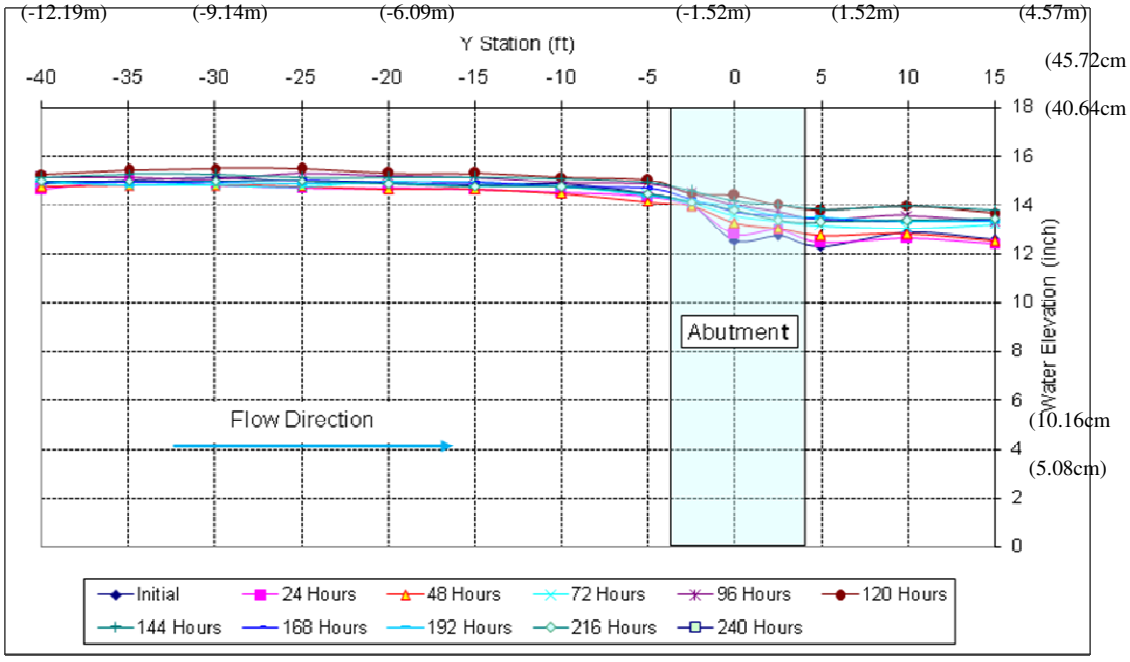

FIG 6.10 Water Surface Profile At Different Time Steps For Test Case 15

With respect to the velocity in the contracted zone, there is a tendency for the velocity to decrease gradually with the development of scour. This is also in confirmation with what Li (2002) observed in the rectangular channel with cohesive soil bed. It is also observed in the compound channel that the highest velocity and the lowest water surface elevation occur roughly at the same downstream location confirming the validity of the flow continuity assumptions.

6.5 HEC RAS

In order to expand the usage of this present methodology to predict scour in prismatic compound channels to channels with irregular cross sections, the population

1 dimensional flow simulation program HEC RAS is used to simulate the present test conditions. A comparison between the HEC RAS simulated flow parameters for the same discharge and flow geometry against the flume test measurements helps in identifying the differences in prediction based on the software program and the actual flow parameters. Fgure 6.11 shows the comparison of HEC-RAS predicted flow velocities the measured velocities from the flume tests at the contraction section for different test cases. It is observed that HEC RAS predictions are closer to the actual averaged velocities at the contraction section for the compound channel tests than the rectangular channel cases. It is also observed that HEC RAS was not found to be very sensitive to variations in water depth. A stepped increase or decrease in the water surface elevations was observed in all the test cases.

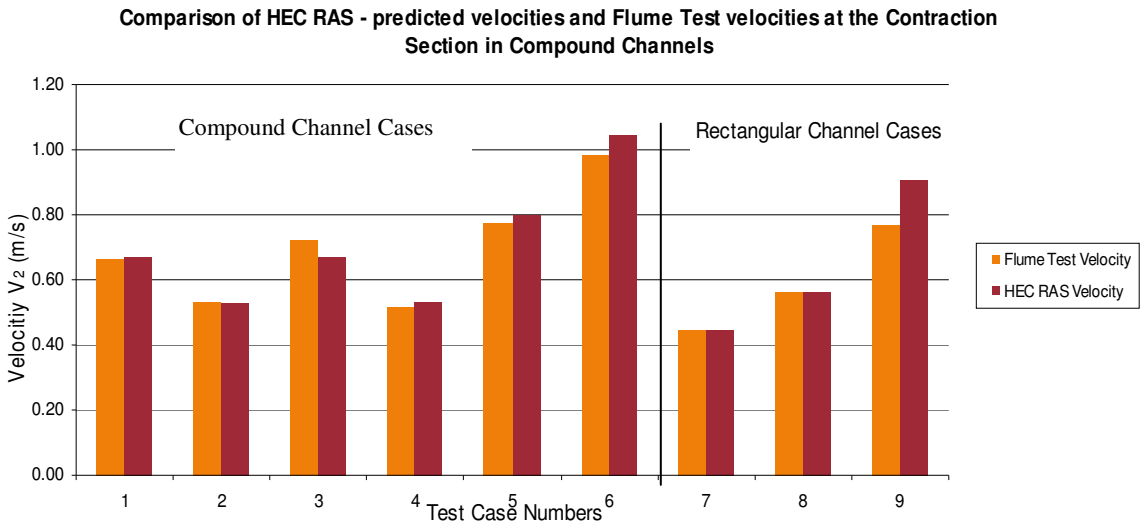

FIG 6.11 Comparison Of HEC RAS Predicted Velocities And Flume Test Velocities

Though a close prediction of flow velocities to the actual measured flow velocities was observed in HEC RAS, a correction factor of 1.02 is proposed to achieve better regression values while comparing the HEC RAS predicted the velocities and the actual velocities measured from flume tests for compound channels.

Figure 6.12 shows the comparison plot between HEC RAS predicted velocities and the actual measured velocities.

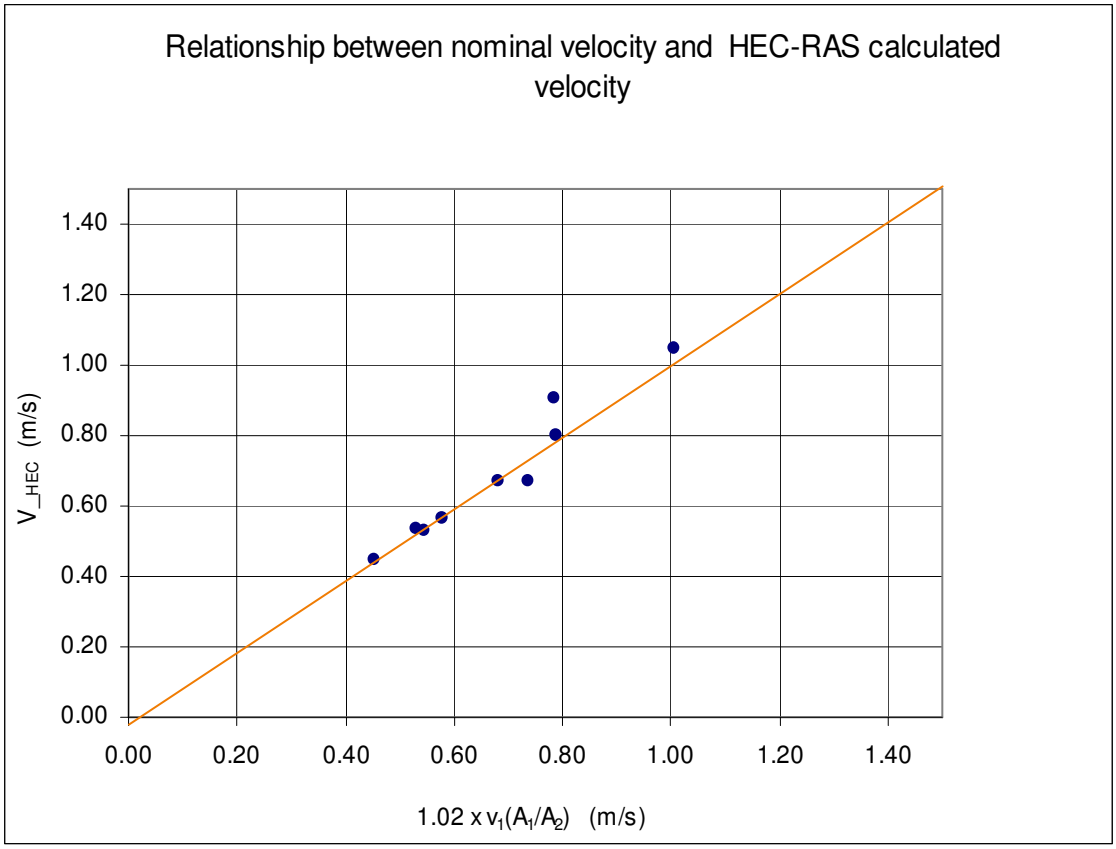

FIG 6.12 Relationship Between HEC RAS Estimate Of Velocities And Flume Test Velocities

$$V_{HEC} = 1.02 \text{ x } V_1 \ (A_1/A_2) \tag{6.1}$$

The test results from all the cases have been given in the Table 6.1. From the hyperbolic model results, the scour values are extrapolated to arrive at maximum scour values.

The focus has been on three characteristics in compound channel contraction scour namely the maximum scour depth (Z_{max}), the uniform scour depth (Z_{unif}) which extends both in the upstream and well as downstream sides of the maximum scour hole and the distance to the maximum scour hole from the center of the contraction section (X_{max}).

CHAPTER VII

METHODOLOGY DEVELOPMENT AND SCOUR PREDICTION

7.1 BACKGROUND

New methodologies are developed based on the results of flume tests and observations as detailed in Chapter 6. To evaluate the effects of different flow parameters in the development of scour, critical shear stress is employed as the resistive parameter against scour. This new methodology predicts all the three important characteristics namely the maximum scour depth, its location and also the uniform scour depth. A procedure to construct a complete geometry of the scour hole in a compound channel is also described. Equations to predict scour are also modified to include HEC-RAS predicted flow parameters in order to arrive at scour depths without any field measurement of flow parameters at the contraction section. Finally, a verification study of the proposed methodology is carried out to check its applicability to real life stream data.

7.2. MAXIMUM SCOUR DEPTH

The major advantage of this research on contraction scour in compound channels is that it identifies the maximum scour hole and distinguishes it from the uniform scour depth. The maximum scour depth (Z_{max}) is the depth of scour hole in the contraction zone. The contraction zone can be identified from the flow lines near the contraction zone. Figure 7.1 shows the flow lines around the contraction section which converge toward the center of the channel. These flow lines converge upto a certain distance (or vena contracta) and diverge again.

The boundary for contraction scour can be delineated from the streamline tangential to the contraction abutment for there is no particulate transfer across a stream line. According to Li (2002), the maximum scour depth is more critical than the uniform scour depth for two reasons.

(1) The maximum scour depth represents the most severe scour and therefore is of more critical importance to the bridge foundation evaluation.

(2) The maximum scour hole is closer to the contraction inlets and bridge piers are abutments are in its influence zone.

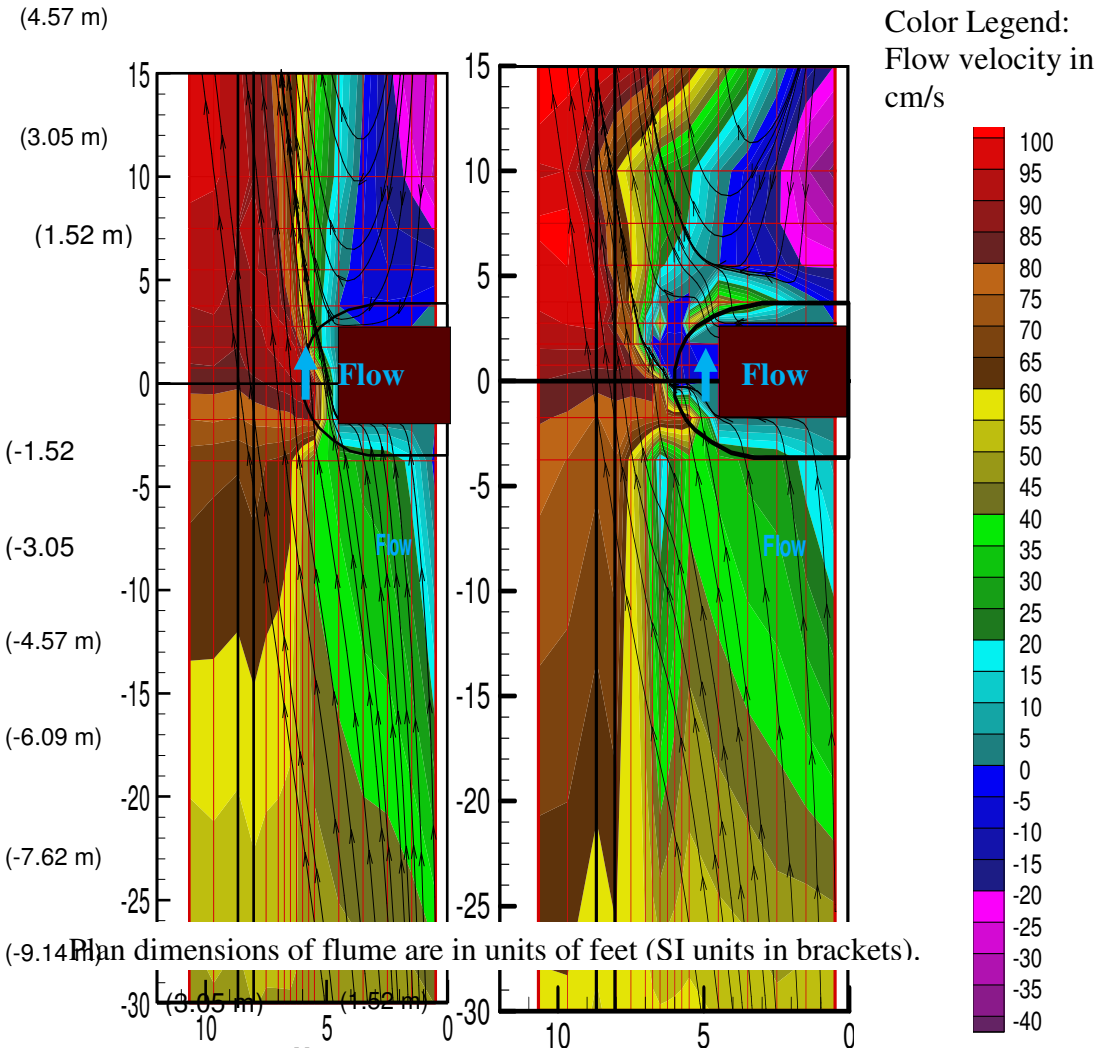

FIG 7.1 Velocity Stream Line Plots For Test Cases 3 And 5

Earlier findings by Li (2002) on contraction scour in cohesive soils for a rectangular channel indicate that Froude number is found to be a better correlation factor compared to Reynolds number. This research compares the relationship between the

maximum scour depth with the Froude number in the contraction section for a compound channel. Figure 7.2 shows the different geometrical parameters at the contracted section of the channel.

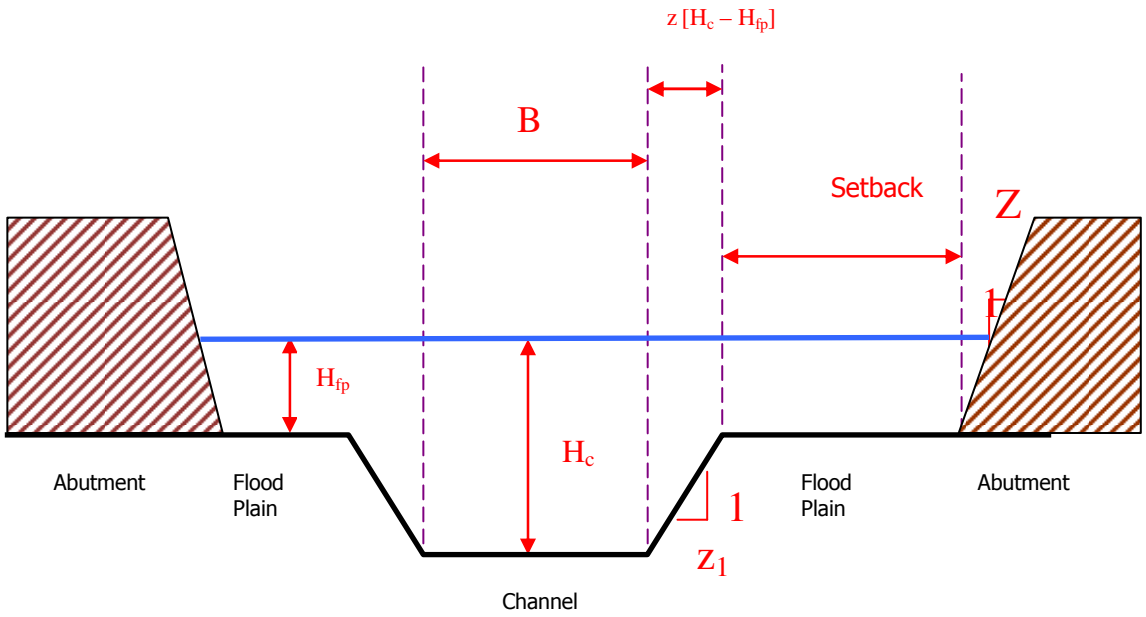

FIG 7.2 Geometry Of The Contracted Section

A relationship between the scour depth and Reynolds number has been evaluated in the following Figure 7.3. It is found that Reynolds number does not correlate well with the observed scour depths of the maximum scour hole and the uniform scour zone.

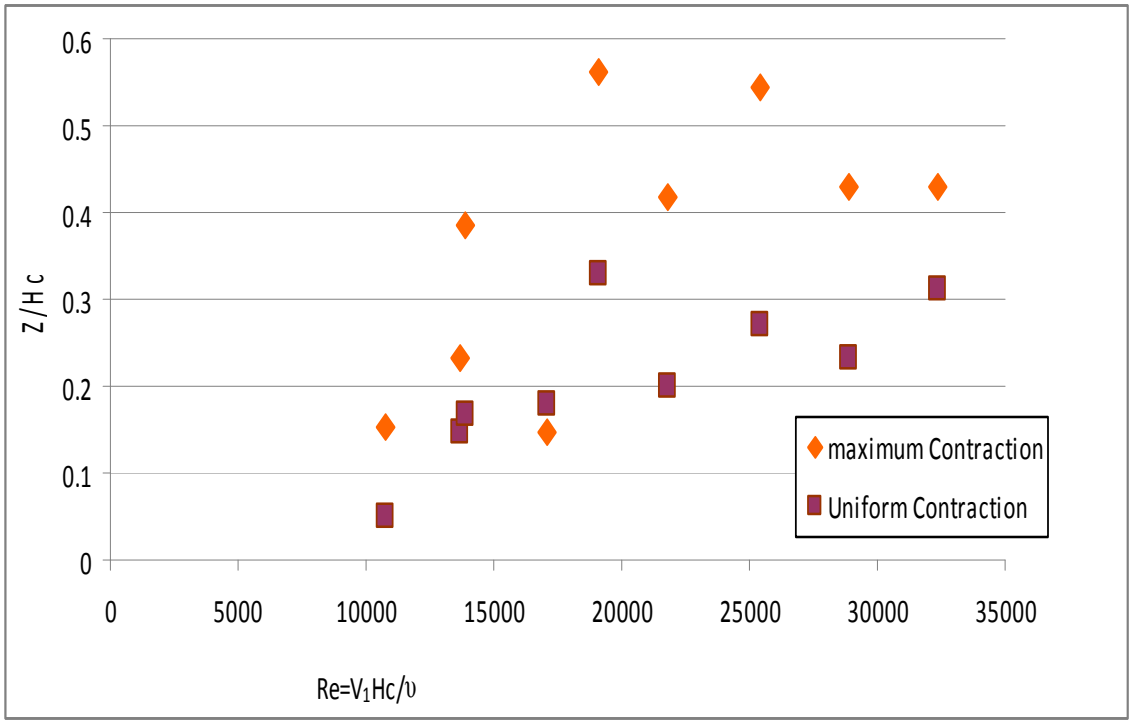

FIG 7.3 Correlation Of Scour Depth Against Reynolds Number

Figure 7.4 shows the relationship between maximum scour depth and Froude number in the contraction section (Fr) and the critical Froude number (Fr_c) for a given flow geometry and soil condition.

$$\alpha_1\left\{\frac{\beta_1 V_2}{\sqrt{gHc}}-\frac{\left[\frac{\tau_c}{\rho}\right]^{\frac{1}{2}}}{gnHc^{\frac{1}{3}}}\right\}\times[M]^{\gamma}$$

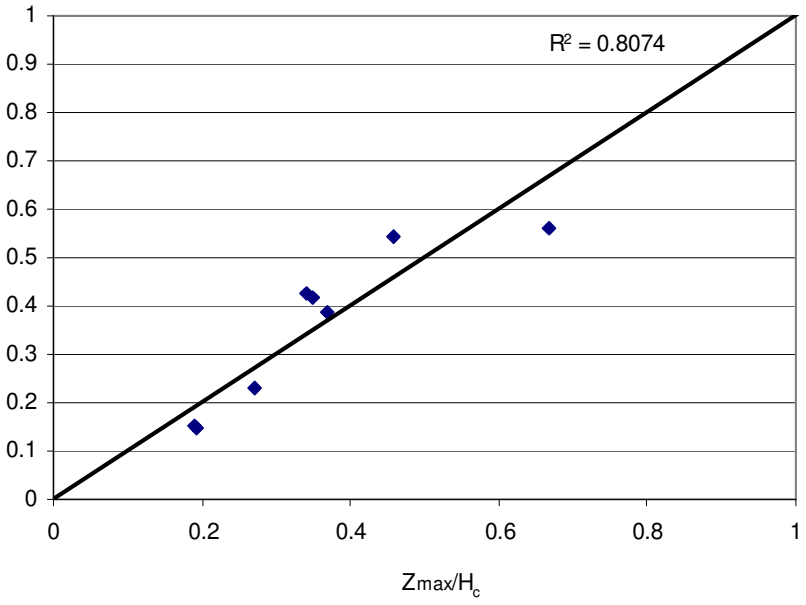

FIG 7.4 Relationship Between Maximum Scour Depth And Froude Number

$$\frac{Z_{\max}}{Hc}=\alpha_1\left\{\frac{\beta_1 V_2}{\sqrt{gHc}}-\frac{\left[\frac{\tau_c}{\rho}\right]^{\frac{1}{2}}}{gnHc^{\frac{1}{3}}}\right\}\times[M]^{\gamma} \qquad (7.1)$$

$\alpha_1 = 1.20$

$\beta_1 = 2.35$

$\gamma = 1.1\left[\frac{A_{fp}}{A_{mc}}\right]$ $\qquad 0 \le \frac{A_{fp}}{A_{mc}} \le 1$

Where A_{fp} is the area of flood plain; A_{mc} is the area of main channel; M is the contraction ratio. $M = \frac{A_2}{A_1}$ Where A_2 is the area of flow of the contracted channel and A_1 is the area of flow of the uncontracted channel.

The above equation 7.1 can be written incorporating upstream velocity V_1 as given below (Equation 7.2) where V_2 has been replaced by the relationship between the flow and the area of the contracted section.

$$\frac{Z_{\max}}{Hc} = \alpha_1 \left\{ \frac{\frac{\beta_1 V_1}{M}}{\sqrt{gHc}} - \frac{\left[\frac{\tau_c}{\rho}\right]^{\frac{1}{2}}}{gnHc^{\frac{1}{3}}} \right\} \times [M]^{\gamma} \tag{7.2}$$

Where L_s is the setback length of the contraction abutment from main channel bank.

The background behind the derivation of the above equation to predict maximum scour depth in a compound channel can be given as follows. The right side of Equation 7.2 can be discussed first. The nominal velocity in the channel at the contracted section can be defined as $v_2 = v_1\left(\frac{A_1}{A_2}\right)$ where v_1 is the average velocity of the channel in the far

upstream approach section, A_1 and A_2 are the flow areas in the far upstream and contracted section respectively. Therefore, the nominal Froude number in the contracted section would be

$$Fr^* = \frac{v_1}{\sqrt{gH_1}}\left(\frac{A_1}{A_2}\right) \tag{7.3}$$

In the above equation, H_1 (Hc) has been used instead of H_2 as the flow levels are assumed to be the same between the upstream and the contracted sections before scour starts and also the velocity is constant across the profile of the channel at the contracted section. A correction factor is applied to account for the errors in this assumption which has been described in detail later in this chapter.

Based on Manning's equation and the equilibrium between the gravity potential and the hydraulic potential for an open channel flow, shear stress (τ_c) and critical velocity (v_c) have been related by Richardson and Davis (1995) through the following equation.

$$\tau_c = \frac{\rho g n^2 v_c^{\,2}}{H_1^{1/3}} \tag{7.4}$$

Therefore, the critical Froude number Fr_c can be defined as

$$Fr_c = \frac{v_c}{\sqrt{gH_1}} = \frac{\left(\frac{\tau_c}{\rho}\right)^{1/2}}{gnH_1^{1/3}} \tag{7.5}$$

Bringing Equation 7.4 into Equation 7.5, the equation for contraction scour can be written as

$$\frac{Z}{Hc} = \alpha\left(\beta Fr* - Fr_c\right) \tag{7.6}$$

A similar approach also has been used by Li (2002) for predicting contraction scour in a rectangular channel with cohesive soil. In the above Equation 7.6, α and β are dimensionless coefficients with definite physical meaning. The coefficient β accounts for the difference in the velocities between the contracted section and the vena contracta as the latter is the section with maximum velocity and contraction. It also accounts for the variation in velocity across the contraction section. The coefficient α is defined as the contraction modulus (Li, 2002) which accounts for the change in the flow geometry between the approach and the contraction sections.

The coefficient γ defined in the Equation 7.2 represents a reduction factor applied to the scour estimate based on a rectangular channel in order to factor the complex flow patterns that occur at the contraction section in a compound channel.

In the above equation, HEC RAS predicted velocity (V_{HEC}) can be used and the Equation can be revised as given below.

$$\frac{Z_{\max}}{Hc} = \alpha_1 \left\{ \frac{0.98\,\beta_1 V_{HEC}}{\sqrt{gHc}} - \frac{\left[\frac{\tau_c}{\rho}\right]^{\frac{1}{2}}}{gnHc^{\frac{1}{3}}} \right\} \times [M]^{\gamma} \qquad (7.7)$$

$\alpha_1 = 1.20$

$\beta_1 = 2.35$

$$\gamma = 1.1\left[\frac{A_{fp}}{A_{mc}}\right] \qquad 0 \le \frac{A_{fp}}{A_{mc}} \le 1$$

7.3 LOCATION OF MAXIMUM SCOUR DEPTH

The knowledge of the location of the maximum scour hole is crucial in making decisions from a bridge design perspective. The location of the deepest contraction scour hole influences the risk posed to bridge pier or abutment by contraction scour. The observed distances of the maximum scour hole from the center of the contracted section

for the various test cases of the flume tests have been given in the Table 6.1. The following relationship between the distances of the maximum scour hole from the center of the contracted section (X_{max}) has been found to predict the distances more accurately than the prediction methodology used for the rectangular channels by Li (2002).

$$\frac{X_{\max}}{B_2} = \left[\frac{A_2}{A_1}\right]^{2.5} + 0.4 \tag{7.8}$$

$$\frac{X_{\max}}{B_2} = M^{2.5} + 0.4 \tag{7.9}$$

In the above Equation 7.9, B_2 stands for the length of the opening at the contraction inlet; X_{max} represents the distance to the maximum scour hole from the center of the contraction section. The plot between the predicted values of X_{max} on the y-axis and the actual measured values of X_{max} on the x-axis has been given in Figure 7.5.

In the downstream side, though a clear boundary for the scour hole could not be identified for lack of test bed, it was noted that contraction scour extends more than atleast twice the length of abutment scour in the downstream direction. In the lateral direction, contraction scour is bound by the farthest stream line which is tangential to the abutment or pier structure giving rise to contraction.

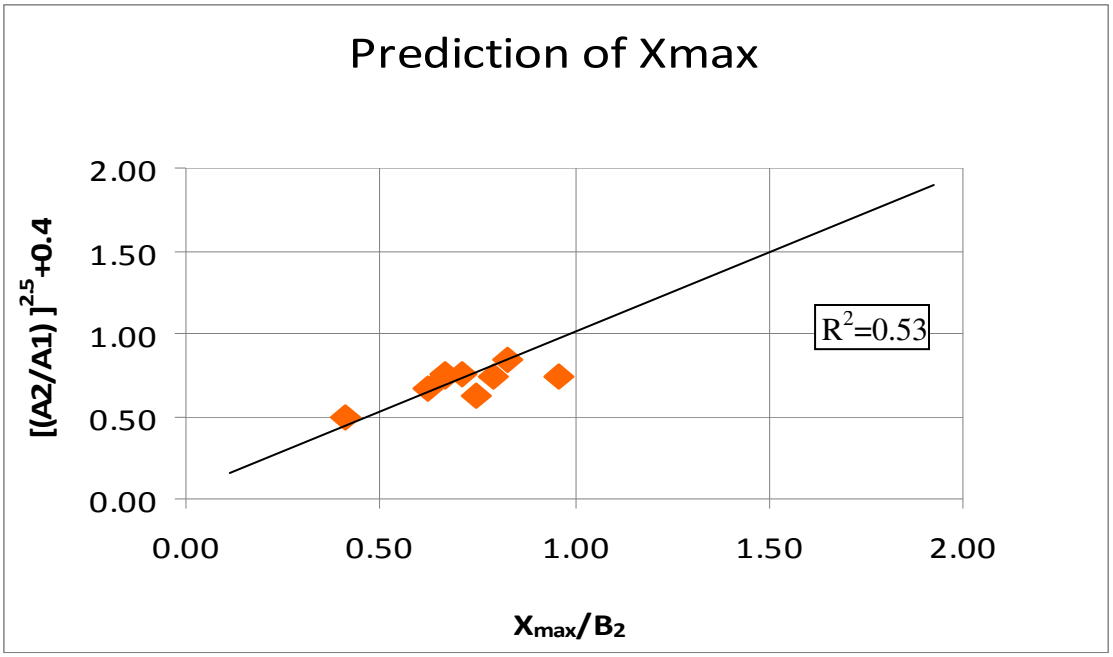

FIG 7.5 Relationship Between X_{max} And Contraction Geometry

7.4 UNIFORM SCOUR DEPTH

Uniform scour depth in a compound channel can be defined as the extent of the scoured area that has a scour depth which is more than atleast 50% of the depth of the maximum scour hole. The uniform scour hole extends well beyond the maximum scour hole and is fairly even in bed elevation. In the flume tests, four values of the uniform scour values have been averaged based on the evenness of scour observed from the time-series plots of scour development. The relationship to estimate uniform scour depth (Z_{unif}) has been given below.

$$\frac{Z_{unif}}{Hc} = \alpha_1 \left\{ \frac{\beta_1 V_2}{\sqrt{gHc}} - \frac{\left[\frac{\tau_c}{\rho}\right]^{\frac{1}{2}}}{gnHc^{\frac{1}{3}}} \right\} \times [M]^{\gamma} \qquad (7.10)$$

$\alpha_1 = 1.10$

$\beta_1 = 1.85$

$\gamma = 1.55\left[\frac{A_{fp}}{A_{mc}}\right] \qquad 0 \le \frac{A_{fp}}{A_{mc}} \le 1$

The contracted section velocity term (V_2) in the above equation can be replaced by the HEC-RAS predicted velocity and the correction can be made as follows.

$$\frac{Z_{unif}}{Hc} = \alpha_1 \left\{ \frac{0.98\,\beta_1 V_{HEC}}{\sqrt{gHc}} - \frac{\left[\frac{\tau_c}{\rho}\right]^{\frac{1}{2}}}{gnHc^{\frac{1}{3}}} \right\} \times [M]^{\gamma} \qquad (7.11)$$

$\alpha_1 = 1.10$

$\beta_1 = 1.85$

$\gamma = 1.55\left[\frac{A_{fp}}{A_{mc}}\right] \qquad 0 \le \frac{A_{fp}}{A_{mc}} \le 1$

A plot of the predicted values of Z_{unif} on the y-axis and the actual measured values of the uniform scour depth on the x-axis is shown in Figure 7.6.

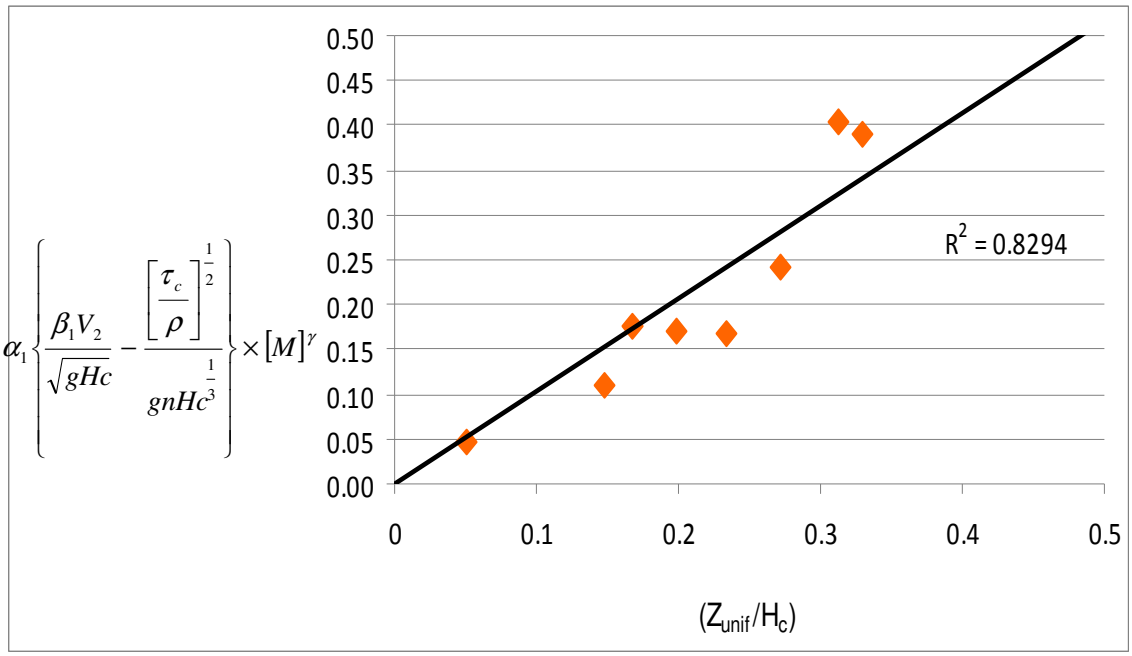

FIG 7.6 Relationship Between Z_{unif} And Froude Number

7.5 VERIFICATION CASE STUDY

An investigative approach to evaluate the precision of the scour prediction equations developed in this research is essential to understand the reliability of the predicted results. Equation 7.1 primarily developed for the estimation of maximum scour depth was used to predict the deepest scour holes due to contraction scour developed in a number of streams and channels of varied geometries and conditions whose scour data was obtained from US Geological Survey's online database (water.usgs.gov). A comparison of the scour depths predicted by the above equation 7.1 has been compared against the scour values measured at various scour sites.

Table 7.1 Contraction Scour Estimates On Real Life Rivers With Compound Channel Geometry

State	Stream Name	Contracted Average Velocity, V_2 (m/s)	Uncontracted Depth, H_c (m)	Contracted Discharge (m^3/s)	Measured Scour (m)	Predicted Scour (m)
OH	Scioto River	0.76	4.9	89.40	0.30	0.46
OH	Clear Creek	0.85	3.8	77.18	0.61	0.82
OH	Massies Creek	0.87	1.9	28.04	0.42	0.50
OH	Maumee River	0.99	5.8	541.38	0.30	1.01
OH	Scioto River	1.21	4.4	558.04	0.61	1.30
OH	Walnut Creek	0.74	2.1	41.92	0.39	0.45
OH	Walnut Creek	0.84	2.9	68.02	0.39	0.65
MN	Pomme De Terre River	1.45	2.4	138.82	1.18	1.17
MO	Chariton River	1.50	5.8	481.38	2.06	2.68
IA	Cedar River	1.70	6.8	671.87	0.76	2.66
SD	James River	1.27	5.4	385.91	1.21	1.46
MS	Conehoma Creek	2.81	4.3	249.12	1.24	1.24
MS	Conehoma Creek	2.80	4.2	187.40	0.91	1.02
WA	Chehalis River	2.30	1.9	694.08	1.30	1.33
WA	Chehalis River	2.76	1.9	832.89	1.51	1.58

The above Table 7.1 shows the various geometrical parameters of the rivers in this case study, the discharges and other relevant parameters. A comparison of the predicted scour depths and the actual measured scour depths by USGS has been given in Figure 7.7. It is to be noted that the uncontracted flow velocity V_1 was greater than the flow velocity at the contracted section V_2 in a few cases due to possible presence of short and narrow floodplains. It should also be noted that predicted scour values are

close to the observed scour depths in a few cases due to the reason that velocity measurements could have been made during non-flood periods prior to flood events causing scour while the recorded scour depth is due to the actual flood event.

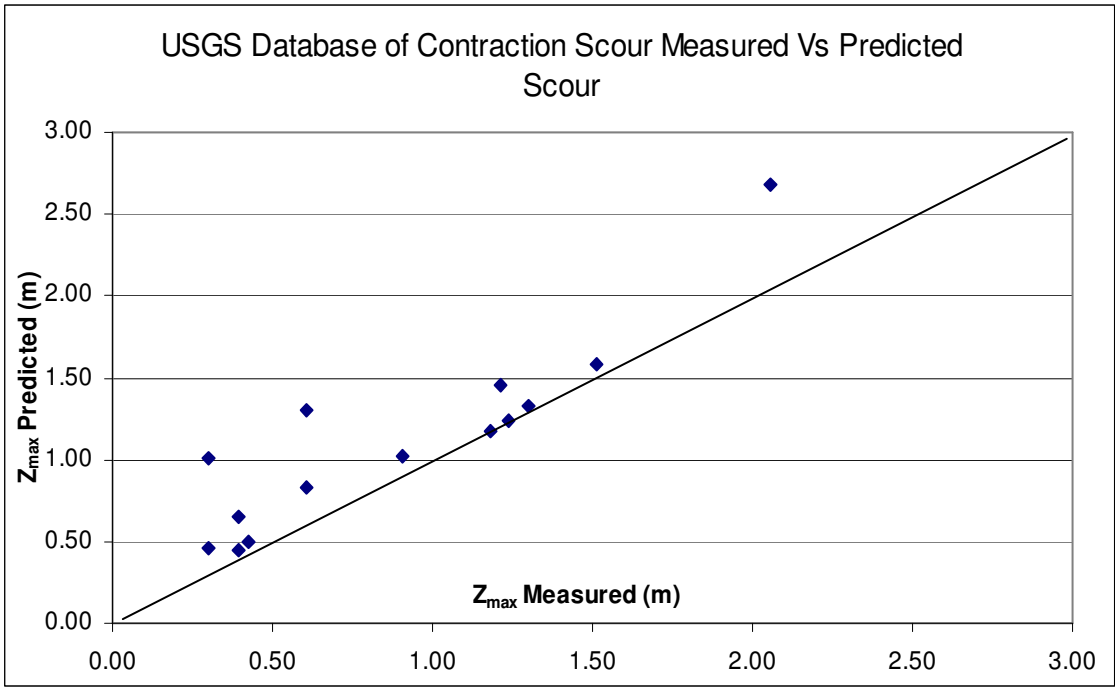

FIG 7.7 Verification Case Studies – Prediction Vs Measurement

The prediction of the proposed equation for maximum contraction scour is found to predict the actual scour measurements from field data fairly well given the fact that the geometries and soil types were differing widely from the test conditions of the flume experiments. Also it should be noted that the predicted scour values are on the conservative side of estimation compared against the field scour measurements.

CHAPTER VIII

CONCLUSIONS AND RECOMMENDATIONS

8.1 CONCLUSIONS

The interaction between the soil bed materials and flow is one of the leading causes for bridge failures in the United States. With respect to contraction scour on cohesive soil beds, on one hand, the soil properties of the clay bed affect specific behavior of scour including the scour rate, the final scour depth and the scour extent or shape. On the other hand, the geometry of the flow contraction affects physical parameters such as flow around the abutment contractions, flow acceleration, formation of vortices and eddies. In this present study, the characteristics of compound channel contraction scour have been highlighted based on the results from a number of flume tests and auxiliary computational analysis.

The following are the main conclusions obtained in this research.

1. The applicability of a hyperbolic model to the estimate the maximum scour depth of a contraction scour hole in a compound channel has been evaluated based on the flume test results and has been verified.
2. Based on flow observations, it has been found that the water surface elevation lowers greatly at the contraction section before scour starts coupled with a

sudden increase in velocity. This difference between the approach section and the contraction section gradually reduces and the water level stays between the approach section water surface elevation and the downstream water surface elevation towards the development of equilibrium scour condition. This again confirms the validity of a methodology to arrive at the scour depth based on the difference between the initial and final water surface elevations at the contracted section.

3. A similar distinction between maximum scour hole and uniform scour zone like in simple rectangular channels with cohesive beds have been identified for the compound channels. The shape and extent of the scour hole and the depth of the maximum scour hole have been found to be a result of the difference between the erosive action of the approach flow characterized by the Approach Froude Number and the resistance to scour offered by the soil at the contraction section characterized by the Critical Froude Number.
4. The extent and boundary of contraction scour in a compound channel is governed by the flow field by being bound by the stream line tangential to the abutment/pier structure. Also, contraction scour happens more near the center of the channel while abutment scour is localized and happens only in the wake of the abutment. It was also observed that contraction scour and abutment scour

superimpose one another upto the development of equilibrium scour when the contraction is harsh.

5. Two sets of equations have been developed to predict maximum scour hole depths and the uniform scour hole depths, one based on a calculation of average representative velocity at the contraction section and the other based on the simulated results from a HEC RAS one dimensional model.
6. An equation to predict the location of the scour hole based on a relationship between the contraction geometry and approach geometry. A method to identify the extent of the scour hole has also been proposed.
7. Flow velocity and depth have crucial effect on contraction scour in a channel with compound geometry. Flow depth directly affects the extent of scour and broadens out the shape of the scour hole while increase in the flow velocity elongates and extends the scour hole far downstream at the contraction section.
8. A vertical wing wall abutment deflects the flow more towards the center of the channel leading to increased velocities causing harsh contractions compared to a spill-through shaped abutment contraction. At the same time, a vertical wall abutment contraction seems to give rise to little scour in the vicinity of the structure itself suggesting that a vertical wall abutment may be more suitable to avoid scour in the close vicinity of the abutment, from a bridge design perspective.

8.2 RECOMMENDATIONS

Most of the current research is based on evaluating the results of flume tests. The singleness of the tested cohesive soil, simplified test conditions might constrain the use of the application of the present research to unique field conditions. The following are the recommendations for future research and investigations.

1. More different kinds of clay should be tested with variations on the shear stresses of clay.
2. Layered cohesive soil formations should be tested under the same flume conditions to test the applicability of the proposed scour equations for layered beds.
3. Flume tests on skewed contraction inlets/abutments should be tested to identify the effects of a skewed inlet geometry on contraction scour.
4. Contraction length effect especially for long contractions should be explored to identify the effect of the length of contraction zone.
5. An integrated approach to evaluate abutment scour and contraction scour in case of harsh contractions should be developed.

REFERENCES

Annandale, G.W. (1995), "Erodibility." *Journal of Hydraulic Research, International Association of Hydraulic Research*, 33(4), 471-494.

Annandale, G.W. and Kirsten, H.A.D., (1994), "On the Erodibility of Rock and Other Earth Materials." *Proc. of National Hydraulic Engineering Conference*, Contonea, G.V. and Bruner, R.R. (ED), ASCE, New York, 68-72.

Ariathurai, R., and Arulanandan, K. (1978). "Erosion Rates of Cohesive Soils." *J. Hydr. Div.*, ASCE 104(2), 279-283.

Arulanandan, K. (1975). "Fundamental Aspects of Erosion in Cohesive Soils." *J. Hydr. Div.*, ASCE, 101(5), 635-639.

Biglari, B. and Sturm, T. W. (1998), "Numerical Modeling of Flow around Bridge Abutment in Compound Channel." *J. Hydr. Div.,* ASCE 124(2), 156-164.

Briaud, J.-L., Ting, F., Chen, H.C., Cao, Y., Han, S.W., Kwak, K.W., (2001a) "Erosion Function Apparatus for Scour Rate Predictions." *Journal of Geotechnical and Environmental Engineering*, ASCE Vol 127, No.2, 105-113.

Cao, Y. (2001), "The Influence of Certain Factors on the Erosion Function of Cohesive Soils." Thesis for Master of Engineering, Department of Civil Engineering, Texas A&M University, College Station, Texas.

Carollo, F. G., Ferro, V., Termini, D. (2005), "Analyzing turbulence intensity in gravel bed channels." *J. Hydraul. Eng.* 131(12), 1050-1061.

Chang, F. and Davis, S. (1998), "Maryland SHA Procedure for Estimating Scour at Bridge Abutments: Part 2-Clear Water Scour." *ASCE Compendium of Conference Scour Papers* (1991 to 1998), 412-416, Reston, VA.

Christensen, R.W. and Das, B.W. (1973), "Hydraulic Erosion of Remolded Cohesive Soils." *Highway Research Board Special Report*, No. 135, 8-19.

Chien, N. and Wang, Z., (1999), "Mechanics of Sediment Transport", *ASCE Press*, Reston, VA.

Barbhuiya, A.K. and Dey, S. (2003), "Vortex Flow Field in a Scour Hole Around Abutments." *Int. J. Sediment Res.*, Vol. 18, No. 4, 2003, 310-325.

Dunn, I. S. (1959). "Tractive Resistance to Cohesive Channels." *J. Soil Mech. And Found. Div.*, ASCE, 85(3), 1-24.

Enger, P. F., Smerdon, E. T., and Masch, F. D. (1968). "Erosion of Cohesive Soils." *J. Hydr. Div*., ASCE, 94(4), 1017-1049.

Ettema, R., Nakato, T. and Muste, M., (2003), "An Overview of Scour Types and Scour-Estimation Difficulties Faced at Bridge Abutments", *Proc. of 2003 Mid-Continent Transportation Research Symposium,* Ames, Iowa, 2-11.

García, C. M., Cantero, M. I., Niño, Y., and García, M. H., (2005), "Turbulence Measurements with Acoustic Doppler Velocimeters." *J. Hydraulic Engineering*, ASCE 131(12), 1062-1073.

Gill, M.A. (1981), "Bed Erosion in Rectangular Long Contraction." *J. Hydr. Div.,* ASCE 107(3), 273-284.

Gudavalli, S. R., (1997), "Prediction Model for Scour Rate around Bridge Piers in Cohesive Soil on the Basis of Flume Tests," PhD. Dissertation, Department of Civil Engineering, Texas A&M University, College Station, TX.

Hoffmans, G.J.C.M. and Verheij, H.J. (1997), *"Scour Manual."* A.A.Balkema, Netherlands.

Iverson (1998), "Scour and Erosion in Clay Soils." *ASCE Compendium of Conference Scour Papers (1991-1998),* Reston, VA, 412-416.

Kelly, E. K., and Gularte, R. C. (1981). "Erosion Resistance of Cohesive Soils." *J. Hydr. Div.,* ASCE, 107(10), 1211-1224.

Komura, S. (1966), "Equilibrium Depth of Scour in Long Contractions." *J. Hydr. Div.*, ASCE 92(5), 17-37.

Kwak, K., (2000), "Prediction of Scour Depth Versus Time for Bridge Piers in Cohesive Soils in the Case of Multi-Flood and Layered Soil Systems." PhD. Dissertation, Department of Civil Engineering, Texas A&M University, College Station, TX.

Lagasse, P. F., Schall, J. D., Johnson, F., Richardson, E. V., and Chang, F. (1991), "Stream Stability at Highway Structures." *Rep. No. FHWA-IP-90-014 (HEC-20),* Federal Highway Administration, Washington, D.C.

Laursen, E. M. (1960), "Scour at Bridge Crossing." *J. Hydr. Div.*, ASCE 86(2), 39-54.

Laursen, E. M. (1963), "An Analysis of Relief Bridge Scour." *J. Hydr. Div*., ASCE 89(3), 94-118.

Laursen, E. M. and Toch, A. (1956), "Scour around Bridge Piers and Abutments." *Bulletin No.4*, Iowa Highways Research Board, Ames, IA.

Li, Y., (2002), "Bridge Pier Scour and Contraction Scour in Cohesive Soils on the basis of Flume Tests." Ph.D. Dissertation, Department of Civil Engineering, Texas A&M University, College Station, TX.

Lim, S. Y. (1998), "Scouring in Long Contractions." *J. Irrigation and Drainage Engineering Div*., ASCE 124(5), 258-261.

Liou, Y. (1970), "Hydraulic Erodibility of Two Pure Clay Systems." PhD. Dissertation, Civil Engineering Department, Colorado State University, Fort Collins, CO.

Lyle, W.M. and Smerdon, E. T. (1965), "Relation of Compaction and Other Soil Properties to Erosion and Resistance of Soil." *Trans., ASAE*, American Society of Agricultural Engineers, St. Joseph, MI, 8(3).

Abscour Users Manual (October 2005), *Office of Bridge Development - Maryland SHA Scour Program,* August 16, 2006, Retrieved May 25, 2007 from http://www.wtbco.com/scour/scour.html

Rana, M.Y. (1986), "Flume Experiments on Sediment Bed in Steady Non-Uniform Flow." M.S. Thesis, Asian Institute of Technology, Bangkok, Thailand.

Richardson, E. V. and Davis, S. R. (1995), "Evaluating Scour at Bridges," *Rep. No. FHWA-IP-90-017 (HEC-18),* Federal Highway Administration, Washington, DC.

Richardson, E. V. and Richardson, J. R. (1994), "Practical Method for Calculating Contraction Scour." *Proc. Of ASCE, National Hydraulics Conference,* Buffalo, NY, 6-10.

Shaikh, A., Ruff, J. F., and Abt, S. R. (1988). "Erosion Rate of Compacted Na-Montmorillonite Soils." *J. Geotech. Engrg.,* ASCE, 114(3), 296-305.

Shirole, A. M., and Holt, R. C. (1991), "Planning for Comprehensive Bridge Safety Assurance Program." *Trans. Res. Rec. 1290, Transportation Research Board,* Washington, DC., 137-142.

Smerdon E. T. and Beasley, R. P (1959), "Tractive Force Theory Applied to Stability of Open Channels in Cohesive Soils." *Research Bulletin No. 715,* Agriculture Experiment Station, University of Missouri, Columbia, MO.

Smith, C. D., (1967) "Simplified Desigh for Flume Inlets." *J. Hydr. Div.,* ASCE 93(6), 25-34.

Straub, L. G (1934), "Effect of Channel Contraction Works Upon Regime of Movable Bed Streams." *Trans. Am. Geophysical Union,* Part II, 454-463.

Sturm, T. W. and Janjua, N. S. (1994), "Clear-Water Scour around Abutment in Flood Plain." *J. Hydr. Div.,* ASCE 120(8), 956-972.

Tey, C. B. (1984), "Local Scour at Bridge Abutment." *Res. Rep. No. 329,* University of Auckland, New Zealand.

U.S. Department of the Interior, U.S. Geological Survey – Kentucky Disctrict June 13, 2000, Retrieved May 24, 2007, from http://water.usgs.gov/osw/techniques/bs/BSDMS/Data_Tables/ContractionScourTable.htm

Wang, J., (2004), "The Sricos-EFA Method For Complex Pier And Contraction Scour." Ph.D. Dissertation, Department of Civil Engineering, Texas A&M University, College Station, TX.

Wei, G., Chen, H. C., Ting, F., Briaud, J. L., et al (1997), "Numerical Simulation to Study Scour Rate in Cohesive Soils." *Res. Rep. Prepared for Texas DOT,* Department of Civil Engineering, Texas A&M University, College Station, TX.

Winterwerp, J. C. (1989), "Cohesive Sediments, Flow Included Erosion of Cohesive Beds." *Rijkswaterstaat/Delft Hydraulics*, Delft, Netherlands.

APPENDIX A

HYPERBOLIC MODEL RESULTS FOR FLUME TESTS

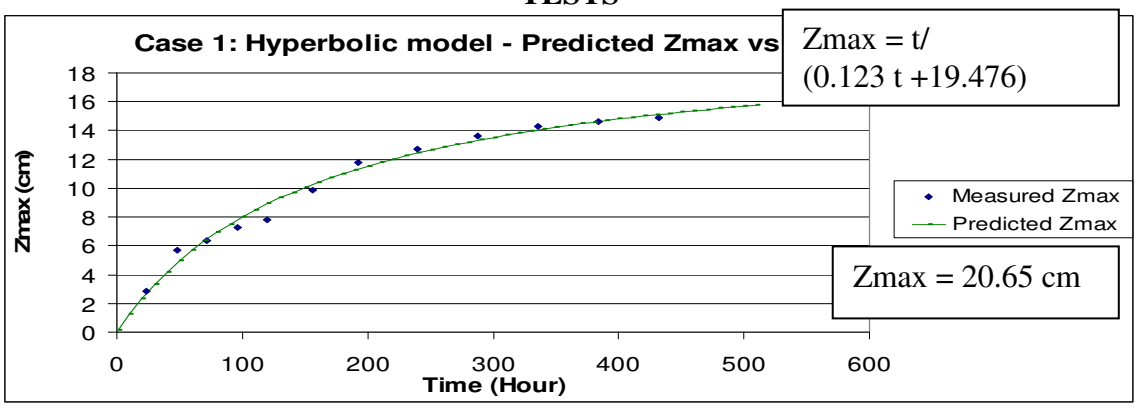

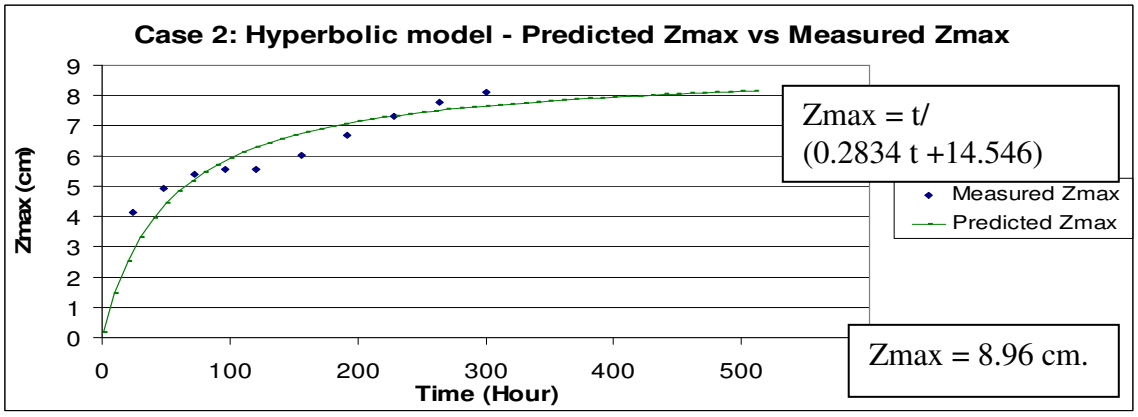

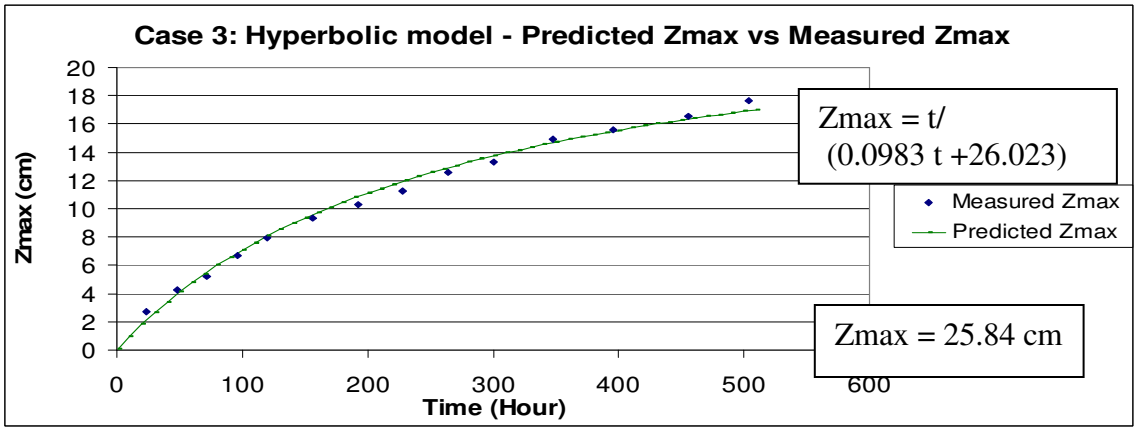

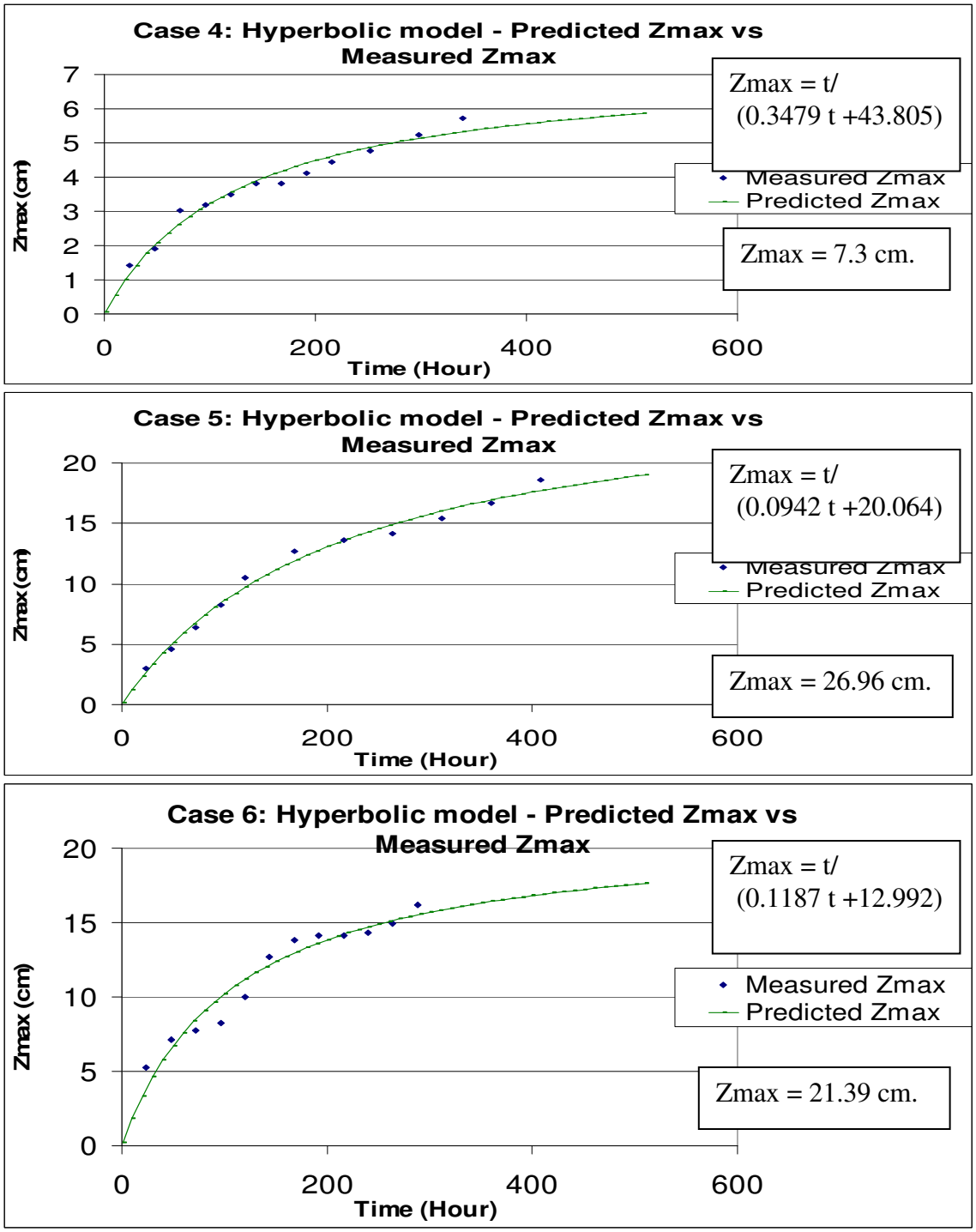
Case 4: Hyperbolic model - Predicted Zmax vs Measured Zmax
Zmax = t/ (0.3479 t +43.805)
Measured Zmax
Predicted Zmax
Zmax = 7.3 cm.
Zmax (cm)
Time (Hour)
0
1
2
3
4
5
6
7
0
200
400
600
Case 5: Hyperbolic model - Predicted Zmax vs Measured Zmax
Zmax = t/ (0.0942 t +20.064)
Measured Zmax
Predicted Zmax
Zmax = 26.96 cm.
Zmax (cm)
Time (Hour)
0
5
10
15
20
0
200
400
600
Case 6: Hyperbolic model - Predicted Zmax vs Measured Zmax
Zmax = t/ (0.1187 t +12.992)
Measured Zmax
Predicted Zmax
Zmax = 21.39 cm.
Zmax (cm)
Time (Hour)
0
5
10
15
20
0
200
400
600

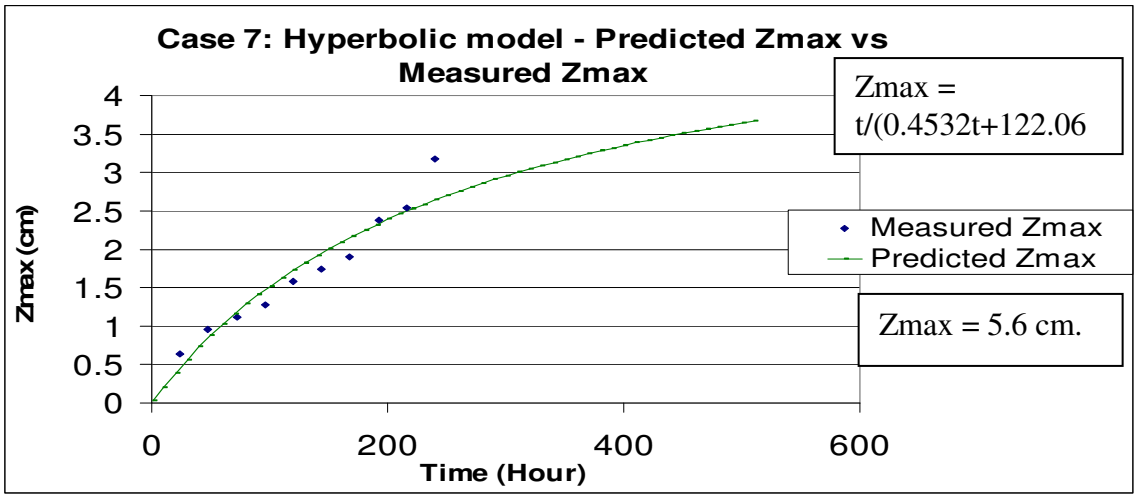
Case 7: Hyperbolic model - Predicted Zmax vs Measured Zmax
Zmax = t/(0.4532t+122.06
Measured Zmax
Predicted Zmax
Zmax = 5.6 cm.
Zmax (cm)
Time (Hour)
0
0.5
1
1.5
2
2.5
3
3.5
4
0
200
400
600

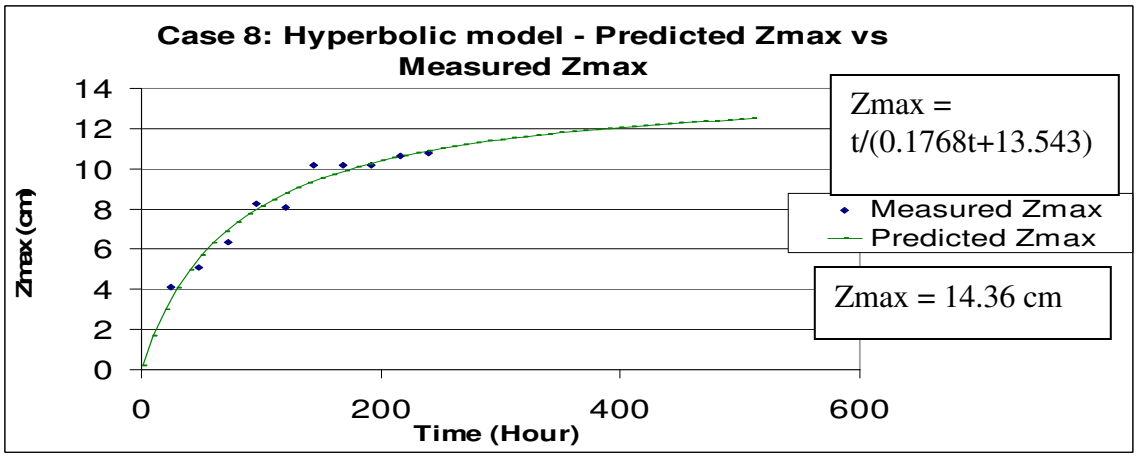
Case 8: Hyperbolic model - Predicted Zmax vs Measured Zmax
Zmax = t/(0.1768t+13.543)
Measured Zmax
Predicted Zmax
Zmax = 14.36 cm
Zmax (cm)
Time (Hour)
0
2
4
6
8
10
12
14
0
200
400
600

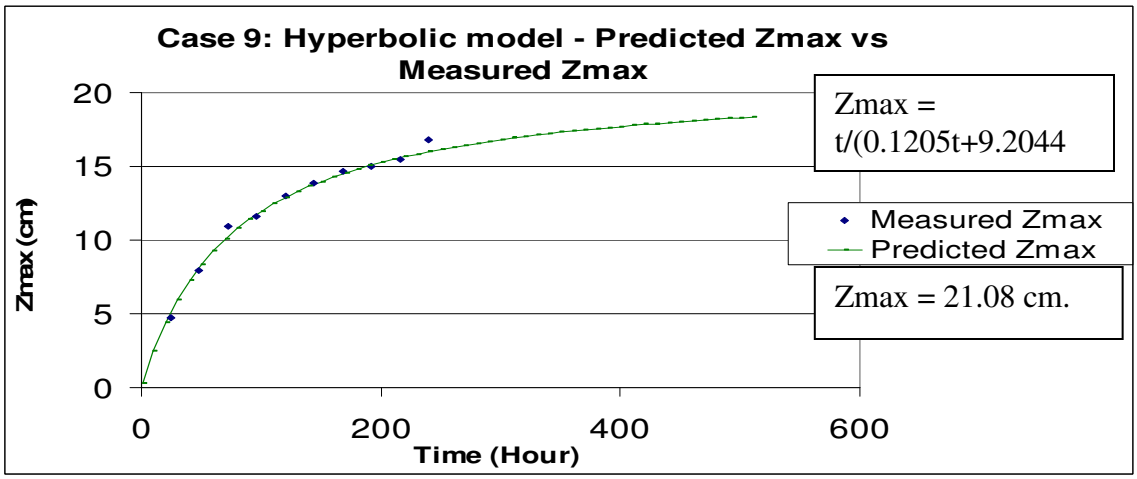
Case 9: Hyperbolic model - Predicted Zmax vs Measured Zmax
Zmax = t/(0.1205t+9.2044
Measured Zmax
Predicted Zmax
Zmax = 21.08 cm.
Zmax (cm)
Time (Hour)
0
5
10
15
20
0
200
400
600

APPENDIX B

TIME VERSUS (T/Zmax) PLOTS FROM FLUME TESTS

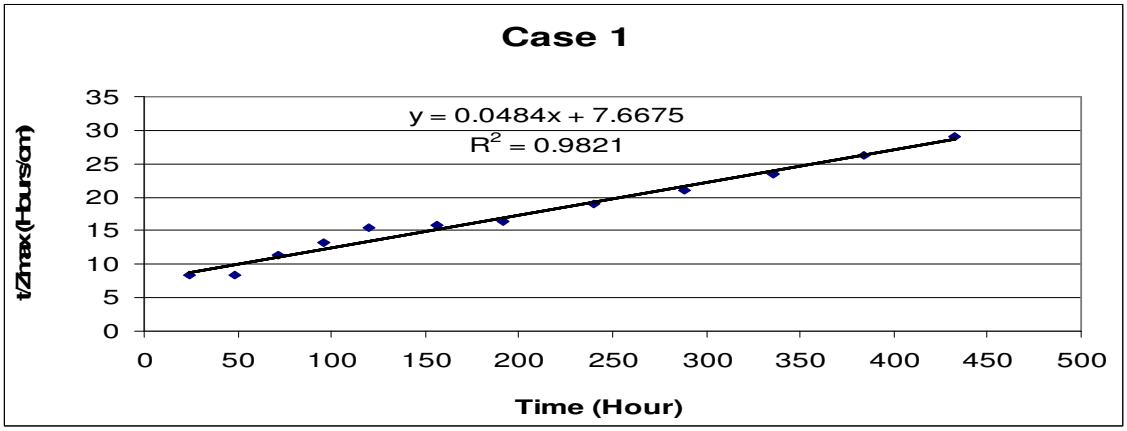

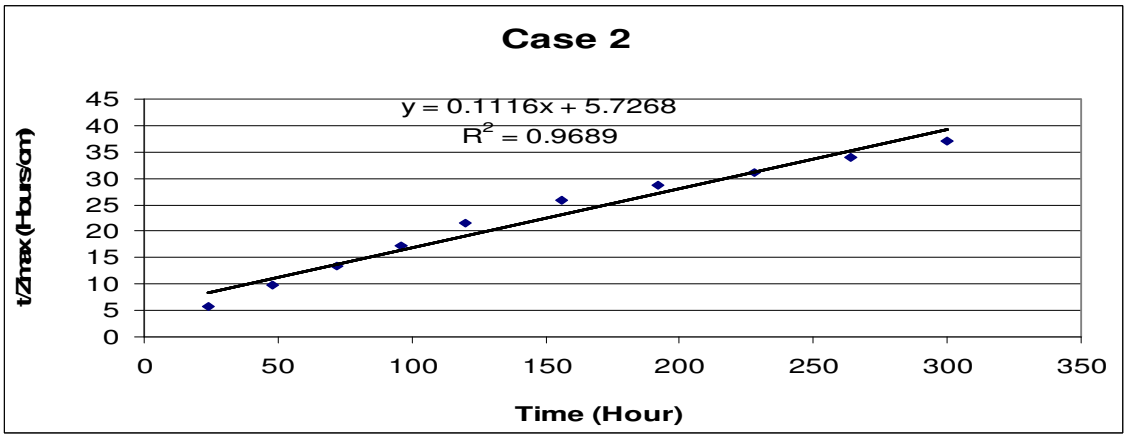

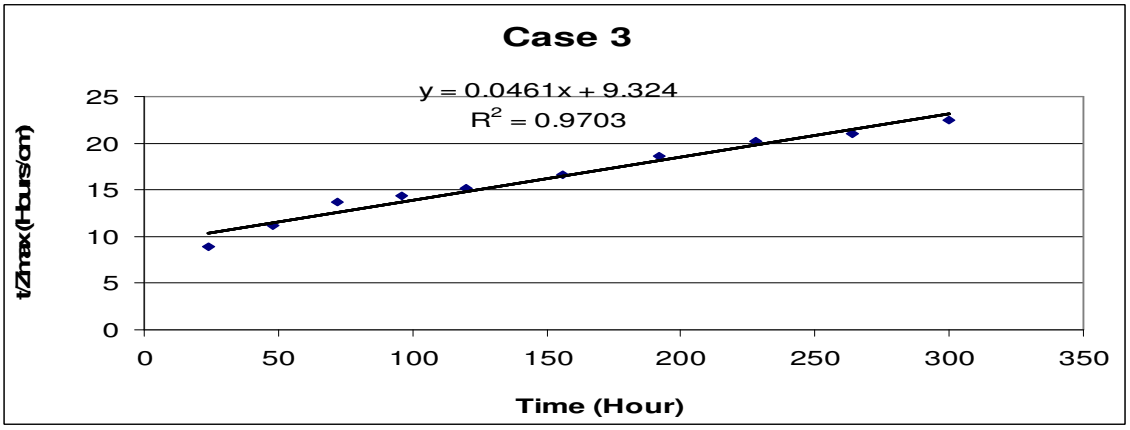

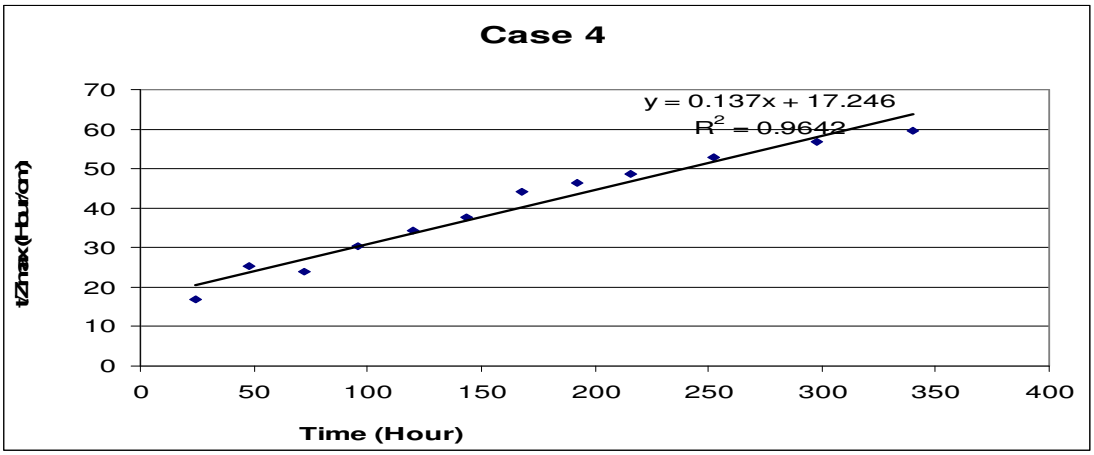
Case 4
y = 0.137x + 17.246
R2 = 0.9642
t/Zmax(Hour/cm)
Time (Hour)
0
10
20
30
40
50
60
70
0
50
100
150
200
250
300
350
400

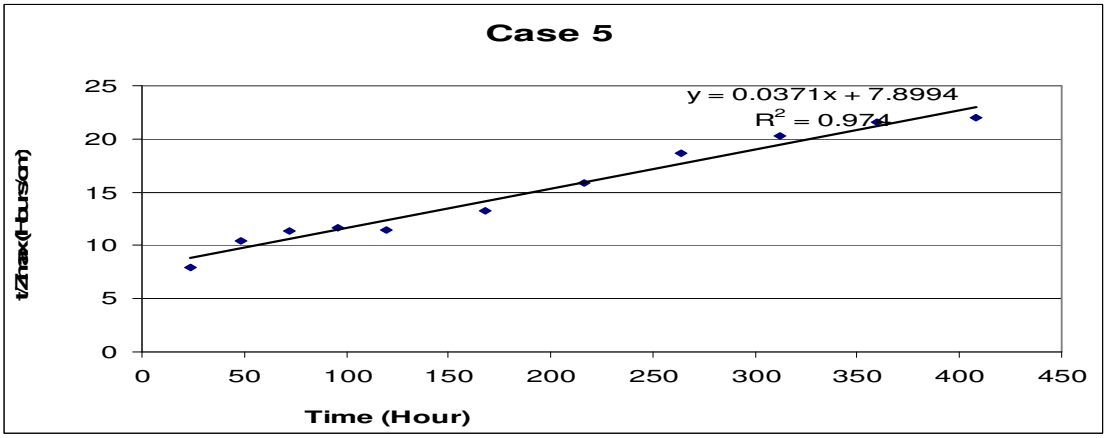
Case 5
y = 0.0371x + 7.8994
R2 = 0.974
t/Zmax(Hours/cm)
Time (Hour)
0
5
10
15
20
25
0
50
100
150
200
250
300
350
400
450

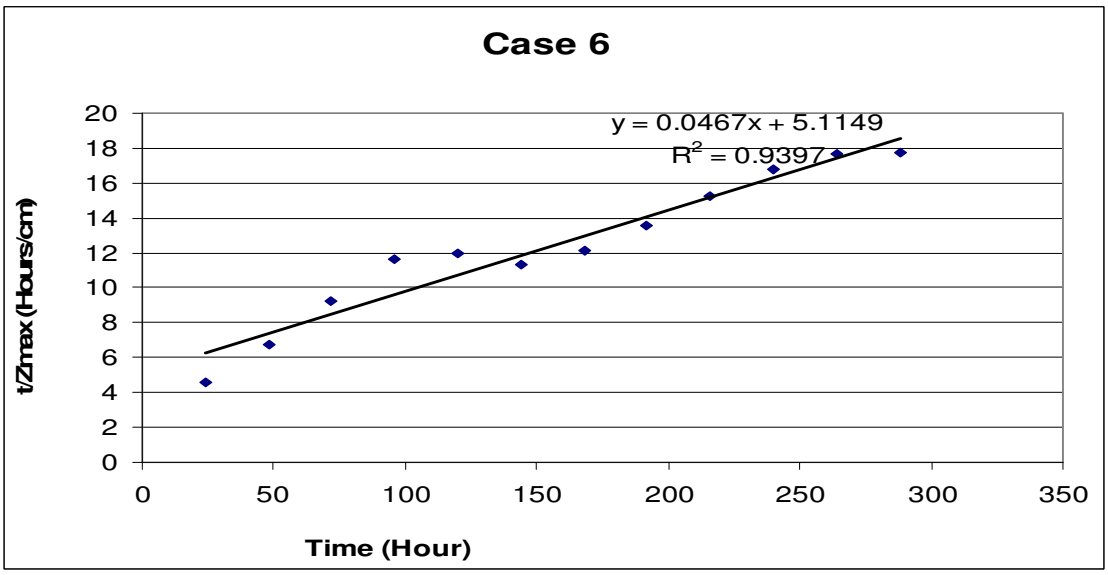
Case 6
y = 0.0467x + 5.1149
R2 = 0.9397
t/Zmax (Hours/cm)
Time (Hour)
0
2
4
6
8
10
12
14
16
18
20
0
50
100
150
200
250
300
350

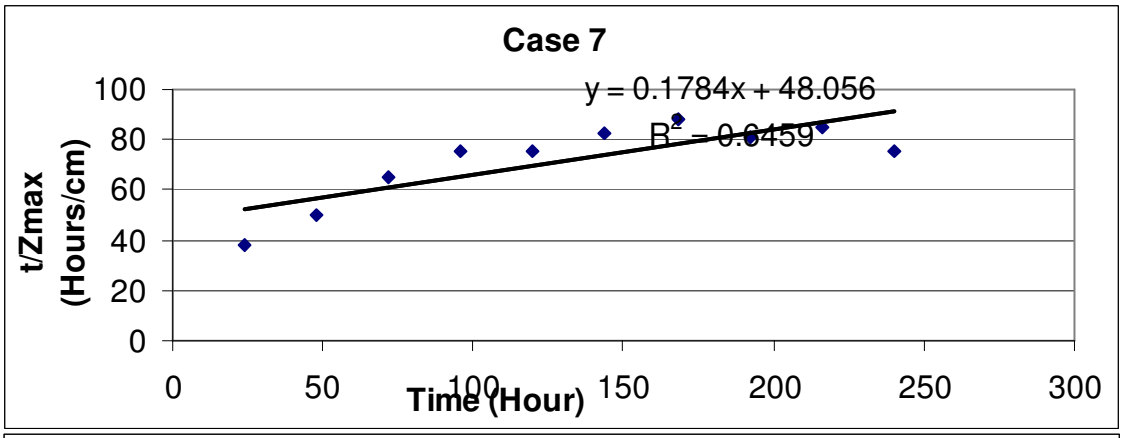
Case 7
y = 0.1784x + 48.056
R² = 0.6459
t/Zmax (Hours/cm)
Time (Hour)
0
20
40
60
80
100
0
50
100
150
200
250
300

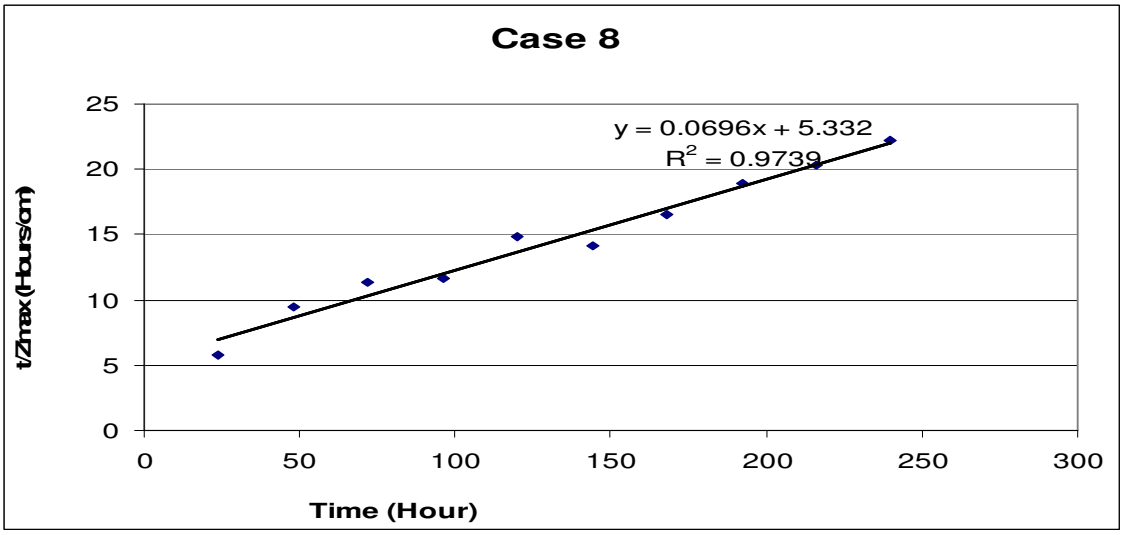
Case 8
y = 0.0696x + 5.332
R² = 0.9739
t/Zmax (Hours/cm)
Time (Hour)
0
5
10
15
20
25
0
50
100
150
200
250
300

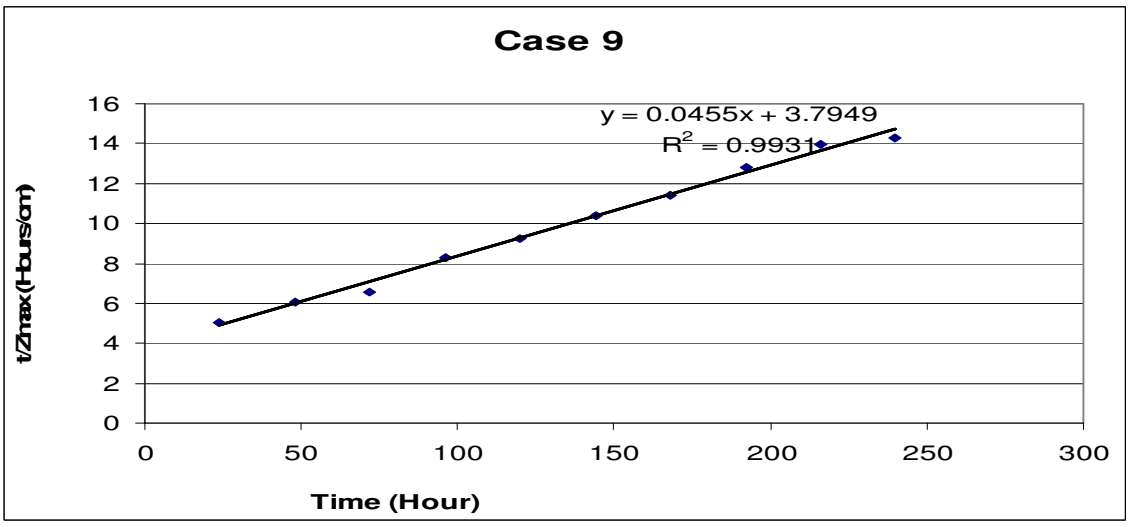
Case 9
y = 0.0455x + 3.7949
R² = 0.9931
t/Zmax (Hours/cm)
Time (Hour)
0
2
4
6
8
10
12
14
16
0
50
100
150
200
250
300

APPENDIX C
MEASURED MAXIMUM SCOUR DEPTH AS A FUNCTION OF TIME

Time (Hour)	Max scour (Zmax)	
	(in)	(cm)
24	1.13	2.87
48	2.25	5.72
72	2.50	6.35
96	2.88	7.32
120	3.06	7.77
156	3.88	9.86
192	4.63	11.76
240	5.00	12.70
288	5.38	13.67
336	5.63	14.30
384	5.75	14.61
432	5.88	14.94

Case 1

Time (Hour)	Max scour (Zmax)	
	(in)	(cm)
24	1.63	4.14
48	1.94	4.93
72	2.13	5.41
96	2.19	5.56
120	2.19	5.56
156	2.38	6.05
192	2.63	6.68
228	2.88	7.32
264	3.06	7.77
300	3.19	8.10

Case 2

Time (Hour)	Max scour (Zmax)	
	(in)	(cm)
24	1.06	2.69
48	1.69	4.29
72	2.06	5.23
96	2.63	6.68
120	3.13	7.95
156	3.69	9.37
192	4.06	10.31
228	4.44	11.28
264	4.94	12.55
300	5.25	13.34
348	5.88	14.94
396	6.13	15.57
456	6.50	16.51
504	6.94	17.63

Case 3

Time (Hour)	Max scour (Zmax)	
	(in)	(cm)
24	0.56	1.42
48	0.75	1.91
72	1.19	3.02
96	1.25	3.18
120	1.38	3.51
144	1.50	3.81
168	1.50	3.81
192	1.63	4.14
216	1.75	4.45
252	1.88	4.78
298	2.06	5.23

Case 4

Time (Hour)	Max scour (Zmax)	
	(in)	(cm)
24	1.19	3.02
48	1.81	4.60
72	2.50	6.35
96	3.25	8.26
120	4.13	10.49
168	5.00	12.70
216	5.38	13.67
264	5.56	14.12
312	6.06	15.39
360	6.56	16.66
408	7.31	18.57

Case 5

Time (Hour)	Max scour (Zmax)	
	(in)	(cm)
24	2.06	5.23
48	2.81	7.14
72	3.06	7.77
96	3.25	8.26
120	3.94	10.01
144	5.00	12.70
168	5.44	13.82
192	5.56	14.12
216	5.56	14.12
240	5.63	14.30
264	5.88	14.94
288	6.38	16.21

Case 6

Time (Hour)	Max scour (Zmax)	
	(in))	(cm)
24	0.25	0.64
48	0.38	0.97
72	0.44	1.12
96	0.50	1.27
120	0.63	1.60
144	0.69	1.75
168	0.75	1.91
192	0.94	2.39
216	1.00	2.54
240	1.25	3.18

Case 7

Time (Hour)	Max scour (Zmax)	
	(in)	(cm)
24	1.63	4.14
48	2.00	5.08
72	2.50	6.35
96	3.25	8.26
120	3.19	8.10
144	4.00	10.16
168	4.00	10.16
192	4.00	10.16
216	4.19	10.64
240	4.25	10.80

Case 8

Time (Hour)	Max scour (Zmax)	
	(in)	(cm)
24	1.88	4.78
48	3.13	7.95
72	4.31	10.95
96	4.56	11.58
120	5.13	13.03
144	5.47	13.89
168	5.78	14.68
192	5.91	15.01
216	6.09	15.47
240	6.63	16.84

Case 9

VITA

Benjamin Praisy Israel Devadason received his Bachelor of Engineering degree in Civil Engineering from Government College of Engineering, Tamil Nadu in India in 2003. He started his Master's program at Texas A&M University, College Station in the fall of 2005. His special professional interests include Hydraulics, Hydrology and Water Resources Systems Engineering. He worked as a Graduate Research Assistant at Texas A&M University and graduated with a Master of Science degree in Civil Engineering in December 2007.

Mr. Israel's contact mailing address is Civil Engineering Department, c/o Dr. Kuang-An Chang, Texas A&M University, College Station, Texas 77840. He can be contacted at the email address bpraisy1982@hotmail.com.